IOWA STATE UNIVERSITY
Digital Repository

Retrospective Theses and Dissertations

Iowa State University Capstones, Theses and Dissertations

1979

A copperized cadmium flow-through detector for the amperometric determination of nitrate in aqueous samples based on electrocatalytic reduction

Glenn Alwyn Sherwood Jr.
Iowa State University

Follow this and additional works at: https://lib.dr.iastate.edu/rtd

Part of the Analytical Chemistry Commons

Recommended Citation

Sherwood, Glenn Alwyn Jr., "A copperized cadmium flow-through detector for the amperometric determination of nitrate in aqueous samples based on electrocatalytic reduction " (1979). *Retrospective Theses and Dissertations*. 7248.
https://lib.dr.iastate.edu/rtd/7248

This Dissertation is brought to you for free and open access by the Iowa State University Capstones, Theses and Dissertations at Iowa State University Digital Repository. It has been accepted for inclusion in Retrospective Theses and Dissertations by an authorized administrator of Iowa State University Digital Repository. For more information, please contact digirep@iastate.edu.

المنارة للاستشارات

www.manaraa.com

INFORMATION TO USERS

This was produced from a copy of a document sent to us for microfilming. While the most advanced technological means to photograph and reproduce this document have been used, the quality is heavily dependent upon the quality of the material submitted.

The following explanation of techniques is provided to help you understand markings or notations which may appear on this reproduction.

1. The sign or "target" for pages apparently lacking from the document photographed is "Missing Page(s)". If it was possible to obtain the missing page(s) or section, they are spliced into the film along with adjacent pages. This may have necessitated cutting through an image and duplicating adjacent pages to assure you of complete continuity.
2. When an image on the film is obliterated with a round black mark it is an indication that the film inspector noticed either blurred copy because of movement during exposure, or duplicate copy. Unless we meant to delete copyrighted materials that should not have been filmed, you will find a good image of the page in the adjacent frame.
3. When a map, drawing or chart, etc., is part of the material being photographed the photographer has followed a definite method in "sectioning" the material. It is customary to begin filming at the upper left hand corner of a large sheet and to continue from left to right in equal sections with small overlaps. If necessary, sectioning is continued again—beginning below the first row and continuing on until complete.
4. For any illustrations that cannot be reproduced satisfactorily by xerography, photographic prints can be purchased at additional cost and tipped into your xerographic copy. Requests can be made to our Dissertations Customer Services Department.
5. Some pages in any document may have indistinct print. In all cases we have filmed the best available copy.

University
Microfilms
International

300 N. ZEEB ROAD, ANN ARBOR, MI 48106
18 BEDFORD ROW, LONDON WC1R 4EJ, ENGLAND

8000173

SHERWOOD, GLENN ALWYN, JR.
A COPPERIZED CADMIUM FLOW-THROUGH DETECTOR FOR THE AMPEROMETRIC DETERMINATION OF NITRATE IN AQUEOUS SAMPLES BASED ON ELECTROCATALYTIC REDUCTION.

IOWA STATE UNIVERSITY, PH.D, 1979

University Microfilms International 300 N. ZEEB ROAD, ANN ARBOR, MI 48106

PLEASE NOTE:

In all cases this material has been filmed in the best possible way from the available copy. Problems encountered with this document have been identified here with a check mark ✓.

1. Glossy photographs ✓
2. Colored illustrations ______
3. Photographs with dark background ✓
4. Illustrations are poor copy ______
5. Print shows through as there is text on both sides of page ______
6. Indistinct, broken or small print on several pages ______ throughout ______
7. Tightly bound copy with print lost in spine ______
8. Computer printout pages with indistinct print ______
9. Page(s) ______ lacking when material received, and not available from school or author ______
10. Page(s) ______ seem to be missing in numbering only as text follows ______
11. Poor carbon copy ______
12. Not original copy, several pages with blurred type ______
13. Appendix pages are poor copy ______
14. Original copy with light type ______
15. Curling and wrinkled pages ______
16. Other ______

University
Microfilms
International

300 N. ZEEB RD., ANN ARBOR, MI 48106 (313) 761-4700

A copperized cadmium flow-through detector for the amperometric determination of nitrate in aqueous samples based on electrocatalytic reduction

by

Glenn Alwyn Sherwood, Jr.

A Dissertation Submitted to the
Graduate Faculty in Partial Fulfillment of
The Requirements for the Degree of
DOCTOR OF PHILOSOPHY

Department: Chemistry
Major: Analytical Chemistry

Approved:

Signature was redacted for privacy.

In Charge of Major Work

Signature was redacted for privacy.

For the Major Department

Signature was redacted for privacy.

For the Graduate College

Iowa State University
Ames, Iowa

1979

TABLE OF CONTENTS

Page

I. INTRODUCTION 1

II. THE ELECTROCATALYTIC REDUCTION OF NITRATE ON CADMIUM 5

- A. Literature Review of the Reduction of Nitrate to Nitrite for Colorimetric Analysis 5
- B. Electrocatalysis 10
- C. Experimental 20
  - 1. Reagents 20
  - 2. Electronic circuitry and associated apparatus 22
  - 3. Rotating disk and ring disk electrodes 22
  - 4. Scanning electron microscope 29
- D. Results and Discussion 30
  - 1. Comparison of relative, heterogeneous reaction rates in acid 30
    - a. Theoretical basis 30
    - b. Experimental results 37
  - 2. Electrochemical investigations of reduction of nitrate and oxygen on copperized cadmium 45
    - a. Rate of reduction of nitrate 45
    - b. Product of reduction of nitrate 51
    - c. Reduction of oxygen 62
  - 3. Stability of metals on copperized cadmium surface 68
  - 4. Microstructure of copperized cadmium surface 74
  - 5. Electrocatalytic effect of copper 76
    - a. Hypothesis one 79
    - b. Hypothesis two 80

Page

c. Hypothesis three 86
d. Summary of hypotheses 87
e. Experimental observations and discussion 88

III. EVALUATION OF LIQUID CHROMATOGRAPHIC DETERMINATION OF NITRATE 112

A. Review of Recent Methods for Determination of Nitrate 112

B. Experimental 117

1. Reagents 117
2. Preparation of strong anion-exchange columns 118
3. Flow-through electrodes 120
4. Liquid chromatograph 124
5. Experimental procedures 129

C. Results and Discussion 136

1. Evaluation of flow-through disk detector 136
2. Choice of detector potential 151
3. Evaluation of anion-exchange columns 158
4. Interference study 163
5. Effect of chloride loading of sample 167
6. Calibration curves and detection limit 183
7. Precision study 188
8. Analysis of unknown samples 195

IV. SUMMARY 206

V. SUGGESTIONS FOR FUTURE RESEARCH 209

VI. APPENDIX: ELECTROLYSIS AT CONTROLLED POTENTIAL 210

VII. BIBLIOGRAPHY 213

VIII. ACKNOWLEDGEMENTS 219

LIST OF TABLES

Page

Table II-1. Proposed diazotizing and coupling reagents for the colorimetric determination of nitrite 6

Table II-2. Nitrate concentration dependence in 0.10 M sulfuric acid of reduction current at rotating cadmium-disk surfaces produced by nitrate etching, anodization, and hydrogen peroxide etching 42

Table II-3. Dependence of nitrate reduction current on rotation speed of a copperized cadmium-disk electrode in pH 8 buffer 52

Table II-4. Dependence of oxygen reduction current on rotation speed of copperized cadmium-disk electrode in air saturated pH 8 buffer 67

Table II-5. Dependence of nitrate reduction current on rotation speed of monocrystalline cadmium-disk and copperized monocrystalline cadmium-disk electrodes in pH 8 buffer 91

Table III-1. Dependence of iodide oxidation current on rotation speed of a platinum-disk electrode at 0.70 V vs. SCE in 0.10 M sulfuric acid 145

Table III-2. Dependence of mass-transport limited current at working electrode of flow-through disk detector on volume flow rate of solution stream, V_f, and on distance, d, between disk and channel orifice 149

Table III-3. Data for pseudo-voltammograms of nitrate and oxygen reduction current at working electrode of copperized cadmium-disk detector in pH 8 buffer 157

Table III-4. Comparison of efficiencies of anion-exchange columns 160

Table III-5. Detection of 0.50 mM nitrate in the presence of potentially interfering ions 164

Page

Table III-6. Influence of chloride loading phenomenon on retention of nitrate by anion-exchange column packed with Dowex 1-X8 172

Table III-7. Response of liquid chromatograph to nitrate concentration with and without 0.10 M chloride 186

Table III-8. Precision study - summary of data 192

Table III-9. Analytical results 197

LIST OF FIGURES

Page

Figure II-1. Drawing of vertical cross section of disk electrodes 24

Figure II-2. Cadmium-disk surfaces produced by (A) nitrate etching, (B) anodization, and (C) hydrogen peroxide etching 41

Figure II-3. Nitrate concentration dependence in 0.10 M sulfuric acid of reduction current at rotating cadmium-disk surfaces produced by (□) nitrate etching, (O) anodization, and (◇) hydrogen peroxide etching 44

Figure II-4. Voltammograms of 0.10 mM nitrate as a function of rotation speed of a copperized cadmium-disk electrode in pH 8 buffer 50

Figure II-5. Dependence of nitrate reduction current on rotation speed of a copperized cadmium-disk electrode in pH 8 buffer 54

Figure II-6. Cyclic voltammetry of hydroxylamine at a rotating platinum-ring electrode in pH 8 buffer 61

Figure II-7. Voltammograms of air saturated pH 8 buffer as a function of rotation speed of a copperized cadmium-disk electrode 64

Figure II-8. Dependence of oxygen reduction current on rotation speed of a copperized cadmium-disk electrode in air saturated pH 8 buffer 66

Figure II-9. Identity of metal electrochemically etched in pH 8 buffer from copperized cadmium surface without potential control 71

Figure II-10. Scanning electron micrograph of copperized cadmium surface 78

Figure II-11. Model of double layer (A) at a cadmium surface and (B) at a copperized cadmium surface 83

Page

Figure II-12. Dependence of nitrate reduction current on rotation speed of monocrystalline cadmium-disk and copperized monocrystalline cadmium-disk electrodes in pH 8 buffer 90

Figure II-13. Voltammograms of nitrate reduction at a rotating polycrystalline cadmium-disk electrode in pH 8 buffer as a function of time dependent deposition of copper atoms on disk 97

Figure II-14. Voltammograms of nitrate reduction at a rotating monocrystalline cadmium-disk electrode $(10\bar{1}0)$ in pH 8 buffer as a function of time dependent deposition of copper atoms on disk 100

Figure II-15. Voltammogram of nitrate reduction in pH 8 buffer at a rotating copper-disk electrode 104

Figure II-16. Voltammogram of cadmium(II) in pH 8 buffer at a rotating copper-disk electrode 107

Figure II-17. Voltammograms of nitrate reduction current at a rotating copper-disk electrode in pH 8 buffer as a function of time dependent deposition of cadmium atoms on disk 109

Figure III-1. Drawing of vertical and horizontal cross section of flow-through disk detector 122

Figure III-2. Schematic diagram of liquid chromatograph 126

Figure III-3. Two dimensional drawing representing flow patterns near the working electrode within (A) a wall-jet detector and (B) a flow-through disk detector 140

Figure III-4. Dependence of iodide oxidation current on rotation speed of a platinum-disk electrode at 0.70 V vs. SCE in 0.10 M sulfuric acid 144

		Page
Figure III-5.	Dependence of mass-transport limited current at working electrode of flow-through disk detector on volume flow rate, V_f, of solution and on distance, d, between disk and channel orifice	148
Figure III-6.	Pseudo-voltammograms of nitrate reduction at working electrode of copperized cadmium-disk detector in pH 8 buffer	154
Figure III-7.	Pseudo-voltammogram of oxygen reduction at working electrode of copperized cadmium flow-through disk detector in pH 8 buffer	156
Figure III-8.	Comparison of chromatogram of Tender Quick Meat Cure sample to that of nitrate standard	170
Figure III-9.	Variations in nitrate and chloride chromatograms as a function of concentration of chloride in injected sample	174
Figure III-10.	Influence of chloride loading phenomenon on retention of nitrate by anion-exchange column packed with Dowex 1-X8	176
Figure III-11.	Response of liquid chromatograph to nitrate concentration with and without 0.10 M chloride	185
Figure III-12.	Chromatograms of 0.1 M potassium chloride (A) without added nitrate and (B) with 0.1 μM nitrate	190
Figure III-13.	Illustration of construction of base-line for nitrate peak not resolved from oxygen-related injection phenomenon	194
Figure III-14.	Chromatograms (A) of spiked spinach extract and (B) of spinach extract	200

I. INTRODUCTION

A chromatographic method for the determination of nitrate in aqueous samples is described in this thesis. Nitrate is separated from oxygen by anion-exchange chromatography and is detected at a copperized cadmium flow-through detector. The working range of the method is 1.0 µM - 1.0 mM, and the detection limit is 0.1 µM for samples containing large quantities of chloride.

The need to monitor the concentration of nitrate in the environment is great. Nitrate is intimately involved in the nitrogen cycle. Various micro-organisms assimilate nitrate nitrogen by reducing it to ammonia and incorporating the ammonia into the cell structure (1). Such organisms provide a pathway for introducing nitrate nitrogen into the nitrogen cycle as a nutrient for plants which are involved in the food chain. It is understandable, therefore, why there has been an increase in the world consumption of nitrogen fertilizers from 5.2 million tons in 1954 to 40 million in 1974 (2). The result of the use of these and other fertilizers is thought to be one of the primary reasons that there has been an average annual 3% increase in the world production of cereal grain, but at the expense, at least in part, of introducing large amounts of nitrate into the environment.

There are at least two ways reviewed by Davenport (3), that nitrate can have adverse effects in man. Methoglobinemia can result when excessive amounts of nitrate and/or nitrite are consumed (4, 5). Both anions can oxidize the iron(II) in hemoglobin and thereby prevent the transport of life supporting oxygen. In severe cases, death results from hypoxia. Nitrosamines, which are very potent carcinogens, can be formed by reaction of nitrous acid with secondary amines (7). The intestinal bacteria Escherichia coli (8, 9) reduces nitrate to nitrite providing a mechanism by which the presence of nitrate can result in the production of carcinogens. Therefore, the consumption of large quantities of nitrate should be avoided. The amount of nitrate allowed in potable water by the United States Public Health Service is 45 ppm (10). The benefit of analytical methods for accurately monitoring nitrate in the environment is, therefore, great.

Davenport and Johnson developed a chromatographic method for the simultaneous determination of nitrate and nitrite (11). These anions were separated in an anion-exchange column and detected amperometrically with a cadmium tubular detector. It has been found, however, that the sensitivity of the cadmium detector is not reproducible. This research was performed to find a reproducible detector. The rate of nitrate reduction in acidic media at the surface of a rotating cadmium-disk electrode was investigated as a function of the pretreatment of the electrode. It was found that the most reproducible cadmium electrode surface is one prepared by deposition of a thin layer of copper on the cadmium electrode. The copperized cadmium surface cannot be used in highly acidic media and is, therefore, sensitive to nitrate only. Three possible explanations of the electrocatalytic effect of copper on the reduction of nitrate are offered and are considered in light of the results of cyclic voltammetric investigations performed with rotating cadmium, copperized cadmium, and copper disk electrodes. The primary product of the reduction of nitrate on a copperized cadmium electrode at pH 8 under conditions of rapid mass transport was determined to be nitrite.

A copperized cadmium flow-through disk detector was developed and interfaced with a liquid chromatograph. The separation developed was based on anion exchange and was similar to that described by Davenport and Johnson (11). Experimental procedures were developed to determine nitrate in a variety of aqueous samples. When analysis was performed on a sample containing a large amount of chloride, it was found that the chloride favorably altered the interaction of the nitrate with the anion-exchange column resulting in increased analytical sensitivity. This chloride phenomenon was investigated and incorporated into the procedures used to analyze other samples. Preliminary investigations were made of the chemical oxidation of nitrite to nitrate for determination of nitrite in the presence of nitrate by a difference method.

II. THE ELECTROCATALYTIC REDUCTION OF NITRATE ON CADMIUM

A. Literature Review of the Reduction of Nitrate to Nitrite for Colorimetric Analysis

Analytical methods for the determination of nitrate that have been published recently will be reviewed in Section III.A. One procedure for determining nitrate that has been used extensively involves the reduction of nitrate to nitrite, which is then determined by the sensitive diazotization method proposed by Griess (1879) (12). The method of Griess is a colorimetric procedure involving the chemistry of diazonium salts. Organic diazonium salts are the characteristic product of the quantitative action of nitrous acid on primary aromatic amines. These salts are coupled to other aromatic compounds which contain strongly electron-releasing groups such as hydroxyl and amines or substituted amines, to form highly colored azo compounds (13). Griess originally determined nitrite by diazotizing sulfanilic acid and coupling the product to 1-naphthylamine to form 4(4-amino-1-naphthylazo)benzenesulfonic acid. Many other organic reagents have been proposed for the same purpose. A few of these are shown in Table II-1. More pertinent to this thesis is a review of the methods that have been proposed to reproducibly reduce nitrate to nitrite so that the above colorimetric procedure can be applied.

Table II-1. Proposed diazotizing and coupling reagents for the colorimetric determination of nitrite

Diazotizing Reagent	Coupling Reagent	Reference
sulfanilic acid	1-naphthol-7-sulfonic acid	14
sulfanilic acid	1-naphthylamine	15
sulfanilic acid	1-naphthol	16
sulfanilic acid	N-(1-naphthyl)ethylenediamine	17
sulfanilamide	N-(1-naphthyl)ethylenediamine	18
sulfathiazole	1-naphthol	19
8-aminoquinoline	8-aminoquinoline	20
1-naphthylamine	1-naphthylamine	21
4-aminophenyl(trimethyl)-ammonium ion	N,N-dimethyl-1-naphthylamine	22
4-aminoacetophenone	1,3-phenylenediamine	23
4-amino-benzenearsonic acid	N-(1-naphthyl)ethylenediamine	24

The earliest of the reduction methods employed powdered zinc metal which was mixed in the aqueous sample and later removed by filteration (25, 26). Chow and Johnstone further developed the method but reported a low reduction yield, 85-90%, which they suggested was due to competing reactions (27). A zinc reductor column was used in an automated method (28), but the efficiency of the column was reported to be low and varied significantly from day to day.

Hydrazine was proposed by Mullin and Riley for the homogeneous reduction of nitrate to nitrite (29). The reaction is catalyzed by copper(II) (30). The method was modified by Austin and Strickland, and required 24 hr at constant temperature (31).

In 1960, Potzl and Reiter suggested the use of cadmium in a reductor column to reduce the nitrate in sea water samples to nitrite (32). In 1965, Brewer and Riley observed a 5% loss of nitrite when a standard nitrite solution was passed through a column of cadmium fillings, but concluded that this loss was smaller for pure cadmium than for binary metal reductor columns that had been suggested previously (33). Follett and Ratcliff used spongy cadmium for the reductor column (16). Fudge and Truman reduced nitrate to nitrite by shaking the sample with a controlled amount of spongy cadmium (34). Morris and Riley investigated several metals for the reduction of nitrate to nitrite and reported that amalgamated cadmium could be used successfully in a reductor column (35). It was suggested that the cadmium metal be washed with nitric acid before amalgamation because this supposedly increases available surface area. Later workers, using the amalgamated cadmium reductor column, suggested using alkaline ammonium chloride (36) or EDTA (37) to complex cadmium(II) which would otherwise precipitate as cadmium hydroxide and shorten the life of the column.

Copperized cadmium reductor columns are prescribed for the official colorimetric method for the determination of nitrate by the Environmental protection Agency of the U.S. (38). The use of copperized cadmium in a reductor column has been investigated by Wood, Armstrong, and Richards, who report a yield of 99 ± 1% (39). A different mode of effecting the reduction of nitrate using copperized cadmium, suggested by Lambert and Dubois, involves adding a mixture of copper(II)sulfate, ammonium chloride, cadmium powder, and dibasic sodium phosphate to the sample (40). Three recent publications illustrate continued interest in the use of copperized cadmium for this reduction. Nydahl has investigated the optimum conditions for the reduction of nitrate on cadmium and concluded that copperization of cadmium is superior to amalgamation if faster rates of reduction are desirable and if somewhat larger errors can be tolerated

(41). Otsuki has suggested that a column be recopperized following extensive use with a solution containing 0.05 M copper(II) in 0.1 M EDTA adjusted to pH 7 (42). He observed that copper is deposited in a granular form; and postulated that insoluble compounds of cadmium(II) and other metal cations that foul the surface of the cadmium are removed by the formation of metal-EDTA complexes. Stainton has replaced the conventional reductor column filled with copperized cadmium, for use in automated methods, by a Teflon tube (1.0 m x 1/32 inch i.d.) threaded with a cadmium wire (1.0 m x 1 mm) the surface of which had been copperized (43).

Difficulties are encountered in applying all of the reduction methods mentioned above. Either the reduction process is slow, requiring lengthy reaction times, or the reducing agent reacts with nitrite resulting in the loss of the desired product. Therefore, it is necessary to carefully control the conditions for reduction. Lowe and Hamilton solved this problem by using the specificity of an enzyme reaction. They were able to reduce nitrate to nitrite in an automated method with nitrate reductase (44). Enzymatic methods, however, are not very practical for routine analysis because of the difficulty of handling the reagents.

Davenport and Johnson suggested a method for the determination of nitrate which avoids the problems associated with the prior reduction of nitrate to nitrite for colorimetric analysis (11). They interfaced the reactive cadmium surface, in the form of a potentiostated tubular electrode, with a flow system containing an anion-exchange column. The column provided a means of separating nitrate from nitrite. The current resulting from the reduction process at the tubular surface allowed for amperometric detection of nitrate and nitrite in the chromatographic effluent. Using this approach, they also avoided the somewhat cumbersome organic chemistry required by the colorimetric methods.

It seemed apparent from the fact that copperized cadmium is used so frequently in the colorimetric method that this surface might also be used for an amperometric method of determining nitrate. The rate of the reduction of nitrate on cadmium is in fact electrocatalyzed when the cadmium surface is copperized. In the next section I define and discuss electrocatalysis. The remainder of the thesis is devoted to observations of the electrocatalytic effect of the copper and to the development of an amperometric method for the determination of nitrate.

B. Electrocatalysis

Amperometric methods of analysis are based on the measurement of the current produced when the analyte is oxidized or reduced at an electrode surface. Such electrode processes can be specific for a single analyte or they may be selective for a group of analytes. However, some selective electrode porcesses exhibit characteristics of slow charge transfer and can only be used to develop a sensitive amperometric method of analysis if the rate of charge transfer can be increased. The study of those factors that can be changed to cause such an increase is called "electrocatalysis". It is beyond the scope of this thesis to review the many examples of electrocatalytic phenomena that have been reported in the literature. Several such reviews have been published (45, 46, 47). In this section I will consider the present understanding of electrocatalysis and cite a few examples from the literature as illustrations.

The development of an expression for the rate of charge transfer processes occurring at an electrode surface parallels that for the rate of a homogeneous chemical reaction. A heterogeneous rate constant, k, is defined in terms of the activation barrier of the reaction, $\Delta G_{\neq}$, as in Equation II-1.

$$k = A\exp(-\Delta G_{\neq}/RT) \qquad \text{(II-1)}$$

In Equation II-1:

A = preexponential constant,

R = universal gas constant,

T = absolute temperature.

The rate of the process is expressed as the product of this rate constant and the activities of all the chemical species that are involved in forming the activated complex of the reaction. As in homogeneous kinetics, this expression for the rate of the heterogeneous reaction is descriptive of only those steps in a reaction mechanism up to and including the rate limiting step. The rate of a heterogeneous process is related to the electrode current by Faraday's law and is, therefore, more conveniently monitored than are the rates of homogeneous reactions. The relationship between electrode current and the rate constant is given by Equation II-2 (48).

$$I = nFAkC_{x=0} \tag{II-2}$$

In Equation II-2:

I = electrode current,

n = number of electrons transfer in the reaction up to the rate limiting step,

A = area of electrode,

$C_{x=0}$ = concentration of reacting specie at the electrode surface.

It will be instructive to consider in some detail the activation barrier metnioned above as it relates to electrocatalysis. Equation II-3 is an expression for the activation barrier for a reduction process at an electrode where the reactants are a solution ion and the electrons in the electrode surface.

$$\Delta G_{\neq} = \Delta G^{\circ}_{\neq} + \alpha_c F(E_M - E_R) + zFE_R \qquad \text{(II-3)}$$

In Equation II-3:

$\Delta G^{\circ}_{\neq}$ = standard electrochemical free energy of activation;

α_c = transfer coefficient for the activation barrier;

E_M = potential of the electrode material measured relative to the potential of the solution, E_S;

E_R = potential of the reaction plane parallel and a distance, x_R, from the electrode surface where charge transfer occurs, also measured relative to E_S;

z = charge on the reactant.

Complete derivations of Equation II-3 and of the analogous equation for the oxidation process may be found in Reference 48. There are three terms in the expression for $\Delta G_{\neq}$, each of which deserves further attention here.

The first term, $\Delta G^{\circ}_{\neq}$, is the measure of the activation barrier that is involved if the reaction occurs under standard conditions. The word "standard" implies that the reaction occurs at a temperature and pressure of 25 °C and 1 atm, respectively; that the activities of all reacting species are equal to one; and that the activation barrier is not modified by the application of an interfacial potential difference, i.e., E_M and E_R are zero such that $\Delta G_{\neq}$ is equal to $\Delta G^{\circ}_{\neq}$. The standard free energy of activation, $\Delta G^{\circ}_{\neq}$, is expected to be different for different reaction mechanisms. Therefore, any change in reaction conditions that alters the reaction mechanism to make $\Delta G^\circ_{\neq}$ smaller will electrocatalyze the reaction, i.e., cause the reaction rate to increase. There are many examples in the literature that illustrate this kind of electrocatalysis. A large number of them involve chemisorbed species at the electrode surface that are postulated as providing an electron transfer bridge for the charge transfer reactions. One example was published by Tur'yan and Ruvinskii (49), who found that adsorbed thiourea at a mercury electrode is responsible for a prewave in the polarogram obtained for the reduction of nickel(II). They concluded that the chemisorbed thiourea molecule displaces one of the ligand water molecules of the nickel(II) ion, providing an alternate mechanism for the reduction. There are also examples in the literature where $\Delta G^\circ_{\neq}$ is thought to be smaller, not by virtue of a change in reaction mechanism, but because a chemisorbed reactant or intermediate interacts more strongly with one electrode material than with another. A good example of this kind of electrocatalysis involves the reduction of oxygen on noble metals. The reduction is thought to proceed through an intermediate that involves chemisorbed oxygen. Gold has no unpaired d electrons to participate in the formation of a metal-oxygen bond and has a charge transfer rate 10^8 times smaller than that for other noble metals which do have unpaired d electrons (45, 50). The activation barrier for the reduction of oxygen on gold is higher than on the other metals.

The second term in Equation II-3 comes about because the energy states of the reactants and, to a lesser extent, of the activated complex are dependent on the magnitude of an electrical potential at the electrode surface. The transfer coefficient, α_c, may be considered to be the fractional extent to which the energy state of the activated complex of the reaction is affected by changes of E_M and, like $\Delta G^\circ_{\neq}$, is dependent on the reaction mechanism. Therefore, changes in reaction conditions that alter the reaction mechanism will also effect the magnitude of the second term, but probably to a much smaller extent than such changes effect the first term as discussed in the previous paragraph.

A more important variable in the second term of Equation II-3 is the electrode potential, E_M, which is the single factor that distinguishes reactions at an electrode surface from homogeneous reactions. The ease with which E_M can be varied with external circuitry sometimes makes it possible to increase the rate of charge transfer to a very large extent by decreasing the overall magnitude of the activation barrier. If this change is large enough, the rate of the reaction becomes limited by the rate at which the analyte can be brought to the surface, i.e., by the rate of mass transport. When this is the case, an amperometric method of analysis can be developed without further efforts to improve the rate of charge transfer, i.e., to electrocatalyze the reaction of interest. These efforts are only needed when the magnitude of $\Delta G^\circ_{\neq}$ is large relative to the free energy equivalent of that potential which can be applied to the electrode surface without the onset of other heterogeneous reactions. Examples of such interfering reactions might include the electrolysis of solvent or other solution constituents, or the dissolution of the electrode material.

Sometimes, interfering reactions can be avoided by changing the electrode material and, in this simple way, the electrocatalytic benefit of the dependence of $\Delta G_{\neq}$ on E_M can be maximized. For example, the reduction of nitrate has been observed at several metals, but with very slow rates of charge transfer (51, 52, 53). The most negative potential that can be applied to a metal when used in a protic solvent is limited by the activation overvoltage of hydrogen on that metal. Davenport and Johnson (11) investigated cadmium as a possible electrode material for the reduction of nitrate because of its large activation overvoltage for hydrogen evolution (54) and found that potentials sufficiently negative to increase the rate of nitrate reduction could be applied to cadmium without excessive hydrogen evolution. They were able to develop a sensitive amperometric method for the determination of nitrate based on this electrocatalyzed reduction.

The third term in Equation II-3 represents the electrostatic contribution to the activation barrier involved in the heterogeneous reaction. The free energy equivalent of this term is directly proportional to the potential gradient that a reacting ion must traverse as it approaches the reaction plane at a distance x_R from the surface. That potential gradient is a function not only of the potential difference between the electrode surface and the bulk of the solution but also of the structure of the electrode-electrolyte interface, called the double layer. A comprehensive model of the structure of the double layer was given by Bockris, Devanathan, and Muller in 1963 (55). Their model will be considered in more detail in Section II.D.4. Here it is important to note that in the double layer there is a charge density gradient, which effects the potential at some distance x from the surface, due to ions and cations present in the double layer but not chemisorbed to the electrode surface. These electroinactive ions are said to be specifically adsorbed in the double layer creating an electrostatic environment at or near the reaction plane which attracts or repels the reacting ion. For example, if the charge density at the reaction plane, q_R, is positive, an anion will come to the reaction plane more easily and the overall activation barrier will be smaller. Conversely, the activation barrier is larger if the charge at the reaction plane and that of the analyte ion have the same sign.

The experimental consequence of the dependence of $\Delta G_{\neq}$ on this electrostatic term is that the logarithm of the rate constant, or the electrode current, varies linearly with the charge density of the double layer at a constant electrode potential. The slope of such a linear relationship can be predicted from electrostatic theory and compared to experimental slopes, providing the charge densities can be measured or represented by some other measurable parameter. Good agreement between the theoretical and experimental slopes is interpreted to mean that the change in the rate of charge transfer in the presence of different electroinactive ions is indeed a function of the decrease in $\Delta G_{\neq}$ through the electrostatic term.

Work performed in the laboratory of Guidelli and co-workers provides strong evidence that the magnitude of the electrostatic term can be large enough to account for observed changes in reaction rate (56). They investigated the electrostatic effect of specifically adsorbed halides, pseudohalides, and the monovalent thallium cation on the electroreduction of tetrathionate ion at a mercury electrode (57, 58). Their predicted slopes for plots of the logarithm of the rate constant vs. charge density agreed satisfactorily with experimental slopes. In later publications, they reported similar success in interpreting the electrostatic electrocatalysis of specifically adsorbed halides and pseudohalides on the electroreduction of perbromate ion at a mercury electrode (59).

The identity of the electrode material may enter into the magnitude of the electrostatic term by virtue of the potential of zero charge, E_{zc}, which is different for different materials. The E_{zc} is that potential where, in the absence of any charge transfer processes, the charging current changes from positive to negative. This dependence of the point of zero charge on the identity of the electrode material is evidence that the double layer structure of electroinactive ions depends on the interaction of those ions with the metal surface. Therefore, the charge density at the reaction plane may be increased, and the overall magnitude of $\Delta G_{\neq}$ decreased, by selecting the right material for the electrode.

The foregoing discussion, even though it is greatly simplified, shows how complex electrocatalytic phenomena can be. It can, therefore, be very difficult to determine how a change in a reaction condition for a particular electrode process brings about higher rates of charge transfer. This has been particularly true for the electrocatalytic phenomenon that is examined in this thesis, i.e., the effect that copperizing a cadmium surface has on the rate of the reduction of nitrate at that surface. Therefore, no attempt is made to rigorously explain this phenomenon. Instead, several observations concerning the reduction of nitrate on cadmium and on copperized cadmium are recorded in Section II.D.4. Also, several speculative ideas concerning those observations are offered for future experimental verification.

C. Experimental

1. Reagents

All chemicals were Analytical Reagent Grade and were obtained, except where noted, from Fisher Scientific Co., Fair Lawn, NJ. Aqueous solutions were prepared with water which had been distilled and demineralized. Supporting electrolytes were 0.1 M sulfuric acid and a pH 8 buffer composed of 0.1 M trishydroxymethylaminomethane (THAM) and 0.056 M hydrochloric acid.

Potassium nitrate and potassium nitrite were dried at 90 °C for four hours and stored in a desiccator over Drierite from Midland Scientific, Inc., Omaha, NE. Stock soltuions of potassium nitrate and potassium nitrite were prepared by dissolving the dried salts in supporting electrolyte.

Stock solutions of copper(II) were prepared by dissolving copper sulfate pentahydrate in water. Stock solutions of cadmium(II) were prepared by dissolving cadmium wire from Research Inorganic/Organic Chemicals, Belleville, NJ, in a minimum volume of boiling perchloric acid dihydrate from G. Frederick Smith Chemical Co., Columbus, OH. The dissolved cadmium was then diluted with appropriate volumes of water.

Test solutions were prepared by standard addition of the stock solutions to approximately 300 mL of electrolyte in the voltammetric cell described in Reference 3. The oxygen content of most test solutions was diminished to a very low level by bubbling prepurified nitrogen through the solutions. A blanket of nitrogen was maintained over the test solutions during experimentation. Oxygen was not removed from only those test solutions in which the reduction of oxygen was to be observed.

All volumes were measured with standard laboratory glassware. The masses of dry reagents were determined with an Ainsworth Type 28 N Analytical Balance or, when less accuracy was required, with an Ainsworth Digimetric Top-loading Balance. Both balances were from Wm. Ainsworth and Sons, Inc., Denver, CO.

2. Electronic circuitry and associated apparatus

Voltammetric studies were made with disk electrodes rotated with a Model PIR Rotator from Pine Instrument Co., Grove City, PA. The potential of the working electrode was controlled relative to a saturated calomel electrode, Corning Scientific Instruments, Medfield, MA, with a Model RDE3 Potentiostat from Pine Instrument Co. Current and voltage measurements were made with a Fairchild Model 7050 Multimeter, Sunnyvale, CA. Voltammograms were recorded with a Model 7035B X-Y Recorder from Hewlett Packard, San Diego, CA, or with a Plotamatic Model 815 X-Y Recorder from Bolt, Beranek and Newman, Inc., Santa Anna, CA.

3. Rotating disk and ring-disk electrodes

Several rotating disk electrodes were used in this research. These were made by screwing different working electrode tips onto the end of a single shaft. The shaft, designated by the letter A in Figure II-1, was made of stainless steel in the Chemistry Shop at Iowa State University. One end was machined to fit the rotator described in the previous sections. The other end was threaded internally with 1/4 inch x 28 threads so that the different tips with matched external threads could be easily attached to the shaft. The diameter of the shaft at the end where the working electrode tips attached was 7/16 inch.

Figure II-1. Drawing of vertical cross section of disk electrodes

A Electrode shaft

B Disk supports

C Polycrystalline cadmium disk

D Monocrystalline cadmium disk

E Copper disk

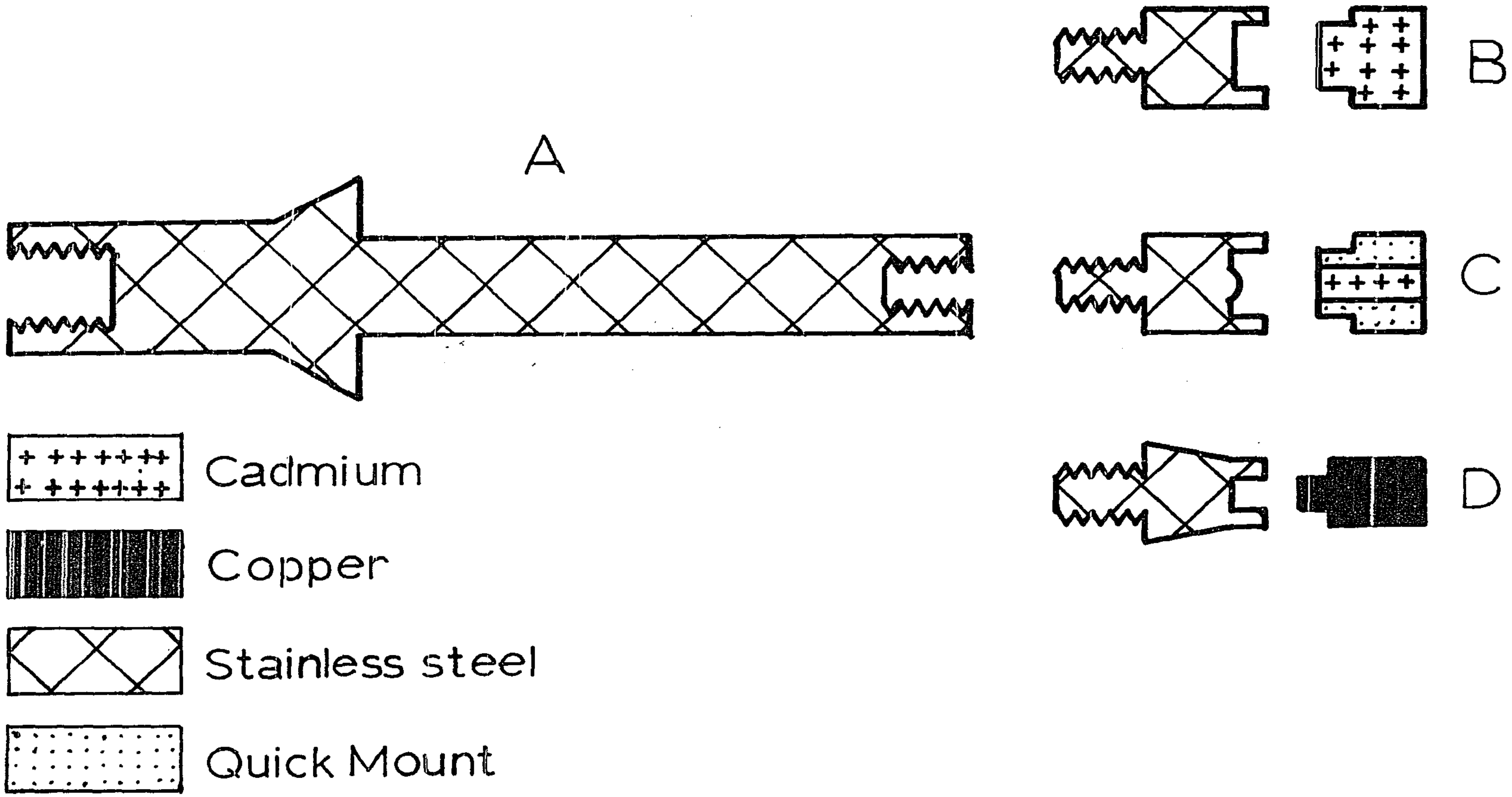
A
B
C
D
Cadmium
Copper
Stainless steel
Quick Mount

Five tips were constructed in the Chemistry Shop. The polycrystalline cadmium disk electrode, referred to frequently in later sections of this thesis as the "cadmium disk electrode", was made from a piece of polycrystalline cadmium (B). The cadmium specimen was prepared as described in Reference 3. It was machined to the shape of a short cylinder, about 1/4 inch long and with a diameter of 7/16 inch, except that one end was further machined so that it could be pressed into the recess of a stainless steel support as shown in Figure II-1. When assembled, Teflon tape was tightly wrapped around the electrode covering the cylindrical stainless steel and cadmium surfaces. The wrapping prevented solution contact with the electrode except at the disk end surface of the assembly. Each of the electrodes described below was similarly wrapped with Teflon tape. Photographs of the polycrystalline cadmium disk were taken by Mr. Harlan Baker of the Department of Metallurgy, Iowa State University.

Three monocrystalline cadmium tips, one of which (C) is shown in Figure II-1, were prepared by mounting three single crystals on three stainless steel supports. As obtained from Aremco Products, Inc., New York, the single crystals were cylindrical in shape about 1 inch long with a 1/4 inch diameter. A different crystal face was oriented perpendicular to the cylindrical axis of each of the crystals. These faces corresponded to the (0001), $(10\bar{1}0)$, and the $(11\bar{2}0)$ crystal planes of cadmium. Press fitting and/or machining the single crystals of cadmium, which is relatively soft, would probably have destroyed the integrity of the single crystals. Therefore, the crystals were mounted onto the electrode supports by a rather complicated procedure. They were first encapsulated in Quick Mount® from Fulton Metallurgical Products, Inc., Pittsburg, PA, which comes in the form of a course powder and a solvent. A mixture of the powder and solvent hardens into an acrylic plastic. The crystals were carefully balanced in cylindrical molds with 1 inch diameters and 2 inch lengths so that the cylindrical axis of the crystals closely approximated the cylindrical axis of the molds. The soft Quick Mount mixture was then poured into the molds around the crystals. The molds were filled to a level well above the top of the crystals so that clamps used to hold the encapsulated crystals in later machining steps would apply pressure to only the Quick Mount. The molds were removed and the Quick Mount on each tip was lathed down to a 7/16 inch diameter. Slabs 1/4 inch thick were cut from the encapsulated crystals as follows. One end of each encapsulated crystal was removed by cutting through the crystal perpendicular to the cylindrical axis with one of two identical Model 650 Low Speed Diamond Wheel Saws from South Bay Technology, Inc., El Monte, CA. Mr. Harlan Baker cut one of the crystals in his laboratory and I cut the other two crystals in a laboratory of the Department of Physics, Iowa State University. The cylindrical surface of the exposed ends of each of the crystals was then lathed to fit the corresponding stainless steel support. The diamond saws were again used to make a second cut parallel to the first such that one of the three crystal faces identified above was exposed on each of the crystal slabs. Epoxy was used to glue the crystal slabs to the stainless steel supports. It can be noted in Figure II-1, that small protrusions were left at the center of the recesses in the stainless steel supports to insure that there would be electrical contact between stainless steel and cadmium. The assemblies of these tips and the electrode shaft are referred to as the monocrystalline cadmium disk electrodes.

When the rotating monocrystalline cadmium disk electrodes with (0001) and $(10\bar{1}0)$ faces were used in experiments described in Section II.D.4., interpretable results were obtained. It was concluded that the preparation of these two electrodes was satisfactory. The third electrode with the $(11\bar{2}0)$ face exposed, however, was not successfully used in the same fashion. Successive background voltammograms obtained with this electrode varied in an erratic fashion, as did background currents measured continuously at constant potential as a function of time. It is possible that the $(11\bar{2}0)$ face of cadmium is very unstable, but it seems more likely that the preparation of this electrode tip was unsuccessful and that there were capillary leaks allowing electrical contact between stainless steel and solution. It was not possible to use this tip.

Copperized cadmium disk electrodes, both polycrystalline and monocrystalline, were prepared by copperizing the cadmium disk electrodes. This was accomplished by swirling the freshly polished cadmium disks in 0.08 M copper sulfate for about 10 sec.

A cylindrically machined piece of polycrystalline copper was mounted onto the stainless steel portion of the fifth tip (D) in the same fashion as the polycrystalline cadmium was mounted onto the first tip. The copper was obtained from Research Inorganic/Organic Chemicals. The diameter of the copper cylinder was only 11/32 inch, so the stainless steel tip was tapered, as shown in Figure II-1, to make it possible to evenly wrap the tip with the Teflon tape.

A platinum-ring glassy carbon-disk electrode, described in Reference 3, was also used in this research. It was converted to a platinum-ring cadmium-disk electrode by depositing cadmium onto the glassy carbon disk while holding the potential of the disk at -1.0 V vs. SCE. The deposition solution was composed of 3 mM cadmium perchlorate and pH 8 buffer. The deposition current was observed to be approximately 1.3 mA and was constant for the duration of the deposition which lasted about 5 min. The square root of the rotation speed used was 6.47 rad$^{1/2}$ sec$^{-1/2}$. The platinum-ring cadmium-disk electrode was converted to a platinum-ring copperized cadmium-disk electrode in two different ways. Copper was deposited on top of the cadmium layer on the glassy carbon-disk electrode under conditions identical to those used for the cadmium deposition. The deposition solution was 3 mM copper sulfate and the copper deposition current observed was 0.65 mA. Alternately, copperization was accomplished without potentiostatic control by dipping the surface into a 0.015 M copper sulfate solution for 10 sec.

Electrode surfaces were polished according to standard metallurgical polishing procedures. The final step in the polishing procedure was accomplished with 1 μ diamond paste. This last step was repeated at the beginning of each work day, and as required to renew the surface between experiments.

4. Scanning electron microscope

Micrographs, recorded on Polaroid film, of a copperized cadmium surface were obtained with a Model JSM-U3 Scanning Electron Microscope from JEOL, Inc., Medford, MA. The microscope is housed in the Energy Research Institute of Iowa State University, and was operated by Mr. Jerry Amenson.

D. Results and Discussion

1. Comparison of relative, heterogeneous reaction rates in acid

It was stated in Chapter I of this thesis that the activity of a cadmium surface toward nitrate reduction is not reproducible, i.e., the rate of nitrate reduction on cadmium varies greatly. Various pretreatments of cadmium electrode surfaces that have been found effective for improving the rate of nitrate reduction on cadmium in acid are described and discussed in Part b of this section. Methods of comparing electrochemical reaction rates are considered in Part a.

a. Theoretical basis The rate of an electrode process is indicated by the magnitude of electrode current, I, which can be easily measured. Electrode current can be limited by either the rate at which the electroactive species is transported to the electrode surface (mass-transport limitation) or by the rate of the transfer of electrons from the electrode to the electroactive species (kinetic limitation). Equation II-4, called the heterogeneous rate equation, gives the dependence of electrode current on both mass transport and kinetics.

$$I = \frac{nFAkC^b}{1 + (\delta/D)k} \qquad \text{(II-4)}$$

In Equation II-4:

C^b = the bulk concentration of the electroactive species,

δ = diffusion layer thickness,

D = diffusion coefficient.

The other parameters in Equation II-4 are defined in Equation II-2. The rate of charge transfer is accounted for in Equation II-4 by the value of the heterogeneous rate constant, k. The rate of mass transport is accounted for in Equation II-4 by the value of the diffusion layer thickness, δ. As will be seen from the discussion below, Equation II-4 may be simplified if either the rate of mass transport or the rate of electron transfer limits the electrode current. It has been assumed in writing Equation II-4 that the electrode reaction described thereby is occurring in only one direction, i.e., the back reaction has been ignored. A more general form of the heterogeneous rate equation which accounts for the rate of the back reaction is found in Reference 48. The relation of k to electrode potential has been discussed in Section II.B.

It is frequently quite easy to compare rates of reaction at an electrode surface by comparing values of k. It is possible to obtain values for k for an electrochemical reaction from measurements of current as a function of electrode potential in the vicinity of the corresponding half-wave potential. Unfortunately, the half-wave potential for the reduction of nitrate on cadmium is more positive than that potential at which oxidation of the cadmium surface, i.e., dissolution of cadmium metal occurs. Therefore, electrode currents measured in the appropriate potential region would be the sum of two processes; nitrate reduction and cadmium oxidation. One might attempt to make current measurements in the presence and absence of nitrate and take the difference to obtain the contribution to the total current-potential response from the nitrate reduction process. This is impractical because the magnitude of the oxidation current would be much larger than that of the reduction current; and the difference measurement would, therefore, be inaccurate. Also, this approach can not be used to determine the rate constant for the reduction of nitrate on cadmium because, as will be seen from the discussion in Part b of this section, this process is evidently a function of whether or not the cadmium atoms have been removed from the electrode surface by the oxidation process described above.

Another approach to the problem of measuring small rate constants involves the use of an electrode design for which all solution, geometric, and hydrodynamic parameters in Equation II-4 can either be measured or predicted with reasonable accuracy. A rotating disk electrode is of such a design. The diffusion layer thickness δ is expressed mathematically for a rotating disk electrode as in Equation II-5 assuming that the surface of the electrode is uniformly accessible, i.e., 100% of the surface area is available to support the electrochemical process.

$$\delta = 1.62D^{1/3}\nu^{1/6}\omega^{-1/2} \qquad \text{(II-5)}$$

In Equation II-5:

ν = kinematic viscosity,

ω = rotation speed.

For a fully active electrode surface, the concentration of the reacting species is constant across the electrode surface and diffusion of these specie occurs in a direction perpendicular to the electrode surface. A value for k may be obtained by varying C^b and measuring I at constant rotation speed and disk potential, i.e., by performing a concentration study. The slope, m, of a plot of I vs. C^b is given by Equation II-6, which when rearranged to Equation II-7, gives an expression for k.

$$m = \frac{nFAk}{1 + (\delta/D)k} \qquad \text{(II-6)}$$

$$k = \frac{m}{nFA - (\delta/D)m} \qquad \text{(II-7)}$$

It should be pointed out that the equations for I and m can be simplified if one chooses to take the current measurements at high values of rotation speed, ω, because Equation II-5 predicts δ will then be small. For small δ, the second term in the denominator of Equation II-4 will be negligible. The results of this condition are shown in Equations II-8 through II-10.

$$I = nFAkC^b \tag{II-8}$$

$$m = nFAk \tag{II-9}$$

$$k = \frac{m}{nFA} \tag{II-10}$$

It may not be true, however, that the surface is uniformly accessible; for example, when the surface is partially blocked by the accumulation of solution impurities or adsorbed reaction products. It may also be that only a portion of the electrode surface was originally active. For whatever reason it may exist, the condition of non-uniform accessibility has at least two important consequences. First, the actual surface area, A', on which the electrochemical reaction can occur may be substantially less than the geometric area, A, and the electrode current will be significantly smaller. Second, concentration gradients are no longer uniform across the surface of the electrode and non-linear diffusion of electroactive species will occur to the edges of those discrete areas where the reaction is occurring. Therefore, the total electrode current would be increased to a value above that predicted on the basis of the magnitude of A'. Equation II-4 might be rewritten as shown in Equation II-11, but this inequality is not experimentally useful.

$$I > \frac{nFA'kC^b}{1 + (\delta/D)k} \tag{II-11}$$

A more quantitative equation for the current at an electrode which is not uniformly accessible is impossible to derive unless the exact geometry of the discrete, active areas of the surface is known. However, this does not mean that relative reaction rates can not be compared.

Landsberg, et al. have investigated the effect of non-uniform accessibility on the current at an electrode which they had partially blocked with photoresist, such that the active area of the electrode was the sum of N circular areas of constant radius distributed in a regular hexagonal array across the surface (60, 61, 62). They derived and experimentally verified the approximate relationship shown in Equation II-12.

$$I \cong \frac{nFAD(C^b - C_{x=0})}{\delta + A_n \tanh \frac{k_n \delta \sqrt{A}}{\sqrt{N\pi}}} \tag{II-12}$$

In Equation II-12:

A_n = Bessel function,

k_n = zero value of the first order Bessel function.

If Equation II-12 is rearranged to obtain an expression for $C_{x=0}$, which can be substituted into Equation II-2, an expression for I is obtained which is not dependent on $C_{x=0}$. This result is shown in Equation II-13 which looks very much like Equation II-4, except that δ has been increased by a term which is dependent on the amount of the surface which is electroactive.

$$I = \frac{nFAkC^b}{1 + (k/D)(\delta + |\Sigma A_n \tanh \frac{k_n \delta \sqrt{A}}{\sqrt{N\pi}}|)} \qquad \text{(II-13)}$$

Taking this case as a representative example, it can be said that the condition of non-uniform accessibility can be mathematically described at a partially activated disk electrode by increasing δ by an appropriate function of the activated area, f(A'), as expressed by Equation II-14.

$$I = \frac{nFAkC^b}{1 + (k/D)(\delta + f(A'))} \qquad \text{(II-14)}$$

This function is expected to depend on δ, but if ω is held constant, and if A' is not time dependent, f(A') will be a constant. Therefore, the slope of a plot of the current at a partially active disk electrode vs. C^b, given in Equation II-15, should still reflect reaction rate.

$$m = \frac{nFAk}{1 + (k/D)(\delta + f(A'))} \qquad \text{(II-15)}$$

It is impossible at low values of ω to extract a value for k from the slope unless f(A') is known. By imposing the condition that ω be large so that δ, and probably f(A'), are small, Equation II-15 can be simplified to Equation II-3 and values for k obtained.

More important than the mathematical analysis in this research, however, was the investigation of possible ways in which to increase the active area of the electrode. This is particularly true when the information gained may be used to increase the sensitivity of a flow-through electrode design, for which very small values of δ can not so easily be obtained. The flow-through disk electrode described in Section II.B.3 is intended to be used at fairly low flow rates (1-5 mL min^{-1}) and δ for that electrode will be large. Therefore, the relative rates of the reduction of nitrate on cadmium were determined with the rotating cadmium-disk electrode at low values of ω as a function of electrode pretreatment. The composite effect on electrode current of an unchanging rate constant and a variable activated area was investigated. The results of this investigation are given in Part b of this section.

b. Experimental results Davenport reported that the reduction of nitrate and nitrite occurs more reversibly on a rotating cadmium-disk electrode surface which is potentiostated at 0.0 V for 90 sec (3). This anodization removes cadmium atoms such that the polycrystalline structure of the electrode is exposed. It was suggested by Davenport that the crystal planes exposed are active toward nitrate reduction and that the active area of the electrode corresponds directly to the extent of exposure of these crystal planes. An equation relating current to activated area was derived, but the derivation did not take into account the consequences of non-uniform accessibility. Davenport used this pretreatment daily to increase the sensitivity of his cadmium tubular detector.

I observed that the polycrystalline structure of a cadmium surface is exposed to a greater extent when the electrode is dipped, without potential control, into a solution saturated with sodium nitrate containing nitric acid than when the electrode is anodized according to Davenport's anodization pretreatment. In Part a of this section it was concluded that electrode current increases with increasing active area and that the slope of a plot of I vs. C^b is highest for the most active surface. It was, therefore, possible to qualitatively test Davenport's suggestion that the magnitude of the area of a cadmium electrode active toward nitrate reduction is related to the degree of exposure of the polycrystalline structure of the electrode. This was accomplished by pretreating the mechanically polished surface of the cadmium-disk electrode in three different ways. (1) The electrode was dipped for about 2 min into a saturated sodium nitrate solution which contained 2 mL concentrated nitric acid. (2) The electrode was anodized according to Davenport's procedure. (3) The electrode was dipped for about 2 min into 30% hydrogen peroxide.

Photographs of the disk surface were taken after each treatment, and then a concentration study was performed. The photographs are shown in Figure II-2.

As may be observed by comparing the first two photographs in Figure II-2, the polycrystalline structure of the cadmium disk was exposed to a greater degree when the surface was etched in the acidic nitrate solution than when the surface was anodized. None of the polycrystalline structure of the cadmium disk is observable in the photograph of the surface etched with hydrogen peroxide. The currents obtained with each of these surfaces as a function of bulk concentration of nitrate is shown in Table II-2 and plotted in Figure II-3. The slope of the plot for the surface etched in the acidic nitrated solution is by far the largest. The slope of the plot for the surface etched with hydrogen peroxide is virtually zero, indicating that there is almost no active area on this surface. The slope of the plot for the anodized surface is intermediate between the other two slopes. It is concluded that the activation of cadmium toward nitrate reduction by nitrate etching, and to a lesser extent by anodization, is the result of the selective removal of cadmium atoms such that active crystal planes are exposed.

The nitrate etching procedure was not applied to the activation of flow-through amperometric detector, because it does not activate the electrode to the extent that the

Figure II-2. Cadmium-disk surfaces produced by (A) nitrate etching, (B) anodization, and (C) hydrogen peroxide etching

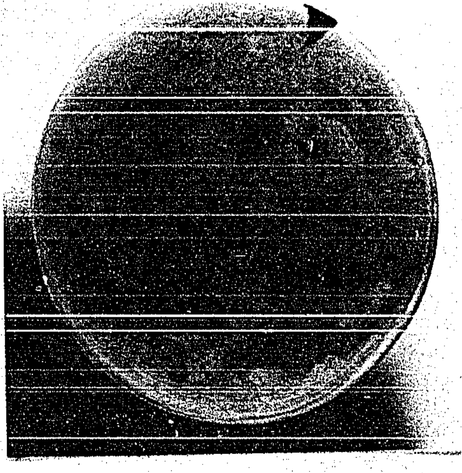

NO_3^- etched

Anodized

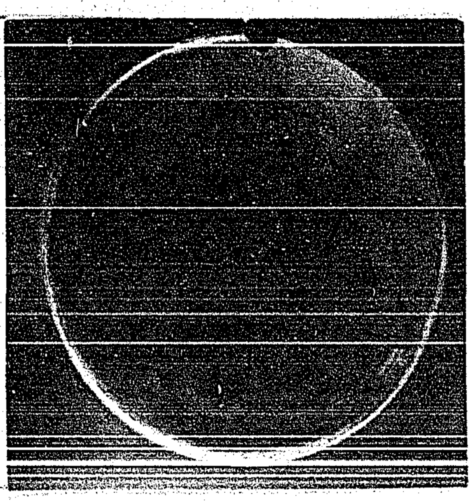

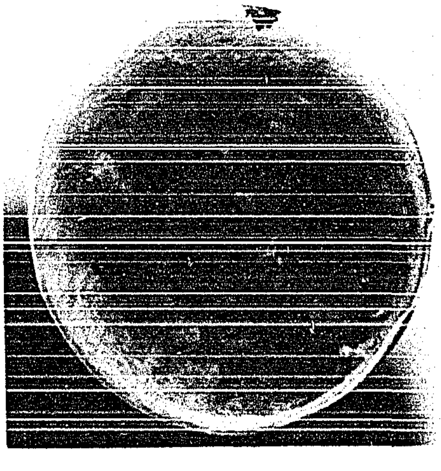

H_2O_2 etched

Table II-2. Nitrate concentration dependence in 0.10 M sulfuric acid of reduction current at rotating cadmium-disk surfaces produced by nitrate etching, anodization, and hydrogen peroxide etching[a]

Nitrate Concentration (mM)	Nitrate reduction current (μA)		
	Nitrate etched surface	Anodized surface	Hydrogen peroxide etched surface
0.00	66	75	168
0.10	430	224	208
0.20	765	375	256
0.30	1120	515	306
0.40	1470	661	348
0.49	1780	792	402
0.59	2050	930	456
0.69	2370	1060	514
0.78	2650	1210	580
0.88	2940	1340	660
0.98	3210	1490	756

[a] Data shown graphically in Figure II-3.

Figure II-3. Nitrate concentration dependence in 0.10 M sulfuric acid of reduction current at rotating cadmium-disk surfaces produced by (□) nitrate etching, (O) anodization, and (◇) hydrogen peroxide etching

Square root of rotation speed = 16.2 $\mathrm{rad}^{1/2}\ \mathrm{sec}^{-1/2}$

Electrode area = 0.95 cm^2

Disk potential = -0.85 V vs. SCE

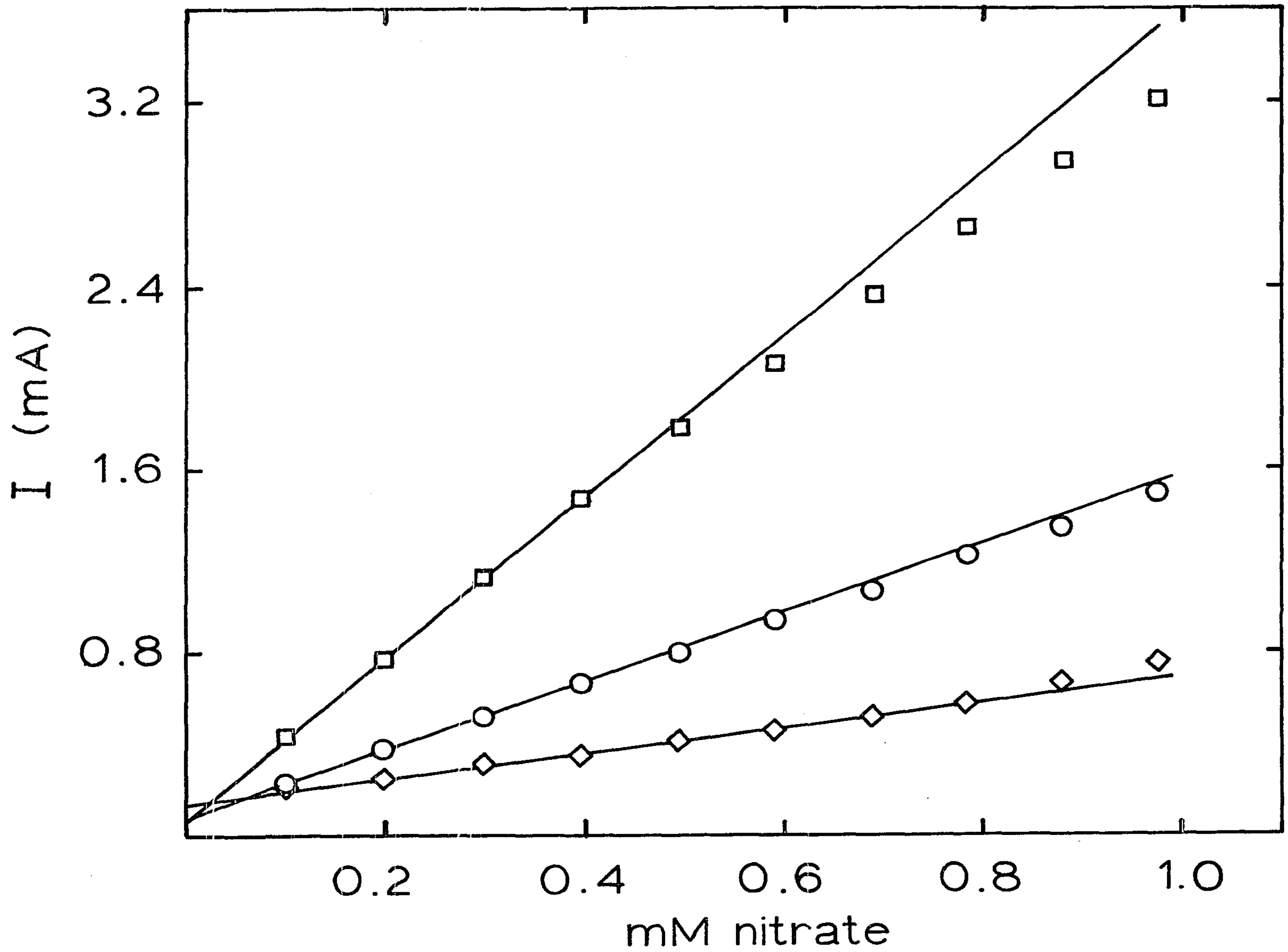
I (mA)
3.2
2.4
1.6
0.8
0.2
0.4
0.6
0.8
1.0
mM nitrate

reduction of nitrate occurs at a mass-transport limit. The theoretical mass-transport limited value for the nitrate reduction current can be calculated from Equation II-17, given in the next section (Section II.D.2). For the highest nitrate concentration used in the studies shown in Figure II-3 this theoretical value is 8.6 mA for a six-electron reduction. The best experimental value obtained on the most active surface was only 3.2 mA. Another cadmium electrode pretreatment, copperization, suggested by the literature is superior to the nitrate etching procedure in this respect. This pretreatment is discussed in detail in the remainder of Chapter II of this thesis.

2. Electrochemical investigations of reduction of nitrate and oxygen on copperized cadmium

On the basis of Nydahl's work with copperized cadmium, which was mentioned in Section II.A, it was postulated that higher rates of nitrate reduction might be observed on a copperized cadmium-electrode surface. In this section results are described of (1) electrochemical investigations of the rate of the nitrate reduction on copperized cadmium, (2) the identity of the product of that process, and (3) the reduction of oxygen on the surface.

a. Rate of reduction of nitrate

Information about the rate of the reduction of nitrate on copperized cadmium was obtained from cyclic voltammetry at a rotating copperized cadmium-disk electrode. In cyclic voltammetry the potential of the working electrode surface is scanned between two limits and the current due to electrochemical processes at the surface is measured. Current-voltage curves (voltammograms) are recorded on a X-Y recorder as a function of the bulk concentration of the electroactive species, of rotation speed, or of scan rate. The shape of the curves obtained can give qualitative information about the magnitude of the rate of charge transfer involved in the electrochemical processes. The current for a process with a very large heterogeneous rate constant changes very rapidly as a function of potential in the vicinity of the half-wave potential for that process. Such electrochemical processes are said to be "reversible". For some reversible processes the rapid change in the current with changing potential is followed by a plateau in the current. The rate of any electrochemical process, occurring at a potential corresponding to a point on a current plateau, is said to be "mass-transport limited".

A current plateau is not always exhibited for processes with large heterogeneous rate constants, however, because of background or interfering processes. Whether or not a process is mass-transport limited in such cases can be tested quantitatively by again applying Equation II-4. If k is large, $(\delta/D)k$ is also large such that $(\delta/D)k >> 1$.

Then Equation II-4 simplifies to Equation II-16 which, for a rotating disk electrode, can be written as in Equation II-17.

$$I = nFADC^b/\delta \qquad \text{(II-16)}$$

$$I = 0.62nFAD^{2/3}\nu^{-1/6}\omega^{1/2}C^b \qquad \text{(II-17)}$$

Equation II-17 is obtained by substituting into Equation II-16 the expression for δ, given in Equation II-5. A plot of current, I, measured at a constant concentration, C^b, and disk potential, E_d, vs. the square root of rotation speed, $\omega^{1/2}$, is linear only if the rate of charge transfer for that potential is large enough to keep $(\delta/D)k >> 1$, i.e., the rate of the electrochemical process is mass-transport limited, over the entire range of rotation speeds used. The linearity of such a plot is evidence that rate of charge transfer is large.

Initial voltammetric experiments with the rotating copperized cadmium-disk electrode were attempted in 0.1 M sulfuric acid but the overvoltage for hydrogen evolution on the copperized cadmium surface was observed to be significantly less than that on pure cadmium. Therefore, it was necessary to work at a higher pH to expand the negative potential range. I chose to use the medium used by Nydahl for the copperized cadmium column so that my results could be correlated to his (41). That medium was a pH 8 buffer, composed of 0.1 M THAM and 0.056 M hydrochloric acid, which results in 100% yield for reduction of nitrate to nitrite for specified rates of flow through the copperized column. Therefore, it was recognized that nitrite does not undergo reduction to any appreciable extent on this material in the pH 8 buffer at the equilibrium potential corresponding to a zero value of net current. It was thought that nitrite might undergo reduction on copperized cadmium at potentials more negative than the equilibrium potential. It was experimentally determined, however, that nitrite does not undergo reduction at a rotating copperized cadmium-disk electrode in the pH 8 buffer at any potential within the working range of that system. Therefore, it should be noted that the *a priori* choice of the pH 8 buffer for experiments with the copperized cadmium surface ruled out the possibility of the amperometric detection of nitrite. The cost of being unable to detect nitrite is, however, offset by the fact that nitrate undergoes reduction more readily on copperized cadmium in the pH 8 buffer than on cadmium in acidic solution, as discussed below.

Cyclic voltammograms for the reduction of nitrate at the rotating copperized cadmium-disk electrode in the pH 8 buffer are shown in Figure II-4 as a function of rotation speed. The nitrate reduction waves exhibit the characteristics of a reduction process with a high heterogeneous rate constant more so than any nitrate reduction waves

Figure II-4. Voltammograms of 0.10 mM nitrate as a function of rotation speed of a copperized cadmium-disk electrode in pH 8 buffer

Potential scan rate = 1.0 V min^{-1}
Electrode area = 0.95 cm^{2}

Curve	
A	Residual at 16.2 rad$^{1/2}$ sec$^{-1/2}$
	Square root of rotation speed (rad$^{1/2}$ sec$^{-1/2}$)
B	6.5
C	9.7
D	12.9
E	16.2
F	19.4
G	22.6
H	25.9
I	29.1
J	32.4

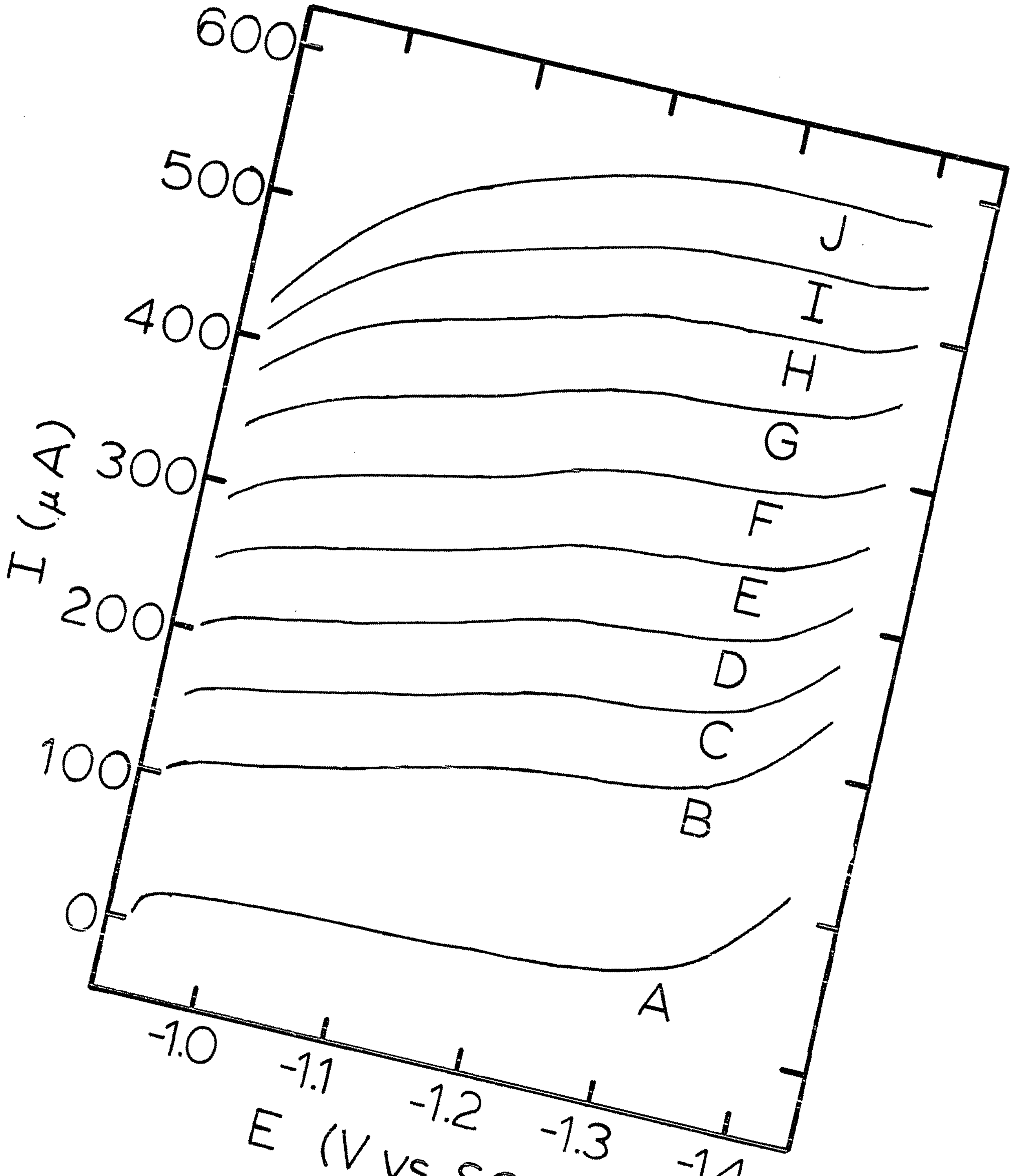
600
500
400
300
200
100
0
I (μA)
-1.0
-1.1
-1.2
-1.3
-1.4
E (V vs. SCE)
J
I
H
G
F
E
D
C
B
A

shown by Davenport (3) or obtained in this work in acid using the nitrate etched cadmium surface. Current data taken from the voltammograms in Figure II-4 is shown in Table II-3 and is plotted vs. $\omega^{1/2}$ in Figure II-5. The plot of data in Figure II-5 is linear. Therefore, it is concluded that the rate of charge transfer is large enough that even at very large rates of mass transport of nitrate to the electrode the nitrate reduction current is mass-transport limited. Furthermore, it seems apparent from these results that a reproducible flow-through detector for nitrate can be designed using the copperized cadmium surface.

b. Product of reduction of nitrate Davenport determined that nitrate is reduced to nitrite (a 2-electron reduction) and that nitrite is further reduced to hydroxylamine (a 4-electron reduction) on pure cadmium in 0.1 M sulfuric acid. It was pointed out in the previous part of this section that nitrite does not undergo reduction at a rotating copperized cadmium-disk electrode in the pH 8 buffer. Sharma, Ahlert, and Saldick have recently shown that it is "thermodynamically feasible" for nitrate to be reduced on cadmium, copperized cadmium, or amalgamated cadmium to a variety of products; dinitrogen tetraoxide, nitrite, nitric oxide, hydroxylamine, and ammonia are examples of species proposed (63). The identity of the product of the reduction depends on the available reaction

Table II-3. Dependence of nitrate reduction current on rotation speed of a copperized cadmium-disk electrode in pH 8 buffer[a]

$\omega^{1/2}$ (rad$^{1/2}$ sec$^{-1/2}$)	I (μA)
6.5	167
9.7	220
12.9	270
16.2	323
19.4	375
22.6	430
25.9	480
29.1	528
32.4	578

[a] Data shown graphically in Figure II-5.

Figure II-5. Dependence of nitrate reduction current on rotation speed of a copperized cadmium-disk electrode in pH 8 buffer

Nitrate concentration = 0.10 M
Electrode area = 0.95 cm^2
Disk potential = -1.3 V vs. SCE

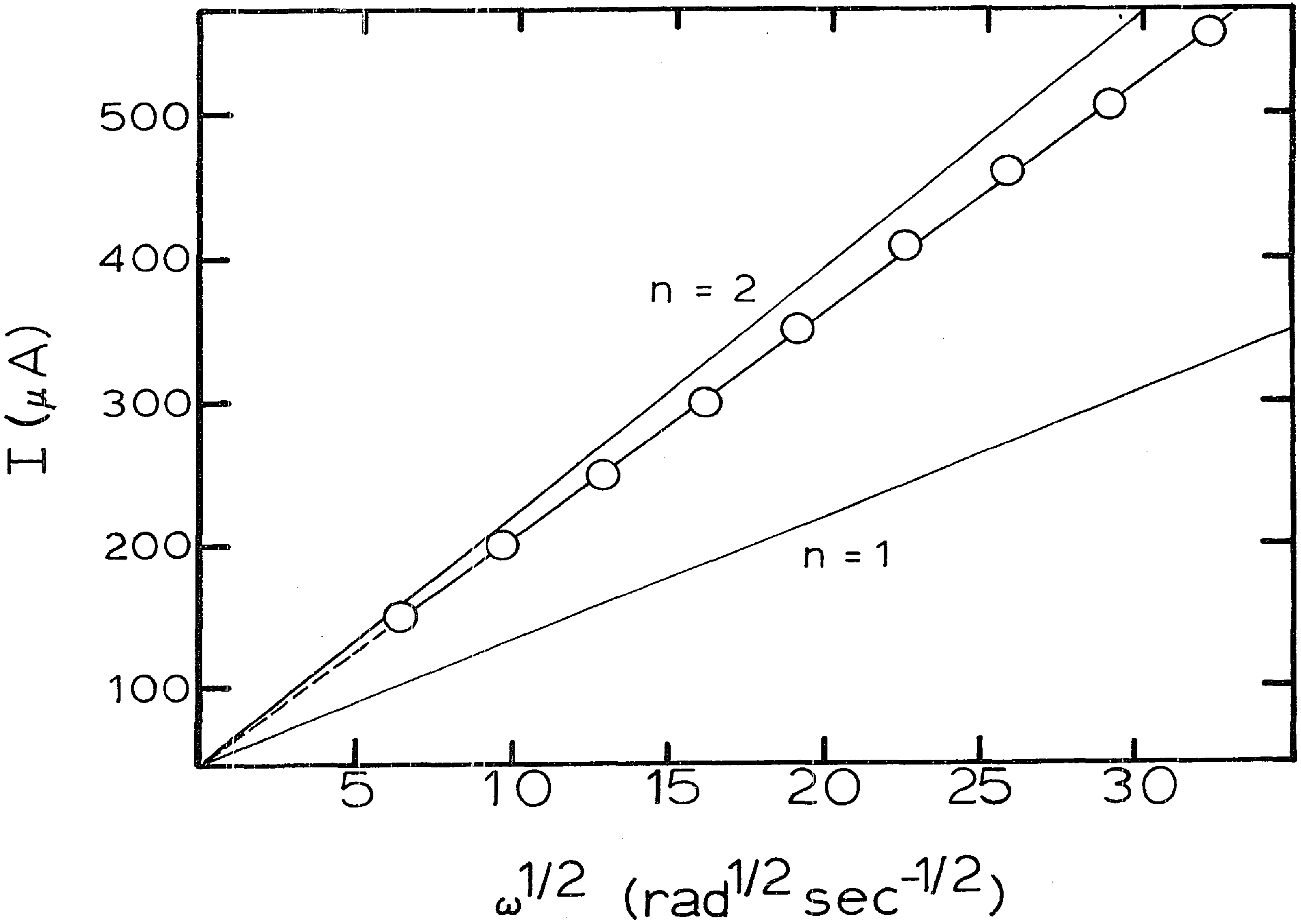
500
400
300
200
100
I (μA)
5
10
15
20
25
30
$\omega^{1/2}$ (rad$^{1/2}$ sec$^{-1/2}$)
n = 2
n = 1

mechanism and associated kinetic considerations as well as thermodynamic feasibility. No reports were found in the literature where any of these compounds have actually been identified as products of the reduction of nitrate on the materials listed above. Therefore, and because Nydahl used copperized cadmium in the pH 8 buffer, it is reasonable to postulate that the product of the reduction of nitrate at a rotating copperized cadmium-disk electrode in the pH 8 buffer is nitrite. The half-reaction for this reduction would be given by Equation II-18.

$$NO_3^- + 2e^- + 2H^+ \rightarrow NO_2^- + H_2O \qquad \text{(II-10)}$$

Several electrochemical techniques were used to gain experimental evidence that would confirm that the identity of this reduction is nitrite.

The number of electrons involved in the half-reaction given in Equation II-18 is 2, i.e., the parameter n in Equation II-17 equals 2. The rate of charge transfer for the reduction of nitrate on copperized cadmium in the pH 8 buffer was concluded to be large on the basis of the results of the voltammetric experiment described in Part a of this section. Therefore, Equation II-18, which is written on the assumption that k is large, can be used to calculate the theoretical slope, m, of the plot of nitrate reduction current vs. $\omega^{1/2}$. The expression for m is given in Equation II-19.

$$m = 0.62nFAD^{2/3}\nu^{-1/6}C^{b} \qquad \text{(II-19)}$$

Using values for D and ν obtained from the literature, $1.9 \times 10^{-5}\ cm^2\ sec^{-1}$ (64) and $0.0101\ cm^2\ sec^{-1}$ (65), respectively, two values of m for values of n = 1 and 2 were calculated. Lines having these slopes are shown in Figure II-5. The slope of the experimental line in Figure II-5 is approximately equal to the calculated slope of the line for which n = 2. This is taken as necessary evidence that nitrite is the reduction product.

A second method was used to determine the value of n. A copperized cadmium-coulometric detector was constructed which was functionally identical to the cadmium-coulometric detector described by Davenport (3), except that 25 mL of 0.08 M copper sulfate solution was passed through the detector without potential control to copperize the cadmium. This coulometric detector was interfaced with the liquid chromatograph which is described in Section III.B.4.

A coulometric flow-through electrode is designed with a large surface so that 100% of the analyte is electrolyzed when injected into a flowing stream passing through the electrode. The charge, Q, that passes during this electrolysis is given by Equation II-20, where N = the number of moles injected.

$$Q = nFN \qquad \text{(II-20)}$$

The electrode is confirmed to be coulometric when the value of n measured is not dependent on flow rate.

The electrode is not expected to be coulometric at high flow rates because the species undergoing electrolysis do not have sufficient time to diffuse to the electrode surface before they pass out of the electrode. At low flow rates, the electrode may behave with an efficiency greater than 100% for an assumed reaction when the product of the principal reaction can undergo further electrolysis. For example, the flow rate may be such that some species A may be reduced to species B with 100% efficiency. If B can be further reduced to some species C, but at very low rates of reaction, a significant amount of C may be produced at low fluid flow rates because B is in contact with the electrode surface for a greater period of time. If the second reduction occurs at flow rates where the electrode is not 100% efficient with respect to the first reduction, there will be no flow rate range where Q is independent of flow rate.

Such seems to be the case for the reduction of nitrate in the coulometric detector. At flow rates between 0.20 and 0.05 mL min^{-1}, n was observed to vary from 2 to 4. The charge measured was not independent of flow rate for any range of flow rates that could be obtained with the liquid chromatograph. Therefore, it was concluded that some nitrite was being further reduced, probably to hydroxylamine, because of slow mass transport of nitrite away from the surface.

A similar argument can be used to explain observations made by Nydahl (41). He found that the reduction efficiency of a copperized cadmium-reductor column is less than 100% if the flow rate of the nitrate containing solution does not fall in an optimum range. As in the coulometric detector, the rate of mass transport in the reductor column of nitrate to the metal surface, and of nitrite from the surface, is the result of convection to a much smaller extent than for the rotating disk electrode.

The products of an electrochemical reaction at a disk electrode can sometimes be identified with the ring of a rotating ring disk electrode. Products generated at the disk are transported by radial convection to the ring electrode, where a cyclic voltammogram of the products can be obtained to aid in product identification.

I attempted to identify the products of the reduction of nitrate in the pH 8 buffer using the rotating platinum-ring copperized cadmium-disk electrode described in Section II.C.3. (Note that the disk of this electrode was prepared by depositing layers of cadmium and copper consecutively onto a glassy carbon disk. The species being investigated were determined not to be active on glassy carbon.) Cyclic voltammograms obtained at the platinum ring with the clean glassy carbon disk potentiostated at 0.0 V, are shown in Figure II-6. Curve A is the background signal obtained at the ring for the conditions specified in the figure. Addition of 1.0 mM nitrite to the cell produced no change in this signal. This is unfortunate because it means that if nitrite is the product of the reduction of nitrate at the copperized cadmium disk, it can not be detected at the platinum ring in the pH 8 buffer. Curve B is the voltammogram obtained at the ring for 0.2 mM hydroxylamine present in the solution bulk. The waves at -0.55 V and 0.50 V correspond to the reduction and oxidation, respectively, of hydroxylamine. Therefore, if a significant amount of hydroxylamine is produced by the disk reaction, it will be detected at the ring.

Cadmium and copper were plated onto the glassy carbon disk and 0.10 mM nitrate was added to fresh buffer solution in the electrolysis cell. Voltammograms were obtained at the disk at four rotation speeds to verify that the process on this disk was the same as it had been on the rotating copperized cadmium-disk electrode used previously. Data were not taken at higher rotation speeds because the cadmium did not adhere well to the glassy carbon substrate of the ring disk electrode and the synthetic surface might have been damaged. The linearity of the plot of current vs. $\omega^{1/2}$ at -1.0 V was taken as an indication that the process at the

Figure II-6. Cyclic voltammetry of hydroxylamine at a rotating platinum-ring electrode in pH 8 buffer

Square root of rotation speed = 16.2 $rad^{1/2}$ $sec^{-1/2}$

Potential scan rate = 1.0 V min^{-1}

A Residual curve

B 0.2 mM NH_2OH

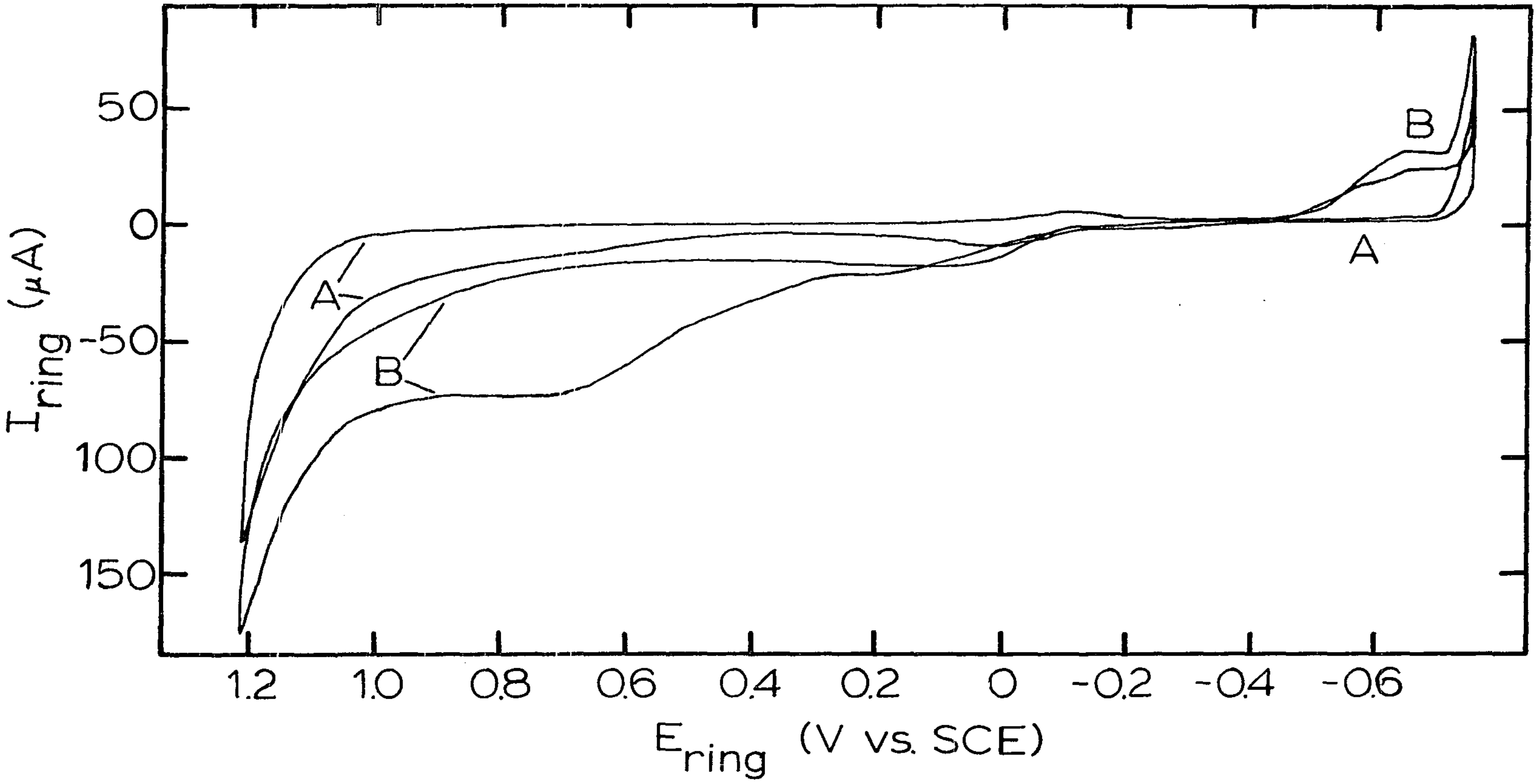
50
0
-50
100
150
I_ring (μA)
1.2
1.0
0.8
0.6
0.4
0.2
0
-0.2
-0.4
-0.6
E_ring (V vs. SCE)
A
B
A
B

disk is mass transport limited on this surface up to and including the rotation speed used to detect reduction products at the ring. When the disk was potentiostated at -1.0 V and the potential of the ring scanned, the voltammogram obtained was identical to Curve A in Figure II-6. It was concluded that no hydroxylamine is produced from the reduction of nitrate in the pH 8 buffer at the rotating copperized cadmium-disk electrode.

None of the experimental evidence given in this section conclusively proves that nitrite is the product of reduction of nitrate at pH 8 on copperized cadmium. No more can be concluded, therefore, than the following: the primary product of the reduction, under conditions of large rates of mass transport, is most likely nitrite.

c. Reduction of oxygen Voltammetric waves obtained for the reduction of oxygen at the copperized cadmium surface in the pH 8 buffer are shown in Figure II-7. The waves seem to be less reversible than those for the reduction of nitrate shown in Figure II-4; however, the plot of electrode current vs. $\omega^{1/2}$ shown in Figure II-8, is quite linear. The data for Figure II-8 is shown in Table II-4. It is important to note that oxygen does readily undergo reduction under the conditions used for the detection of nitrate, and it is, therefore, necessary to remove oxygen, or to separate nitrate from oxygen, if nitrate

Figure II-7. Voltammograms of air saturated pH 8 buffer as a function of rotation speed of a copperized cadmium-disk electrode

Potential scan rate = 1.0 V min^{-1}

Electrode area = 0.95 cm^2

Curve	Square root of rotation speed ($\text{rad}^{1/2}$ $\text{sec}^{-1/2}$)
A	6.5
B	9.7
C	12.9
D	16.2
E	19.4
F	22.6
G	25.9
H	29.1
I	32.4

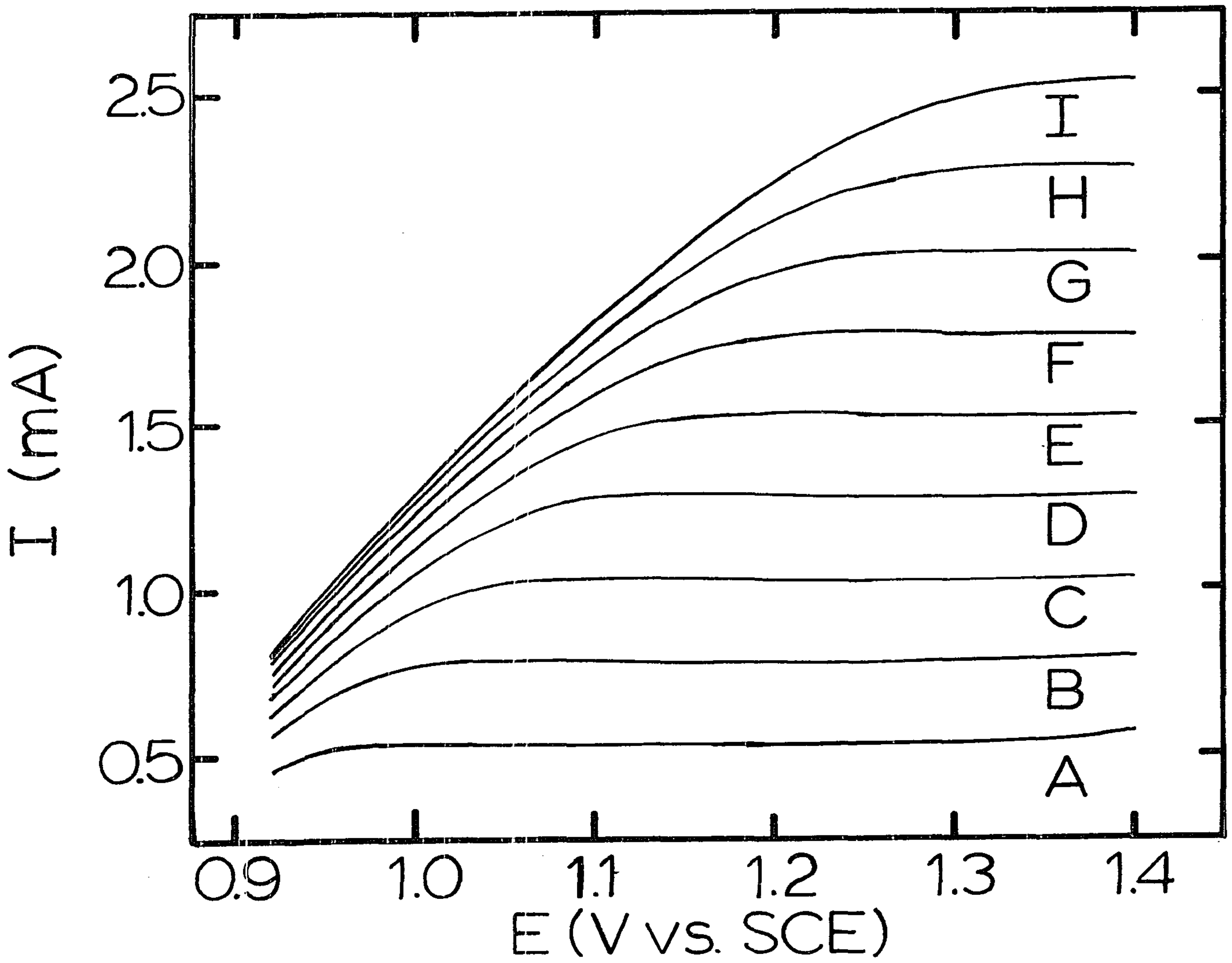

I (mA)
2.5
2.0
1.5
1.0
0.5
0.9
1.0
1.1
1.2
1.3
1.4
E (V vs. SCE)
I
H
G
F
E
D
C
B
A

Figure II-8. Dependence of oxygen reduction current on rotation speed of a copperized cadmium-disk electrode in air saturated pH 8 buffer

Electrode area = 0.95 cm^2

Disk potential = -1.35 V vs. SCE

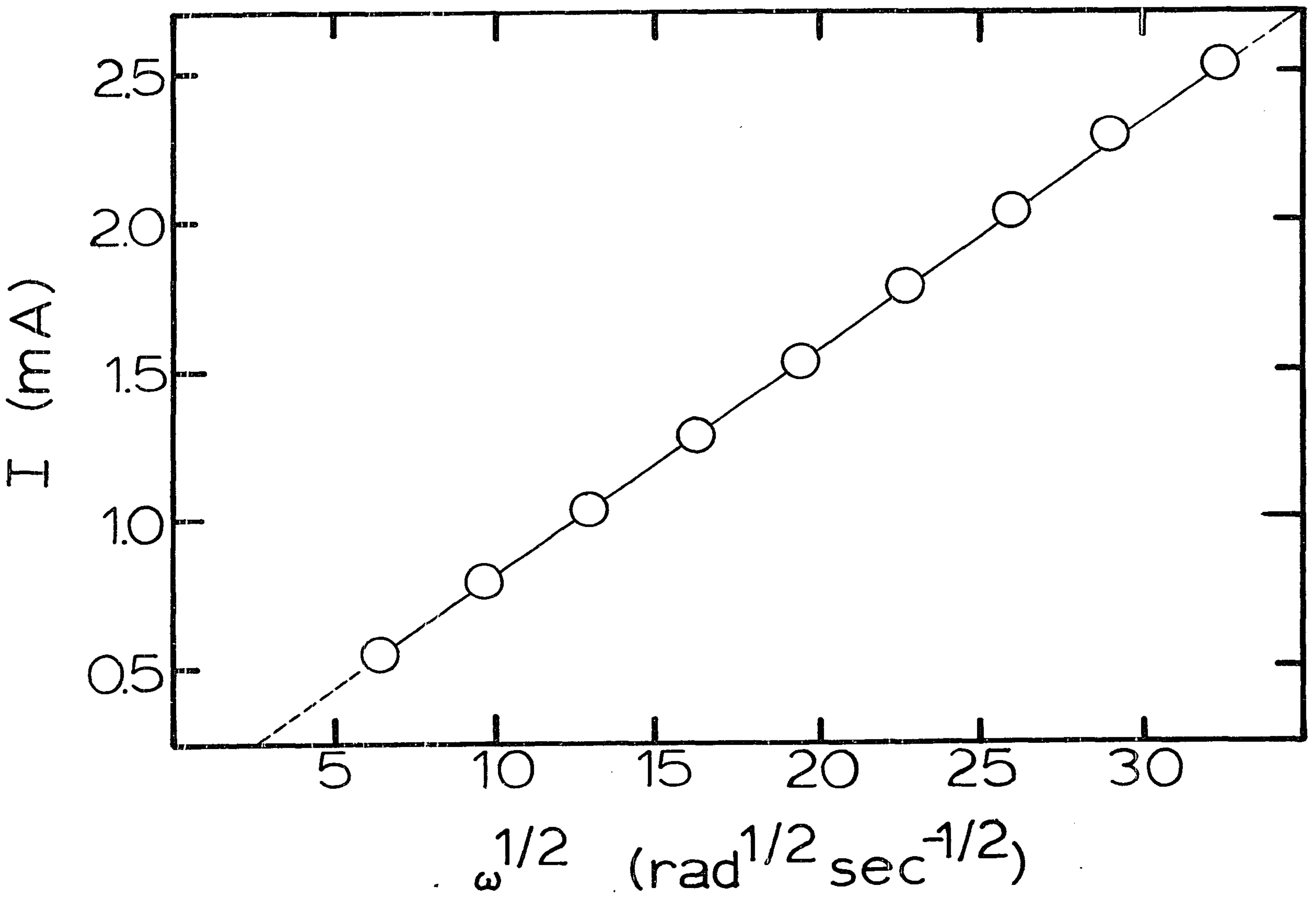
2.5
2.0
1.5
1.0
0.5
I (mA)
5
10
15
20
25
30
$\omega^{1/2}$ (rad$^{1/2}$ sec$^{-1/2}$)

Table II-4. Dependence of oxygen reduction current on rotation speed of copperized cadmium-disk electrode in air saturated pH 8 buffer[a]

$\omega^{1/2}$ (rad$^{1/2}$ sec$^{-1/2}$)	I (mA)
6.5	0.51
9.7	0.83
12.9	1.06
16.2	1.31
1.94	1.55
22.6	1.80
25.9	2.05
29.1	2.31
32.4	2.55

[a] Data shown graphically in Figure II-8.

is to be determined amperometrically with a copperized cadmium flow-through electrode.

3. Stability of metals on copperized cadmium surface

As illustrated in Section II.D.2, information about an electrochemical process can sometimes be obtained by allowing that process to occur at the disk of a rotating ring disk electrode such that intermediates and/or products of the disk reaction can be electrochemically observed at the ring. A rotating ring disk electrode with a glassy carbon disk, onto which cadmium and copper were deposited, and a platinum ring was used to gain information regarding the identity of the product of the reduction of nitrate on copperized cadmium in the pH 8 buffer. Here, experiments will be described that utilize the same electrode to gain information regarding the stability of the metals on a copperized cadmium surface during the electrocatalyzed reduction of nitrate.

Recently, Otsuki proposed that the reduction of oxygen by copperized cadmium in a reductor column involves a cationic form of copper as an intermediate (42). This proposal was offered as an explanation of the observation that when copperized cadmium is used in a reductor column to reduce nitrate to nitrite for colorimetric determination, the copper at the entry end of the column is slowly removed for reduction of nitrate samples containing dissolved oxygen. The experiment described below was designed to determine whether or not copper cations are produced by the reduction of nitrate on copperized cadmium.

Voltammograms were obtained at the platinum ring of the aforementioned electrode. The portion of those voltammograms falling between 0.0 and -0.8 V vs. SCE are shown in Figure II-9. Curve A corresponds to the residual curve obtained in the pH 8 buffer before cadmium and copper were deposited on the disk of the electrode and with the disk potentiostated at 0.0 V vs. SCE. Curves B and C were obtained in two separate solutions containing 0.35 mM copper(II) and 0.08 mM cadmium(II), respectively. The peaks at -0.2 V and -0.7 V in Curves B and C correspond to the voltammetric stripping of copper and cadmium, respectively, which was deposited when the potential of the platinum ring was scanned in the negative direction. The mass-transport limited current plateaus in the two curves correspond to the deposition processes for the metals. It may be observed that copper or cadmium deposited on a platinum electrode increases the overvoltage for hydrogen evolution on that surface. Curve D was obtained after the cadmium and copper were deposited on the disk as described in Section II.C.3 for a solution which contained 0.05 mM nitrate but no copper or cadmium ions. The potential of the copperized

Figure II-9. Identity of metal electrochemically etched in pH 8 buffer from copperized cadmium surface without potential control

A Residual platinum ring curve
Potential scan rate = 1.0 V min^{-1}

B Copper stripping peak
Copper concentration = 0.38 mM
Potential scan rate = 1.0 V min^{-1} with no hold at negative limit

C Cadmium stripping peak
Cadmium concentration = 0.08 mM
Potential scan rate = 1.0 V min^{-1} with no hold at negative limit

D Open circuit nitrate ethcing metal product
No copper(II) or cadmium(II) in solution
Nitrate concentration = 0.05 mM
Potential scan rate = 1.0 V min^{-1} with 1.0 min hold at negative limit

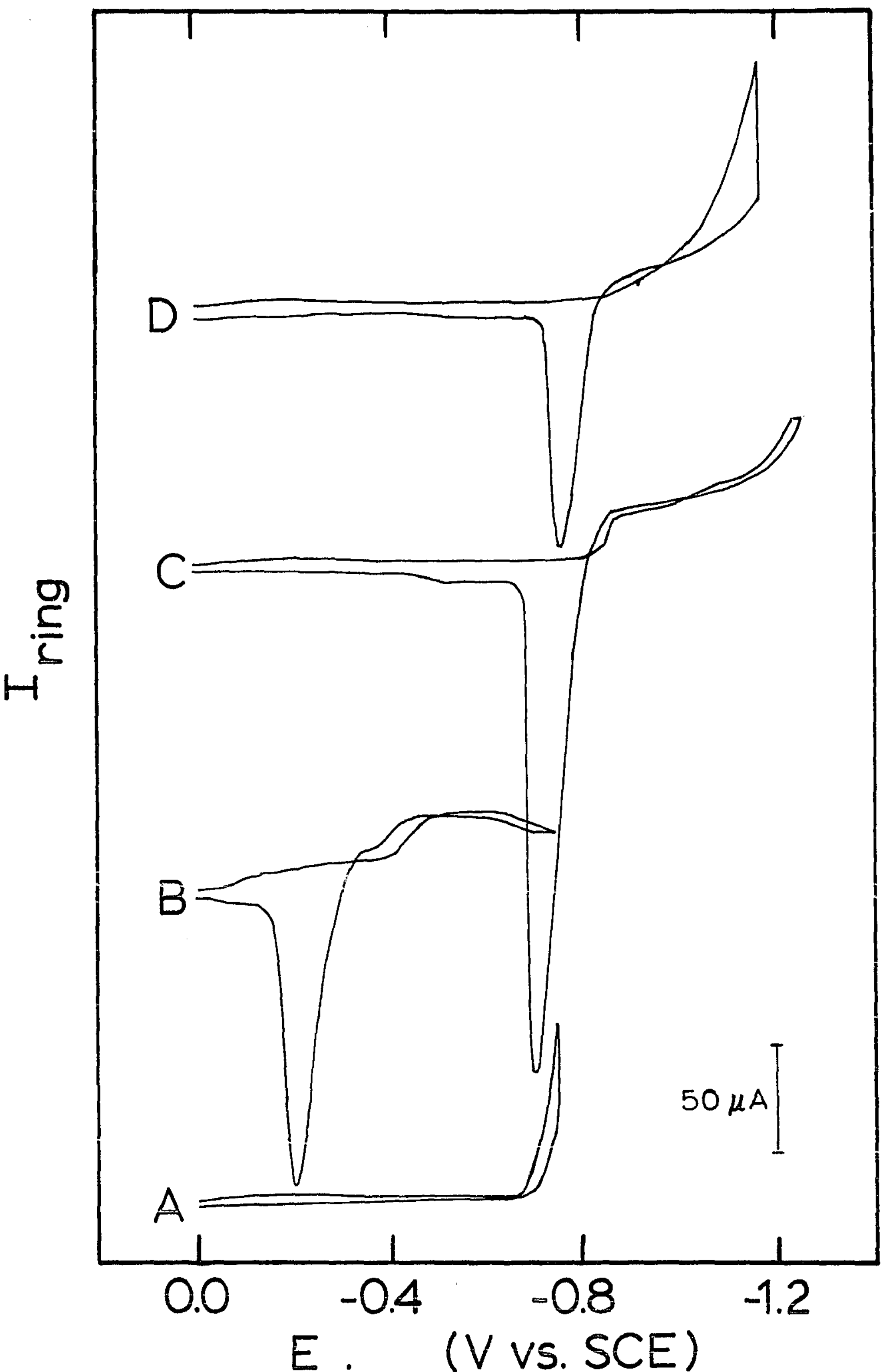
D
C
B
A
50 μA
I ring
0.0
-0.4
-0.8
-1.2
E ring (V vs. SCE)

cadmium disk was not controlled so that the only available source of electrons needed to support the nitrate reduction process results from the oxidation of one or both of the metals on the disk surface. The potential of the ring was scanned to -1.20 V vs. SCE and then held constant for 1 min. The stripping peak at -0.7 V vs. SCE was obtained when the potential of the ring electrode was scanned in the positive direction.

It is concluded from Curves B and C that it is possible to determine the identity of the metal deposited at the ring under the conditions used to obtain Curve D. It is apparent from Curve D that only cadmium ions were deposited at the ring electrode, and therefore, that only cadmium ions are produced as a result of nitrate oxidation of a copperized cadmium surface. Copper ions are evidently not involved in the mechanism of the reduction of nitrate on copperized cadmium. This result may seem inconclusive, because one would expect that any cations of copper produced at the disk without potential control would react immediately with the cadmium on the disk surface before they could get to the platinum ring. The reaction of the cations of copper with the cadmium would, of course, be the same as the reaction involved in the copperization process. On the other hand, the rate of mass transport from the disk to the ring of the rotating electrode is very high and so it is reasonable to expect that some of the cations of copper if produced at the disk would escape the disk before being reduced by the cadmium. While the amount of copper cations escaping might be small, the anodic stripping technique used at the ring has a very low detection limit. Therefore, the conclusion that no cations of copper are involved in the nitrate reduction mechanism on copperized cadmium seems valid, and it is concluded that the deposit of copper is very stable on the cadmium surface.

A few comments should be made concerning the observation that cadmium is removed from the disk during the open circuit reduction of nitrate. This result was anticipated so the experimental evidence that cadmium ions were collected at the ring electrode is unimportant, except that it serves to amplify one criticism that can be made about use of the reductor column for reducing nitrate to nitrite. The cadmium ions formed during the reduction are very easily introduced into the general environment because they are constituents of waste solutions from the colorimetric analysis. Effort should be expended to prevent that from happening, because cadmium is very toxic. This problem is avoided when the copperized cadmium surface is used for amperometric detection.

It was possible to verify that no cadmium ion is released from the disk when the potential of the disk is appropriately controlled. This was done by repeating the experiment which corresponds to Curve D in Figure II-9 except that the potential of the disk was controlled at values negative of -0.9 V vs. SCE. No stripping peak for cadmium was observed at the ring under these conditions. Therefore, both metals are stable on the electrode surface when used as an amperometric detector.

4. Microstructure of copperized cadmium surface

The observation made in the last section that cadmium ions are formed during the open circuit reduction of nitrate on copperized cadmium served to inspire a question about the microstructure of the copperized cadmium surface. It was possible to approximate the thickness of the cadmium and the copper layers on the disk used in the studies described (see procedure for preparation of the disk surface in Section II.C.3). These thicknesses were equivalent to about 1200 layers of cadmium and 700 layers of copper (see Appendix). Therefore, it seemed reasonable to ask: How does the cadmium get out from under the copper overlayer? To answer this question a copperized cadmium surface was examined with a scanning electron microscope. It was not, however, possible to examine the actual disk surface used in the experiments described above because the electrode was too large for insertion into the scanning electron microscope. Therefore, the tip of the polycrystalline cadmium disk electrode described in Section II.C.3, which was equivalent to that surface used in the amperometric detector discussed in this thesis, was examined instead.

The cadmium surface was polished as described in Section II.C.3 and then examined through the scanning electron microscope at a magnification of 10,000x. One rectangular area on the surface was scanned for about a half hour as tuning adjustments were made on the scanning electron microscope and associated photographic equipment. The grooves left in the surface by the 1 μ diamond particles used in the last step of the polishing procedure were quite evident but no additional feature was observed to be significant on the surface. The electrode tip was removed from the microscope and copperized as described in Section II.C.3. It was then reinserted into the microscope in exactly the same position and first viewed at only 3,000x magnification. At the center of the viewing scope was a dark rectangle which corresponded to the region which had been scanned previously. When the magnification was increased to 10,000x, it was obvious that no copper had deposited on that portion of the surface. The electrode tip was shifted slightly so that only a corner of the previously scanned area which had not been copperized was visible in the viewing scope and the photomicrograph shown in Figure II-10 was taken. It is apparent that the deposited copper does not exist as a continuous film on top of the cadmium. Instead, there are microspheres, probably consisting of pure copper, present on the surface. The copper microspheres are in a closely packed array with cadmium exposed by the interstitial spaces between the microspheres. Hence, nitrate does have access to the cadmium surface during electrochemical applications of the copperized cadmium surface.

The area of the cadmium electrode tip examined with the scanning microscope that was not copperized was probably covered by a carbonaceous film during the initial microscopic examination of the surface. Organic molecules in the oil used in the vacuum pump of the system travel back into the sample chanber where they can adsorb to the sample surface. The high energy electron beam decomposes those organic molecules leaving the decomposition products to interact with the surface (66). The adsorbed carbonaceous decomposition products apparently prevented deposition of copper.

5. Electrocatalytic effect of copper

The fact that electrocatalytic phenomena can be complex has been noted in Section II.B. For this reason, and because the mechanism of the reduction of nitrate on cadmium

Figure II-10. Scanning electron micrograph of copperized cadmium surface

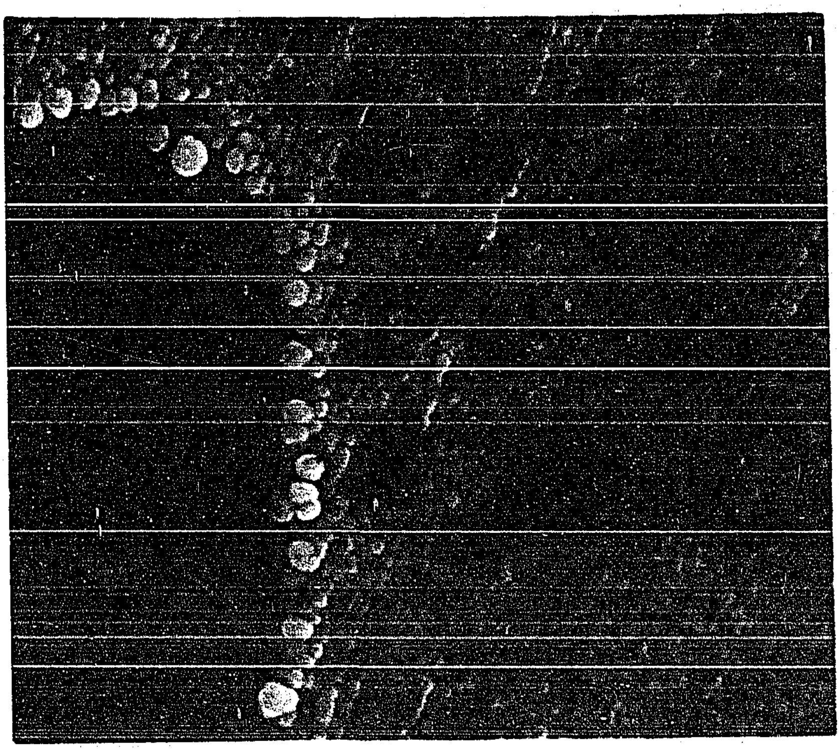

Scanning electron micrograph

Copperized cadmium

(x 10,000)

is not known, no attempt has been made to rigorously investigate the electrocatalytic role of the copper in the mechanism of the reduction at a copperized cadmium surface. Three possible mechanisms for the copper electrocatalysis are discussed in this section and examined in light of the experimental evidence.

a. Hypothesis one The copperization process described in Section II.C.3, involves the removal of cadmium atoms with simultaneous deposition of copper as given in Equation II-21.

$$Cu(II) + Cd \rightarrow Cd(Cu) + Cd(II) \tag{II-21}$$

As the cadmium atoms are removed, a layer of copper atoms is simultaneously deposited. The bulk of the copper layer is not strongly adherent and can be removed by wiping the disk with a piece of soft tissue paper. When this is done, a visual inspection of the cadmium surface reveals that the copperization process removes cadmium atoms selectively in a way which exposes the polycrystalline structure of the cadmium surface. It was pointed out in Section II.D.1 that nitrate etching of a cadmium surface, a process which probably involves the chemical reaction given in Equation II-22, also exposes the polycrystalline structure of the cadmium.

$$NO_3^- + Cd + 2H^+ \rightarrow NO_2^- + Cd(II) + H_2O \tag{II-22}$$

Experimental evidence was given which shows that the apparent rate of nitrate reduction on the crystal faces exposed by the nitrate etching process is faster than on other cadmium surfaces previously prepared. Hence, it is conceivable that the copperization process functions in a similar manner to expose the same set of active crystal faces, and that once this has been accomplished the copper is not further involved in the electrocatalysis. If this explanation is correct, copper atoms deposited during copperization do not prevent interaction between nitrate and the cadmium atoms on the surface.

b. Hypothesis two The copper could be involved in the electrocatalyzed reduction of nitrate in a much more complicated way if the following consideration is important. The reduction of nitrate on cadmium involves the transport of a negative ion to a negatively charged electrode surface. The point of zero charge, which has been defined in Section II.B, is approximately 1 V more positive for copper than that for cadmium when measured in solutions of strong electrolytes (67). It is probably true that the difference between the points of zero charge of these two metals is also large in the pH 8 buffer used in much of this work. The metal having a more positive point of zero charge will have a greater absolute negative charge density when compared to another metal at the same applied negative potential, measured with respect to an arbitrary reference potential. Therefore, the surface of a copper electrode is expected to be more negatively charged than that of a cadmium electrode when they are at the same applied negative potential. The point of zero charge of a copperized cadmium surface probably falls between those of pure cadmium and copper surfaces. Therefore, the presence of the copper on the copperized cadmium surface is expected to increase the negative charge on the surface. It might be concluded that the increased electrostatic repulsion that the increased charge on the surface of the copperized cadmium electrode exerts on the approaching nitrate ion would decrease the rate of reduction of nitrate on that electrode. This conclusion is premature, however, because it has not been recognized that the charge transfer actually takes place a finite distance, x_R, away from the electrode surface where the charge density is different from that on the surface.

The consequences of the fact that x_R is not equal to 0 can best be discussed after considering the model for the double layer which is shown in Figure II-11. The model is quite similar to the model proposed in 1963 by Bockris, Davanathan, and Muller (55). Both solvated and unsolvated ions, as well as solvent molecules, occupy the region between the electrode surface and some plane parallel to

Figure II-11. Model of double layer (A) at a cadmium surface and (B) at a copperized cadmium surface

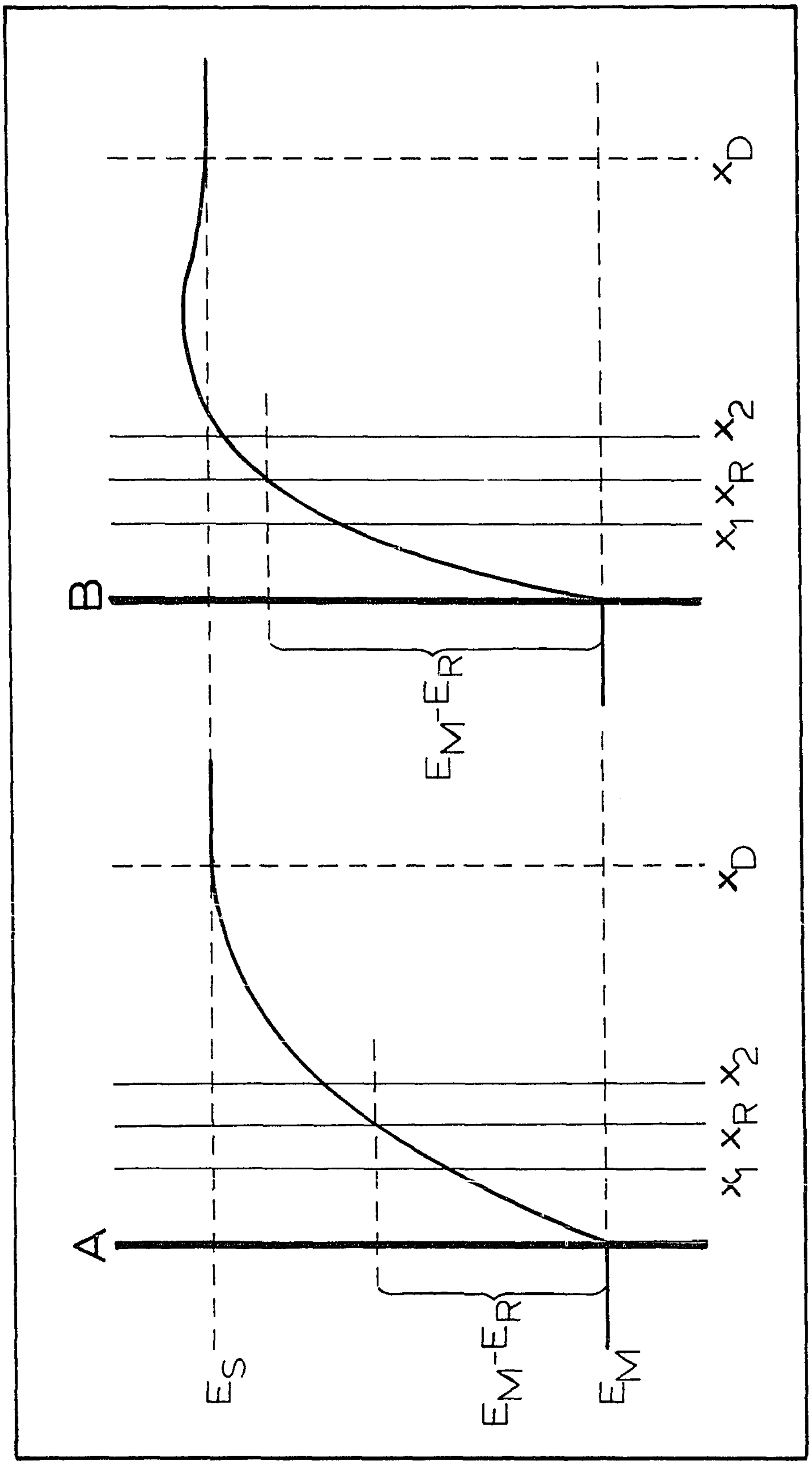
E_S
E_M-E_R
E_M
A
x_1
x_R
x_2
x_D
E_M-E_R
B
x_1
x_R
x_2
x_D

the surface at an undetermined distance, x_D, away from the surface. Let x_D be the distance where solution ions are far enough away from the electrode that they are neither repelled nor attracted by the electrostatic environment at the electrode surface. The distance x_D is the thickness of the double layer region. This double layer region is divided into three smaller regions by planes parallel to the electrode surface. The first region is bounded by the surface and a plane at distance x_1 from the electrode. The distance x_1 is taken to be the radius of an unsolvated ion chemisorbed at the electrode surface. The next region is bounded by the plane at x_1 and a plane at distance x_2 from the surface. The distance x_2 is measured from the surface of the electrode to the center of a solvated ion at its position of closest approach to the surface. The third region is bounded by the planes at x_2 and x_D. This region is the so-called "diffuse region". The planes that divide the double layer region are shown diagrammatically for cadmium and copperized cadmium surfaces, designated by the letters A and B, respectively, in Figure II-11. The plane where the charge-transfer reaction takes place, at a distance x_R is also shown in the figure. The value of x_R was chosen such that it falls between x_1 and x_2. While this particular choice of x_R is not necessary, it helps in the following illustration. The curves in

Figure II-11 are meant to pictorially represent the potential distribution within the double layer as a function of distance from the surface. The curves indicate that the potential of the electric field, E, caused by the charge on the surface increases to the potential of the bulk of the solution, E_S, as x increases. The gradient of the potential distribution near the electrode surface, dE/dx, is expected to be proportional to the number of positively charged cations near the surface. There are undoubtedly more cations near the copperized surface because of the greater absolute negative charge on that surface. Therefore, the potential gradient curve for the copperized surface is expected to rise more rapidly. An approaching nitrate ion at a distance x from the surface will be in an electric field the potential of which E_x is represented by the intersection of a vertical line at x and the curve representing the potential distribution. When x is equal to x_R, E_x will be equal to E_R. If x_R is the same for both surfaces, as shown in Figure II-11, E_R is considerably more positive for the copperized cadmium surface than for the pure cadmium surface. It can be suggested, based on these double layer considerations, that the copper electrocatalyzes the nitrate reduction process by making E_R more positive, i.e., causing an increase in the cation concentration at the surface which shields the approaching ion from the surface charge. A second consequence of a more positive value of E_R is that the difference, $E_M - E_R$ will be more negative. A careful examination of Equation II-3 will reveal that $\Delta G_{\neq}$ will be smaller because both of the last two terms will be negative, and the rate of charge transfer will be larger.

c. Hypothesis three Finally, the copper could be involved in the electrocatalyzed reduction of nitrate in still another way. It is conceivable that the copper enhances the reduction of nitrate on the copperized surface by virtue of a catalyzed adsorption step. Trepak, et al. have concluded, based on the results of a chronoamperometric investigation of the reduction of nitrate on cadmium, that the process proceeds through an adsorption step (68). However, the strength of the cadmium-reactant bond in such an adsorption step would not be expected to be very great because, as in the case of the reduction of oxygen on gold, discussed in Section II.B, cadmium has no unpaired d electrons to aid in the formation of that adsorption bond. The electronic configuration of cadmium is $[Kr]4d^{10}5s^2$. The electronic configuration of copper is $[Ar]3d^{10}4s^1$. If in the presence of neighboring cadmium atoms one of the 3d electrons in the copper atom is shifted into the available vacancy in the 4s orbital of the copper atom, there would be an unpaired d electron to participate in the formation of a metal-reactant bond, in which case the standard free energy of activation for the process would be smaller and the rate of charge transfer would be larger on the copperized cadmium surface than on the cadmium surface.

d. Summary of hypotheses The three possible roles of the copper in the electrocatalyzed nitrate reduction described above can be summarized as in the following statements. Hypothesis one proposes that the amount of active cadmium surface area is increased by copperization. Hypothesis two proposes that the potential of the reaction plane is more positive on copperized cadmium and the overall activation barrier is smaller as a result of the effect copper has on the absolute number of cations near the surface. Hypothesis three proposes that the standard free energy of activation of an adsorption step of the reduction mechanism is reduced as a result of an unpaired d electron in the electronic structure of the copper-cadmium alloy. No data were obtained in this research which proves explicitly any one of these mechanisms. However, the results of experiments described below seem to be consistent with the general conclusion that copper is actively involved in an adsorption step in the mechanism for the electrocatalyzed reduction of nitrate.

e. Experimental observations and discussion Rotation speed studies of the reduction of nitrate were performed with two rotating cadmium-disk electrodes that were fabricated as described in Section II.C.3, from monocrystalline cadmium. One of these electrodes was constructed such that the (0001) plane of the crystal was exposed on the disk surface. The plane exposed on the second disk was the $(10\bar{1}0)$ plane. The four digits used to specify these cadmium crystal planes are called Miller-Bravais indices, and are used whenever referring to a hexagonal close-packed system, of which cadmium is a good example. Definition and discussion of the Miller-Bravais indices may be found in Reference 69.

Plots of nitrate reduction current in the pH 8 buffer as a function of the square root of rotation speed for both of the rotating monocrystalline cadmium disks, and for the same two surfaces when copperized, are shown in Figure II-12. The data for Figure II-12 are listed in Table II-5. The plot for the $(10\bar{1}0)$ face of cadmium is not very linear and the slope of the line drawn through the first five points is only 33% of the theoretical slope, which can be calculated from Equation II-17 assuming a 2-electron reduction. It is concluded, therefore, that the rate of nitrate reduction is slow on the $(10\bar{1}0)$ face of cadmium. Evidently the rate of nitrate reduction on the (0001) face of cadmium,

Figure II-12. Dependence of nitrate reduction current on rotation speed of monocrystalline cadmium-disk and copperized monocrystalline cadmium-disk electrodes in pH 8 buffer

Disk potential = -1.0 V vs. SCE
Nitrate concentration = 0.10 mM
Electrode area (0001) = 0.43 cm^2
Electrode area $(10\bar{1}0)$ = 0.35 cm^2

● Rotating monocrystalline cadmium-disk electrode (0001)

■ Rotating copperized monocrystalline cadmium-disk electrode (0001)

○ Rotating monocyrstalline cadmium-disk electrode $(10\bar{1}0)$

□ Rotating copperized monocrystalline cadmium-disk electrode $(10\bar{1}0)$

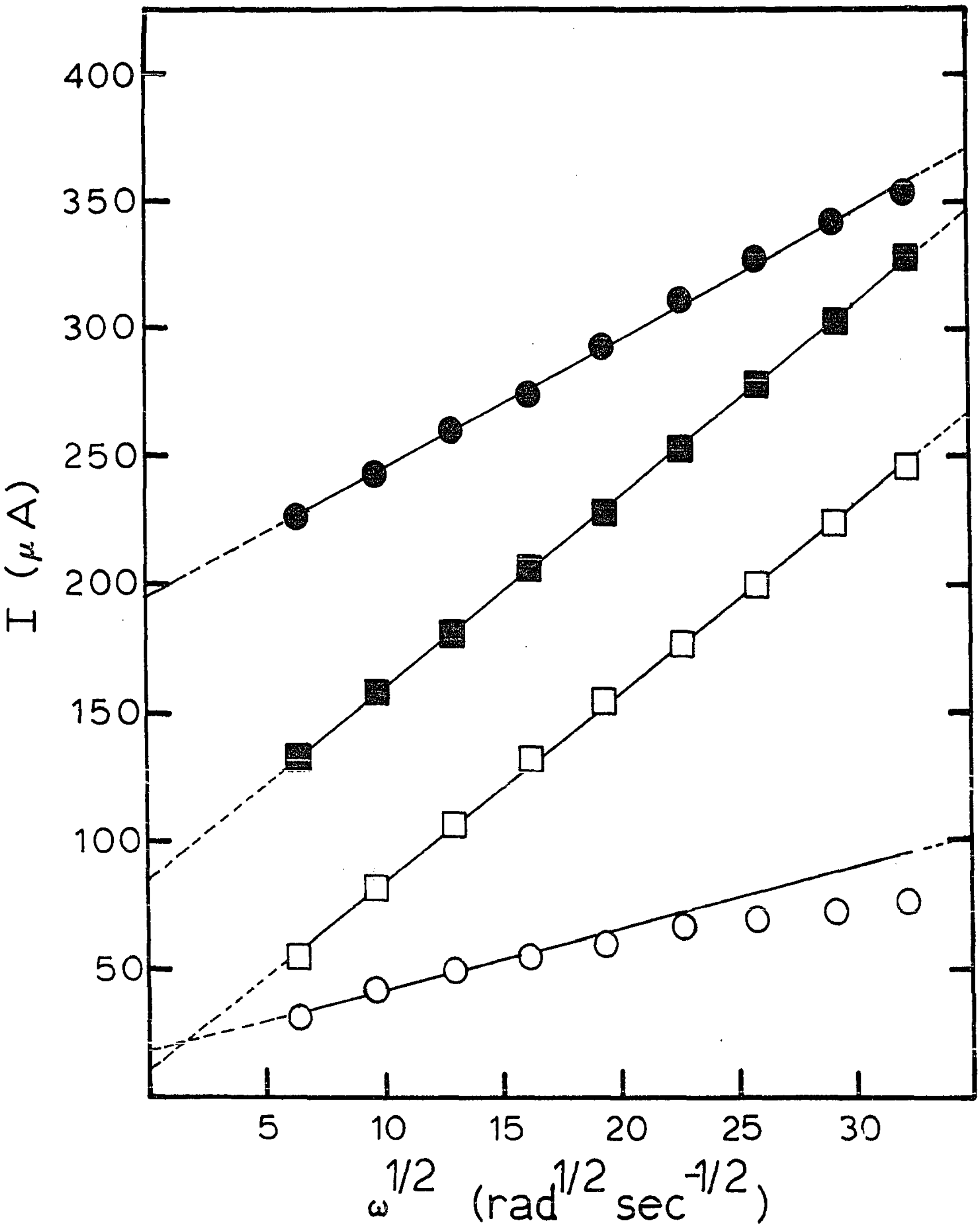
400
350
300
250
200
150
100
50
I (μA)
5
10
15
20
25
30
ω$^{1/2}$ (rad$^{1/2}$ sec$^{-1/2}$)

Table II-5. Dependence of nitrate reduction current on rotation speed of monocrystalline cadmium-disk and copperized monocrystalline cadmium-disk electrodes in pH 8 buffer

$\omega^{1/2}$ (rad$^{1/2}$ sec$^{-1/2}$)	Rotating monocrystalline cadmium-disk electrode currents (μA)			
	(0001)		(10$\bar{1}$0)	
	Pure	Copperized	Pure	Copperized
6.47	228	133	32	55
9.71	244	157	42	81
12.94	260	182	49	107
16.18	275	207	56	133
19.42	293	229	60	155
22.65	310	253	67	177
25.89	327	278	69	199
29.12	342	302	72	224
32.36	354	329	76	246

although it is somewhat faster than on the $(10\bar{1}0)$ face, is also small. In Section II.D.1, it was pointed out that the apparent rate of reduction of nitrate on cadmium in acidic media seems to be a function of the crystal faces exposed at the surface. The observations made here with the monocrystalline cadmium-disk electrodes seem consistent with the conclusion that the dependence of reduction rate on exposed crystal faces is the same in basic media. It is surprising, however, that there is any change in nitrate reduction current at these two crystal faces with rotation speed, because it has been observed that no reduction of nitrate occurs at the polycrystalline disk surface used for other studies in the pH 8 buffer. It was expected that these two crystal faces, as well as other more active crystal faces of cadmium, would have been exposed to some extent on the polycrystalline surface.

The plots of I vs. $\omega^{1/2}$ for both crystal faces when copperized, shown in Figure II-12, are very linear and the slopes of these plots are equal to the aforementioned theoretical slope. It is concluded that the rate of nitrate reduction on these copperized crystal faces is mass-transport limited and that the active areas of the copperized cadmium crystals approach their geometric areas.

The results of the rotation speed studies performed with the bare monocrystalline cadmium disks provide necessary, but not sufficient, evidence that the selective removal of cadmium atoms by the copperization process is responsible for the observed copper electrocatalysis (hypothesis one). The studies performed with the copperized monocrystalline cadmium disks provided no further information concerning the electrocatalysis; however, it should be pointed out that the reduction rate on both crystals was improved to the theoretical mass-transport limit and apparently the copper is capable of causing the same improvement on many different exposed crystal faces. Therefore, copperization of the cadmium surface is considered to be the best method of activating cadmium surfaces for the amperometric determination of nitrate.

The results of the following activation studies are somewhat more revealing as to what might be the role of the copper in the electrocatalyzed nitrate reduction. These activation studies were performed by slowly accumulating copper atoms at a rotating cadmium disk electrode from a very dilute solution of cupric ions. The solution containing a trace amount of copper(II) also contained nitrate at a high enough concentration so that the current observed at any potential, which was within the working range of potentials of the cadmium surface, was virtually all the result of the reduction of nitrate. The rate of reduction of copper(II) was mass-transport limited over the same range of potentials; therefore, the potential of the cadmium disk was scanned within that range without changing, to any significant degree, the rate of the accumulation of copper atoms on the surface and successive voltammograms were obtained as a function of the accumulation of copper. The shape of the nitrate reduction wave was expected to become more and more reversible as copper atoms were accumulated on the surface, i.e., a mass-transport limited plateau was expected to develop for the nitrate reduction curve due to the electrocatalytic effect of the accumulated copper atoms. Because the copper accumulation process is mass transport limited, it was possible to calculate the number of moles of copper atoms, $N^a{}_t$, that were on the surface at any time, t, during the activation study as a function of the number of moles of cupric ions, $N^b{}_{t=0}$, present in the bulk of the solution at the beginning of the study. The derivation of the expression for $N^a{}_t$ is given in the Appendix. The result of that derivation is given in Equation II-23.

$$N^a{}_t = N^b{}_{t=0}[(1 - \exp(-0.62\ AD^{2/3}\nu^{-1/6}\omega^{1/2}V^{-1}t)] \qquad \text{(II-23)}$$

In Equation II-23, V is the volume of the cupric ion solution: all other variables therein have been defined elsewhere in this thesis.

The voltammograms obtained during the activation, by the process just described, of the rotating polycrystalline cadmium disk electrode are shown in Figure II-13. The values of all experimental parameters used in the activation study are given in the legend to the figure. Curve A in Figure II-13 was obtained at t=0, i.e., before cupric ions were added to the solution. There is no mass-transport limited current plateau in Curve A, but it is believed that the minimum in the curve at about -1.3 V vs. SCE is due to onset of background processes interferring with the nitrate reduction process. The background processes probably include the adsorption of protons and/or their reduction, the rate of the latter process being limited by a very slow rate of charge trasnfer. The other curves in Figure II-13 obtained at various times during the accumulation of copper atoms do indicate that the magnitude of the current for the reduction of nitrate is increased at all potentials in the operating range. The shape of the curve in the vicinity of the current minimum at -1.3 V does not change significantly, probably indicating that the background processes are not effected by the presence of the accumulated copper.

The experiment was repeated using the rotating monocrystalline cadmium disk electrode with the $(10\bar{1}0)$ face exposed. Nitrate reduction curves obtained before and during the activation of the crystal face exposed on this surface

Figure II-13. Voltammograms of nitrate reduction at a rotating polycrystalline cadmium-disk electrode in pH 8 buffer as a function of time dependent deposition of copper atoms on disk

Nitrate concentration = 0.20 mM
Electrode area = 0.95 cm^2
Potential scan rate = 1.0 V min^{-1}
Square root of rotation speed
= 6.47 $rad^{1/2}$ $sec^{-1/2}$
Cell volume = 300 cm^3
Initial copper(II) concentration
= 7.7 x 10^{-4} mM

Before addition of copper(II)
A Residual curve
B Curve for nitrate reduction

After addition of copper(II)

Curve	Number of copper layers on surface at beginning of potential scan in the negative direction
C	.5
D	1.0
E	1.5
F	2.0
G	2.5
H	3.2

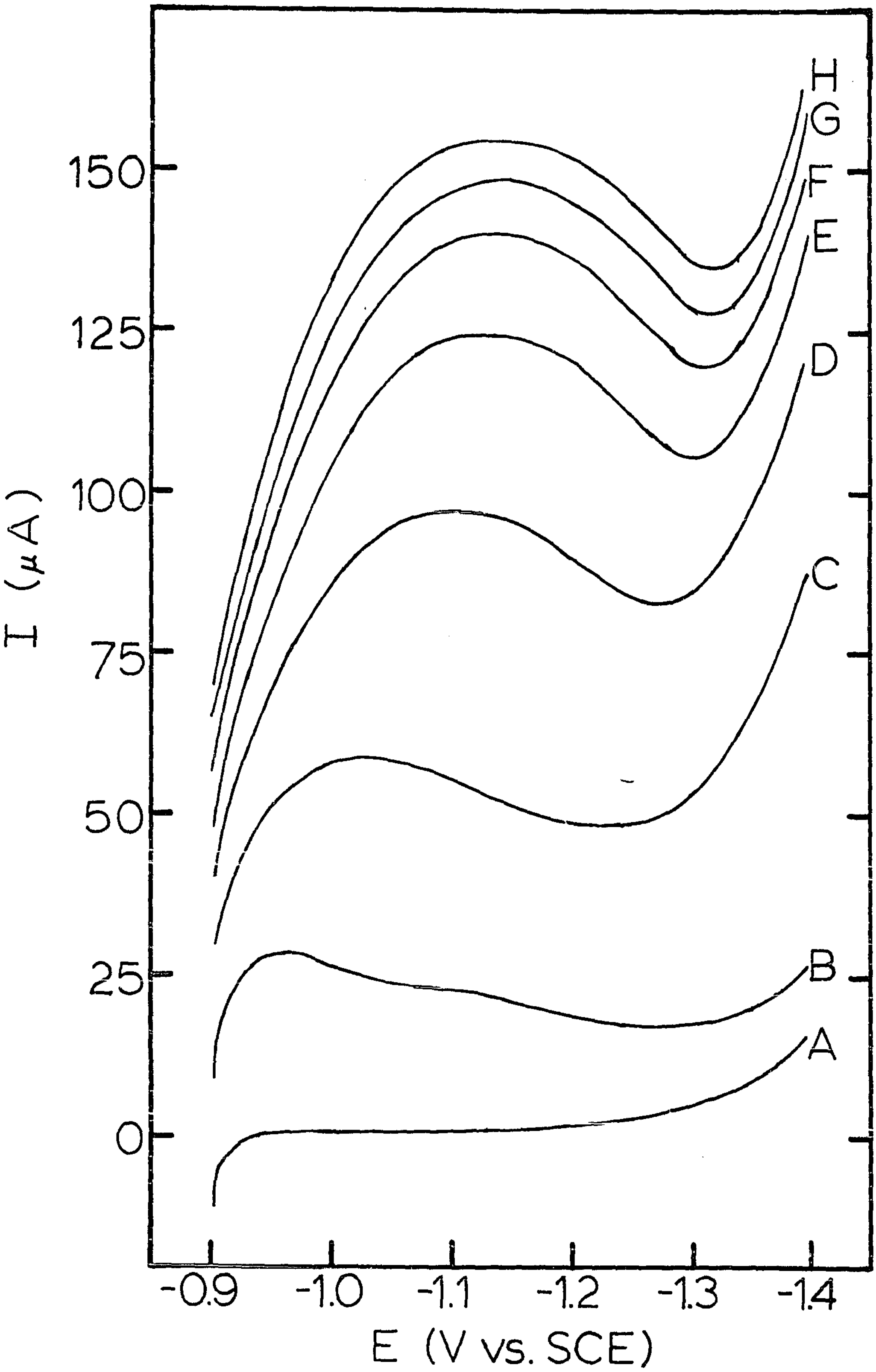
I (μA)
150
125
100
75
50
25
0
-0.9
-1.0
-1.1
-1.2
-1.3
-1.4
E (V vs. SCE)
H
G
F
E
D
C
B
A

by the same process are shown in Figure II-14. Again, the shape of the curve obtained at t=0, indicates that there are some background processes that interfere with the nitrate reduction process on this crystal face. The other curves in Figure II-14 obtained at various times during the accumulation of copper again indicate that the magnitude of the nitrate reduction current is improved at all potentials. Note that on this surface, however, the nitrate reduction current becomes independent of potential over the range from -0.9 to -1.35 V vs. SCE as the amount of copper on the surface approaches the equivalent of 15 layers of hexagonally close-packed copper.

It is concluded that the rate of charge transfer is increased on both the polycrystalline and the monocrystalline cadmium surfaces used in the activation studies, as a result of the slow accumulation of copper. A possible reason that accumulated copper does not affect the background processes of the polycrystalline cadmium disk is that the copper atoms are selectively deposited on only some of the exposed crystal faces. If this is true, background processes occurring on the other exposed crystal faces would not be altered.

One conclusion concerning the role of the copper in the electrocatalyzed nitrate reduction can be made on the basis of the results of the two activation studies just

Figure II-14. Voltammograms of nitrate reduction at a rotating monocrystalline cadmium-disk electrode $(10\bar{1}0)$ in pH 8 buffer as a function of time dependent deposition of copper atoms on disk

Nitrate concentration = 0.30 mM

Potential scan rate = 1.0 V min^{-1}

Square root of rotation speed = 6.47 $\mathrm{rad}^{1/2}$ $\mathrm{sec}^{-1/2}$

Cell volume = 300 cm^3

Initial copper(II) concentration = 2.2×10^{-3} mM

Before addition of copper(II)

A Residual curve

B Curve for nitrate reduction

After addition of copper(II)

Curve	Number of copper layers on surface at beginning of potential scan in negative direction
C	0.2
D	1.4
E	3.6
F	6.8
G	14.7

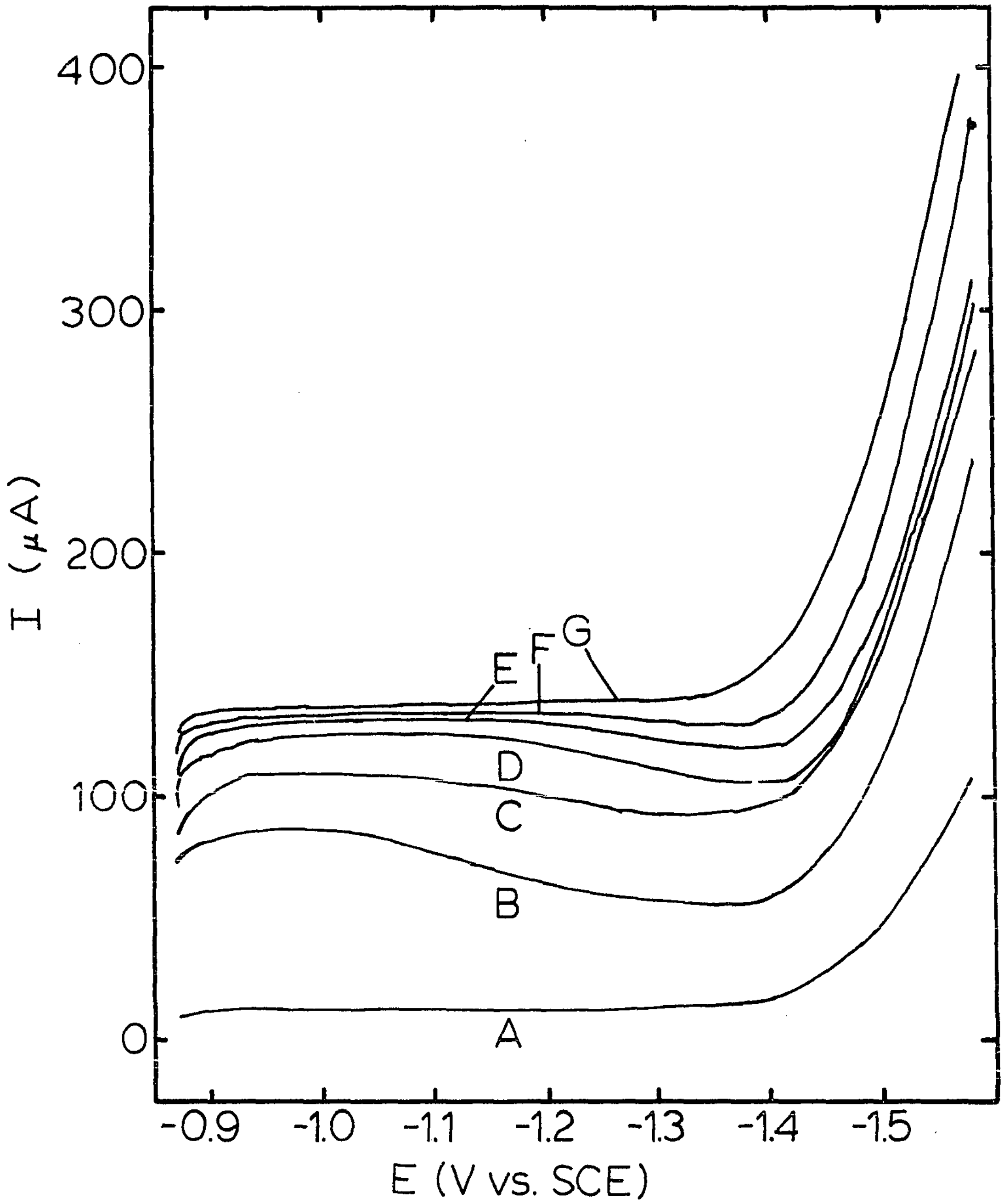
400
300
200
100
0
I (μA)
-0.9
-1.0
-1.1
-1.2
-1.3
-1.4
-1.5
E (V vs. SCE)
A
B
C
D
E
F
G

described. These two activation studies involved the controlled deposition of copper, i.e., no cadmium was removed as the copper was deposited. Therefore, no selective exposure of a given crystal face or set of crystal faces was possible. It might be argued that if cadmium ions form during the nitrate reduction, they could be redeposited but at a different place on the surface. This could provide a mechanism for the selection of the exposed crystal faces. Section II.D.3 describes a rotating ring-disk study wherein it is concluded that when the potential of the surface is held at values negative of about -0.9 V vs. SCE, no cadmium ions form during the reduction of nitrate. Therefore, it is concluded that the electrocatalysis is not the result of the exposure of an active set of cadmium crystal faces during copperization (hypothesis one).

The explanation for the copper electrocatalysis proposed in hypothesis two, i.e., the possibility that the copper on the copperized cadmium surface increases the reaction plane potential by shifting the point of zero charge, was also determined to be inadequate. Pure copper has a more positive point of zero charge than cadmium or copperized cadmium. Therefore, the rate of nitrate reduction should be higher on copper than on cadmium or copperized cadmium. A copper-disk electrode was constructed as described in Section II.C.3 from polycrystalline copper in order to investigate the reduction of nitrate on copper. The residual voltammogram, Curve A, and the voltammogram obtained in 0.1 mM nitrate, Curve B, in the pH 8 buffer are shown in Figure II-15. The current at -1.0 V vs. SCE is only 18% of the mass transport limited value predicted by Equation II-17 assuming a value of 2 for n. Therefore, it is concluded that the rate of nitrate reduction is not as high on copper as on cadmium. It is also concluded that a more positive value of the reaction plane potential caused by the copper on the copperized cadmium, which would not be as positive as that value would be on pure copper, does not by itself account for the copper electrocatalysis.

The activation studies described previously suggest that both metals must be present in order for the reduction process to be electrocatalyzed. An activation study in reverse, i.e., the activation of the copper-disk surface by the slow accumulation of cadmium atoms, was performed to see if cadmium electrocatalysis of the reduction process would be observed on a cadmiumized copper electrode. This activation was performed in the same fashion as were those previously described for Figure II-13 and II-14 except that cadmium ions were reduced and deposited on copper. It was first necessary, however, to determine the stripping potential of the deposited cadmium so that the positive limit of the potential scan could be set at a value where the deposited cadmium would not be oxidized and

Figure II-15. Voltammogram of nitrate reduction in pH 8 buffer at a rotating copper-disk electrode

Nitrate concentration = 0.05 mM
Potential scan rate = 1.0 V min^{-1}
Square root of rotation speed = 6.47 $\text{rad}^{1/2}$ $\text{sec}^{-1/2}$
Electrode area = 0.60 cm^2

A Residual curve
B Curve for reduction of nitrate

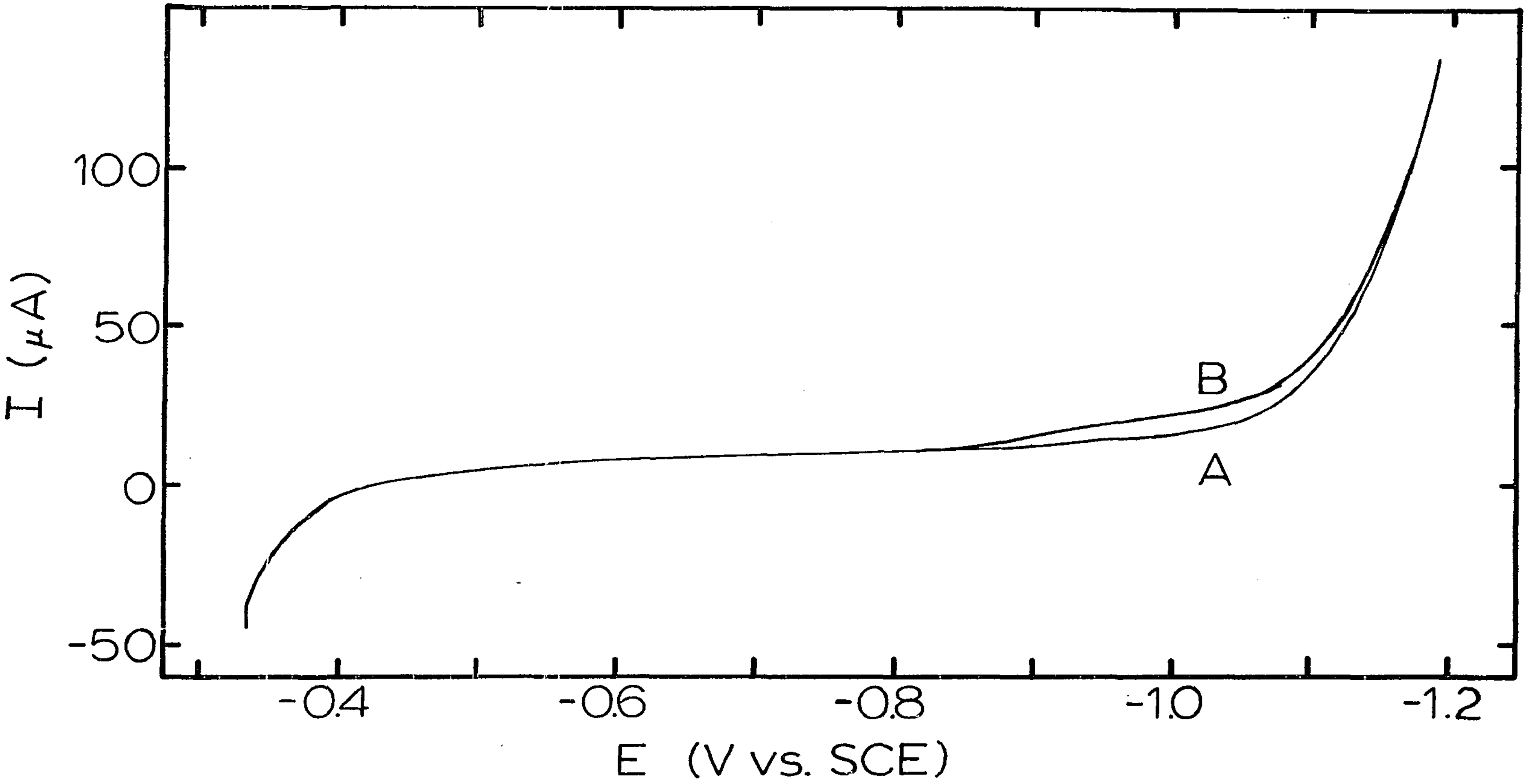
I (μA)
100
50
0
-50
B
A
-0.4
-0.6
-0.8
-1.0
-1.2
E (V vs. SCE)

removed from the surface, i.e., so that the rate of accumulation of cadmium would be mass-transport limited. Figure II-16 shows the voltammogram obtained at the copper disk in 0.14 mM cadmium(II). The stripping potential of the cadmium was determined to be about -0.77 V vs. SCE. Therefore, the positive limit of the potential scan for the activation study was set at -0.93 V vs. SCE.

Figure II-17 shows the voltammograms obtained at the copper disk for 0.1 mM nitrate in the pH 8 buffer during the activation of the disk by the accumulation of cadmium. The reduction wave for nitrate becomes more reversible as cadmium is accumulated, again indicating that both metals are involved in the electrocatalytic phenomenon.

If the copper electrocatalysis is caused by a decrease in the activation barrier of an adsorption step of the reduction process (hypothesis three), it should be possible to derive an expression for the total current, I_T, at any time during the activation studies based on the following assumption. The total current at any time can be expressed by the sum of the current due to the catalyzed reduction occurring on the fraction of the disk which has been covered by the activating atom, I_Θ, and of the current due to the uncatalyzed reduction occurring on the fraction of the disk which has not been covered by the activating atom,

Figure II-16. Voltammogram of cadmium(II) in pH 8 buffer at a rotating copper-disk electrode

Cadmium(II) concentration = 0.14 mM
Potential scan rate = 1.0 V min^{-1}
Square root of rotation speed = 9.71 $rad^{1/2}$ $sec^{-1/2}$
Electrode area = 0.60 cm^2

A Residual curve
B Curve for cadmium(II)

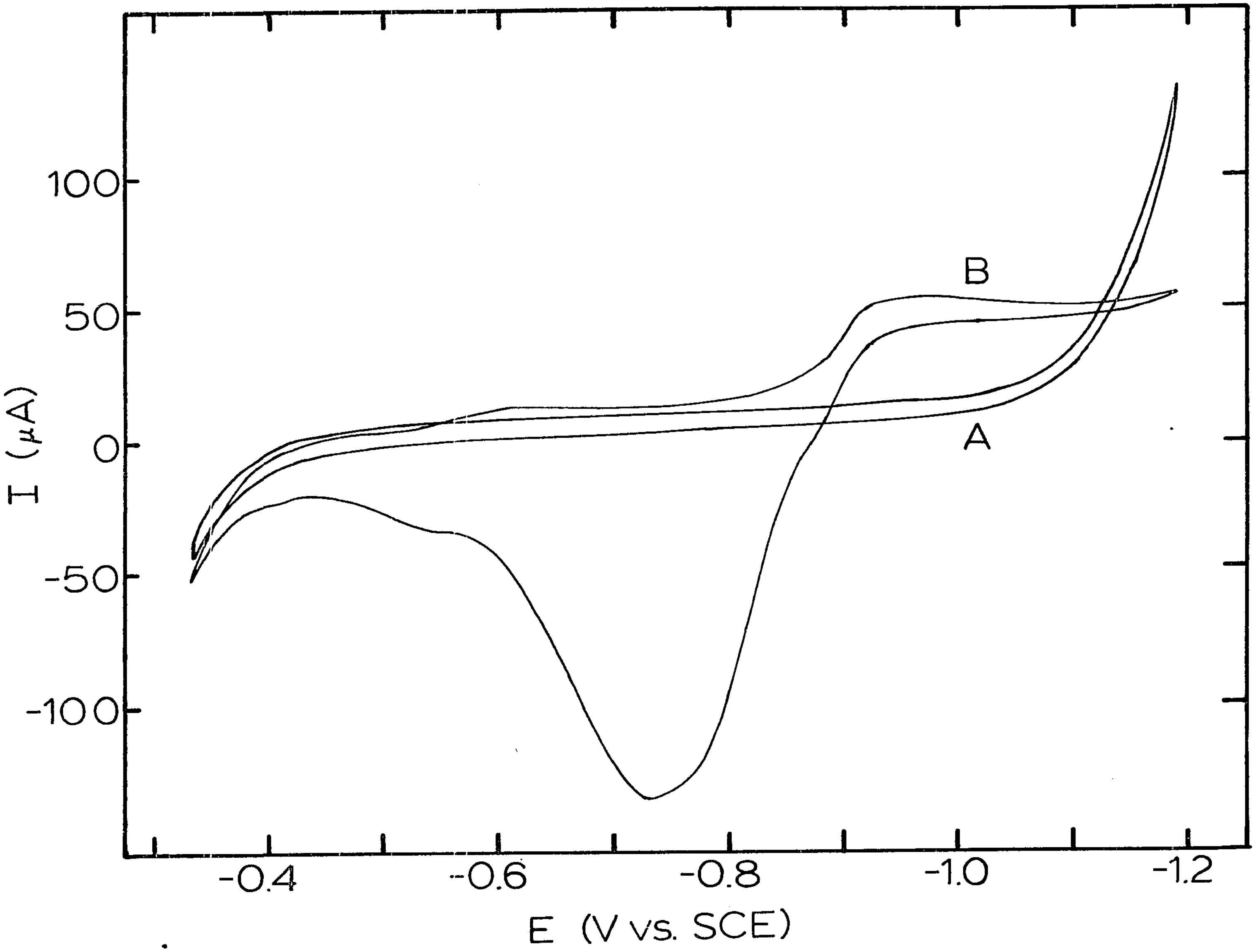
I (μA)
100
50
0
-50
-100
B
A
-0.4
-0.6
-0.8
-1.0
-1.2
E (V vs. SCE)

Figure II-17. Voltammograms of nitrate reduction current at a rotating copper-disk electrode in pH 8 buffer as a function of time dependent deposition of cadmium atoms on disk

Nitrate concentration = 0.50 mM
Potential scan rate = 1.0 V min^{-1}
Square root of rotation speed = 6.47 $rad^{1/2}$ $sec^{-1/2}$
Cell volume = 300 cm^3
Initial cadmium(II) concentration = 4.64 x 10^{-4} mM

Curve	Number of cadmium layers on surface at beginning of potential scan in negative direction
A	0.05
B	0.09
C	0.18
D	0.29
E	0.72
F	1.18

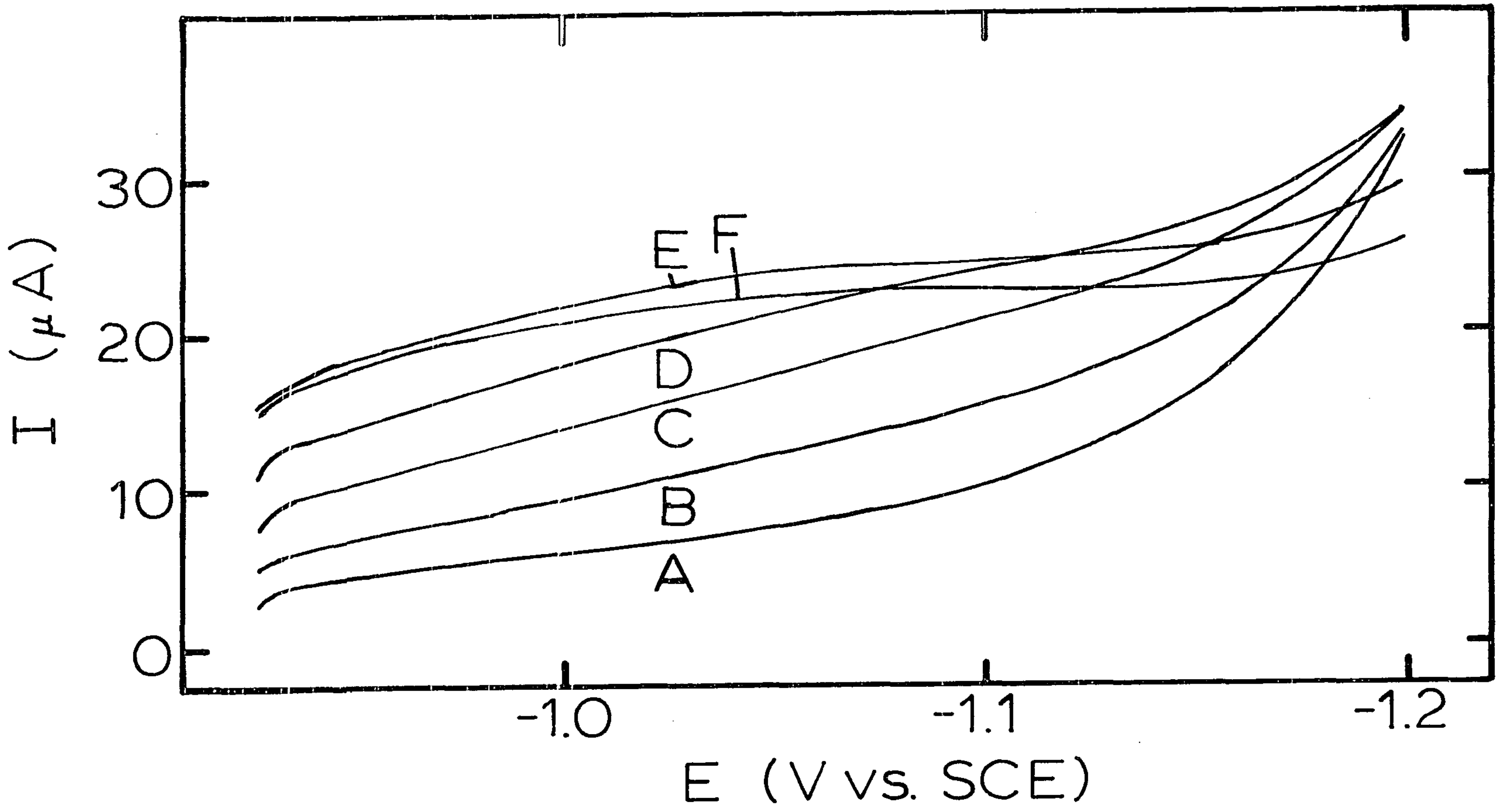
I (μA)
30
20
10
0
E (V vs. SCE)
-1.0
-1.1
-1.2
A
B
C
D
E
F

$I_{1-\Theta}$. This relationship is shown in Equation II-24.

$$I_T = I_\Theta + I_{1-\Theta} \qquad \text{(II-24)}$$

Several attempts were made to derive such an expression but none of the derived expressions could be satisfactorily fit by the experimental data.

Further work needs to be done to mathematically describe the electrocatalysis on the basis of surface coverage, but the following comments can be offered on the basis of the available information. The increase in reduction current during the activation studies does seem qualitatively consistent with the hypothesis that an adsorption of nitrate on the surface is involved in the copper electrocatalysis. No evidence has been presented to show that the activation barrier of that adsorption step is smaller because of the availability of an unpaired d electron as proposed in hypothesis three. This proposal does seem plausible, however, since according to the hypothesis the unpaired d electron only exists when the two metals are both present on the surface. In pure copper the 3d shell is filled, the unpaired electron being an s electron and unavailable to interact with an adsorped reacting species. This in turn accounts for the small reduction rate on copper because the magnitude of the activation barrier of the adsorption step on copper would not be expected to be significantly different from that on cadmium.

In conclusion, the best explanation of the copper electrocatalysis considered in this thesis is that proposed in hypothesis three. I hope that future investigators will be able to show whether or not this explanation is correct.

III. EVALUATION OF LIQUID CHROMATOGRAPHIC DETERMINATION OF NITRATE

A. Review of Recent Methods for Determination of Nitrate

Davenport reviewed the analytical methods for the determination of nitrate, which had been published prior to 1973 (3). While his review is not exhaustive, it is very extensive including about fifty methods for nitrate and about forty-five methods for nitrite. Examples of many different analytical techniques are included. The interested reader is directed to Davenport's thesis for a review of important methods published prior to 1973. Interest in the development of methods for the determination of nitrate has not waned. Since 1973, several methods have been published and these are reviewed here.

Shahine and Ismael have proposed an indirect bromometric method for the determination of trace nitrate involving precipitation with an excess of standard nitron solution (70). The excess nitron in an aliquot of the supernate is brominated with an excess of standard bromine. The excess bromine is then reduced with iodide and the iodine produced is titrated with a standard thiosulfate solution. Nitrite, bromide, iodide, chromate, chlorate, and perchlorate interfere; however, all of these anions except perchlorate can be removed by various chemical schemes. The method was applied to sample aliquots containing between 0.05 and 0.15 mmole of nitrate.

The spectrometric methods for the determination of nitrate that have been published since 1973 include the following. Cresser has measured the gas phase absorption of ultraviolet light by ammonia which was produced by the reduction of nitrate with titanium sulfate (71). The range of nitrate concentrations that gave a linear response was 0-5 ppm; however, this range could be expanded upward at the expense of sensitivity. Senn, Carr, and Klatt have proposed the use of the enzyme nitrate reductase, in conjunction with a radical cation, which is produced by the action of thiosulfate on 1,1'-dimethyl-4,4'-bipyridinium dichloride, to reduce nitrate to nitrite (72). The nitrite so formed is measured colorimetrically after it is quantitatively reacted with sulfanilamide and N-(1-naphthyl)ethylenediamine dichloride to produce an azo dye. The detection limit of this method is 17 ppb nitrate.

Several electrochemical methods for the determination of nitrate have been published since 1973. An air gap electrode was used by Kiang, Kuan, and Guilbault to measure the ammonia produced by the successive reductions of nitrate to nitrite and of nitrite to ammonia with nitrate reductase and nitrite reductase, respectively (73). The range of concentrations of nitrate and/or nitrite that was determined was 5×10^{-5} to 1×10^{-2} M. The use of the enzymes in both the soluble form and in an immobilized enzyme system was investigated. Mertens, Vander Winkel, and Massart have determined nitrate with an ammonia selective electrode using Devarda's Alloy (Cu 50%, Al 45%, and Zn 5%) to reduce the nitrate to ammonia (74). Beads of the reducing agent were successfully imbedded in a polymer for application to a flow-through system. The detection limit for nitrate was 0.1 ppm. Hopirtean, Stefaniga, and Liteanu (75); and Nomura and Nakagawa (76) have described two new nitrate-ion selective electrodes. The former employed genetian violet or tetraphenyl phosphonium bromide in nitrobenzene or tetrachloroethane in a liquid membrane electrode. The latter employed a compressed film of silver diethyldithiocarbamate in a solid electrode. Pfeiffer and Smith (77); and Liedtke and Meloan (78) have reported success in applying commercially available nitrate-ion selective electrodes for the analysis and screening, respectively, of baby foods. A cyclic voltammetric method was published by Bodini and Sawyer using a pyrolytic graphite electrode (79). They spiked their nitrate samples with controlled quantities of cadmium and copper ions which are reproducibly deposited on the working electrode during a linear potential scan in the negative direction. The surface formed catalyses the electroreduction of nitrate. The detection limit is 62 ppb nitrate. Very recently, Cox and Litwinski reported the development of a membrane-clad amperometric sensor for nitrate similar to the Clark oxygen electrode (80). Nitrate is separated from the sample by Donnan dialysis across an ion-exchange membrane and electroreduced at a constrained mercury electrode, the reduction being catalyzed by zirconyl chloride. The detection limit is 6.7 μM nitrate.

At least three methods for the determination of nitrate emphasizing new approaches to the separation of nitrate have been published. Tesch, Rehg, and Sievers have successfully determined nitrate in saliva, blood, water, and suspended particulates by quantitatively reacting the nitrate in the sample with benzene to produce nitrobenzene (81). Gas chromatography, with electron-capture detection, is used to separate and determine the nitrobenzene. The detection limit is 0.1 ppm nitrate in a single drop of saliva or blood. Wheeler and Lott have performed a similar analysis involving the reduction of nitrate to nitrite with either hydrazine or copperized cadmium (82). The nitrite is quantitatively reacted with 2,3-diaminoaphthalene to form the triazole. The triazole is separated by normal and/or reverse phase liquid chromatography. The detection limit for the former separation was 10 ppb nitrate. Small, Stevens, and Baumans have developed a general method for the determination of cations or anions called ion chromatography (83). A low capacity ion-exchange resin is used to separate the ions. The eluting agent is chosen such that it and the separated ions can then be extracted on a high capacity resin to produce water and a base or acid. An acid is produced if anions are being removed and a base is produced if cations are being removed. The conductivity of the acid or base is measured as the effluent passes through a conductivity cell. The detection limit for the method is on the order of 1 ppm. The method was applied for the determination of nitrate.

A description and discussion of a liquid chromatographic method with electrochemical detection for the determination of nitrate is given in this chapter. The development of the amperometric detector is based on the observed electrocatalytic reduction of nitrate on copperized cadmium which is described in the previous chapter. A flow-through disk electrode modeled after the design of Fleet and Little is described and evaluated. The anion-exchange resin used for the separation of nitrate from oxygen is similar to that described by Davenport (3). Also, the observation is made that the interaction of nitrate with the anion-exchange resin described is favorably altered when a large excess of chloride is added to the sample. Investigations of this phenomenon are described. The results of an interference study and a precision study are given. Finally, descriptions are given of the determinations of nitrate in several unknown samples and of an attempted determination of nitrite in one of the unknown samples.

B. Experimental

1. Reagents

The reagents used in the amperometric experiments discussed in this chapter were essentially those used in the voltammetric experiments described in Chapter II except as specified below.

The pH 8 buffer solution contained 0.5 M THAM and 0.22 M perchloric acid. Perchloric acid was used in place of hydrochloric acid because the eluent chosen to be used in the liquid chromatograph, described in Section III.B.4, contained perchloric acid. The high concentration of buffer constituents were necessary to provide adequate buffer capacity when the buffer solution was mixed with the chromatographic effluent before passing through the amperometric detector. The mixing process is described in Section III.C.3.

Because all measurements of nitrate reduction current were made following the separation of the nitrate from the remaining constituents of the test solution, samples were prepared in deionized water rather than in the supporting electrolyte.

2. Preparation of strong anion-exchange columns

Anion-exchange columns were prepared from three commercially available resins: Amberlite IRA-900, Amberlyst A-26, and Dowex 1-X8. The retention of nitrate on each column is discussed in Section III.C.3. Described below are procedures for refining the commercial resins and for packing the columns.

The Amberlite IRA-900 from Rohm and Haas, Philadelphia, PA, was ground by hand with a porcelain mortar and pestle. The ground resin was then passed through a stack of sieves by continuously washing with deionized water. The stack was composed of five sieves with 60, 80, 100, 180, and 250 mesh screens. This process was extremely slow and inefficient. The fine particles electrostatically attached to the 180 to 250 mesh fraction were removed hydrostatically by backwashing a column of the resin in a burette with deionized water. Glass columns were packed with 180-250 mesh resin by applying suction to one end of the column while dipping the other end into a slurry of the resin in deionized water.

Amberlyst A-26, from Rohm and Haas, was similarly prepared except that the resin was ground in a Waring blender. The blender jar was filled less than one-half full with resin and water and the blender was run at its top speed for 3-5 min. The ground resin was sieved as above. The

180-250 mesh fraction was sieved a second time through a 200 mesh screen to produce a 180-200 mesh fraction which was packed as above. This fraction was treated hydrostatically to remove fine particles and packed into a column as described above. The column prepared with Amberlyst A-26 is designated as C-1.

Dowex 1-X8 resin (200-400 mesh) was obtained from Bio-Rad Laboratories, Richmond, CA. This resin was used without additional grinding and screening. The resin was washed with 2-propanol to remove excess water and then spread on a towel so that the 2-propanol could evaporate. The dried resin was dry sieved with a Tyler mechanical sieve. The stack of sieves for this operation was composed of U. S. Sieve No's. 170, 230, 270, and 325; a collection pan was also used. This procedure required no operator attention and is deemed to be superior to the wet sieve method described above. Fine particles in the fraction collected in the collection pans were removed by floatation in 2-propanol, i.e., particles of resin that floated, or settled only very slowly in 2-propanol were decanted. Three 50-mL portions of 2-propanol were mixed with the resin and decanted to insure complete removal of fines. The 2-propanol was washed from the resin with water. A glass column was packed with this resin by delivery under pressure from a plastic syringe containing a slurry of resin in water. This column is designated C-2.

3. Flow-through electrodes

The cadmium flow-through detector, shown in Figure III-1, was constructed in the Chemistry Shop at Iowa State University. The body of the detector was made from a $2^1/4$ inch x 2 inch (diameter) rod of silica-loaded Teflon obtained from Cadillac Plastics of Davenport, IA. The Teflon rod was drilled, and tapped where necessary, to provide chambers for the working, reference, and auxiliary electrodes, and channels for the flow of solution.

Solution entering the detector at Port A impinges normally on the working electrode in chamber B. Two channels provide flow paths to the reference electrode chamber, D, and the auxiliary electrode chamber, E. Finally solution is channeled to a waste collector through exit Ports G and H (see horizontal cross section).

The working electrode chamber is large enough to receive a miniature calomel reference electrode. The dimensions of the upper and lower portions of the working electrode chamber are 3/4 inch x 1/2 inch, and 7/8 inch x 3/16 inch, respectively. A Fetfe o-ring with an internal diameter slightly less than 3/16 inch holds the reference electrode in position and prevents flow of solution out of the top of the chamber.

The Pt-wire auxiliary electrode, F, is inserted through a standard tube-end fitting from Altex, Inc., and through a

Figure III-1. Drawing of vertical and horizontal cross section of flow-through disk detector

A	Entry port
B	Working electrode chamber
C	Retractable working electrode tip
D	Reference electrode chamber
E	Auxiliary electrode chamber
F	Auxialiary electrode
G	Exit port from reference electrode chamber
H	Exit port from auxiliary electrode chamber

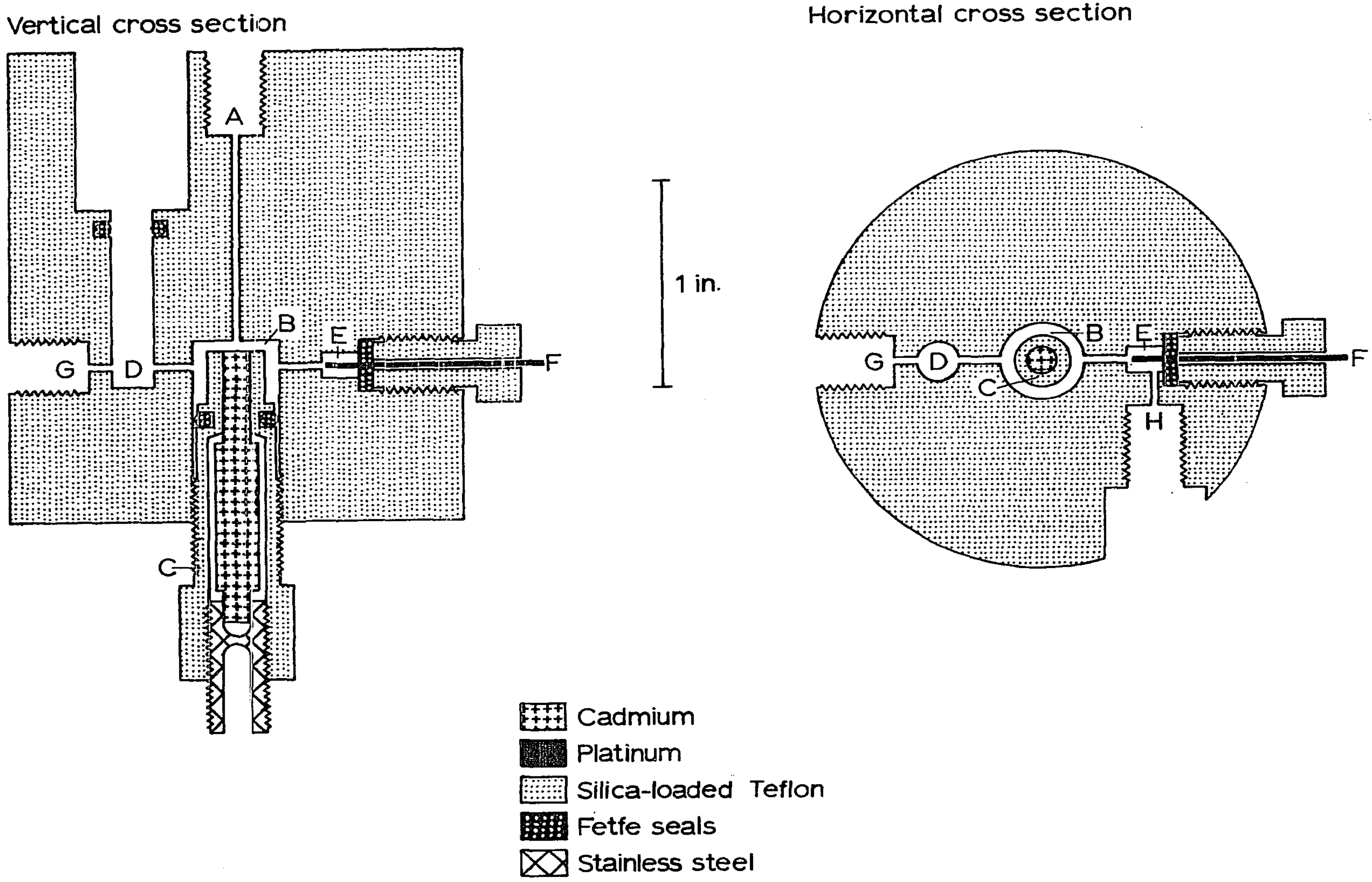
Vertical cross section
A
B
E
F
G
D
C
1 in.
Horizontal cross section
B
E
F
G
D
C
H
Cadmium
Platinum
Silica-loaded Teflon
Fetfe seals
Stainless steel

disk of Fetfe into the auxiliary electrode chamber. Fetfe is a pliable fluoroelastomer from Ace Glass, Inc., Vineland, NJ. Fetfe is inert to strong acids and corrosive solutions and is frequently used for making compression seals.

The retractable working electrode tip, C, is constructed of 3 parts: a cadmium shaft, a silica-loaded Teflon shroud, and a short stainless steel banana jack. The cadmium shaft was prepared by carefully machining one end of a stick of cadmium metal (99.9%), obtained from Fisher Scientific Company, to a 3 mm diameter. The other end was machined to a 1/8 inch diameter such that it could be pressed into one end of the stainless steel banana jack. The diameter of the central portion was left larger (approx. 0.2 inch) to prevent bending of the shaft during machining. The banana jack-shaft assembly was then sealed in the silica-loaded Teflon shroud with Devcon "5 Minute" Epoxy. This shroud was tapped internally to fit the 1/4 inch x 32 threads of the banana jack and externally to fit the 3/8 inch x 32 threads of the detector body. A Fetfe o-ring was again used to provide a solution seal.

The banana jack provides a means of making electrical contact to the working electrode metal. It also makes possible the conversion of the retractable working electrode tip into a tip for the disk electrode shaft described previously in Section II.C.3. For this purpose a 1/2 inch adapter with appropriate threads was machined from stainless steel.

A Pt-working electrode tip was prepared in the same fashion. In order to conserve the precious metal, the bulk of the shaft was made from stainless steel with a 2 mm disk of Pt soldered to its exposed end.

The exposed metal surfaces of the cadmium and platinum working electrode tips were polished in the same manner as previously described.

A silver wire flow-through electrode was made by substituting a 16-gauge silver wire for the platinum wire working electrode in the detector described by Snider (84).

4. Liquid chromatograph

Figure III-2 shows a schematic diagram of the liquid chromatograph used in this work. The design and construction of the chromatograph was similar to that reported by Davenport (3). Components of the chromatograph were connected using Teflon tubing (0.063 inch o.d. x 0.031 inch i.d.), standard tube-end fittings (with 1/4 inch x 28 threads), and Teflon-glass connectors (2 mm i.d. x 7 mm o.d. x $3^1/4$ inch). Tubing, fittings, connectors, the Kel-F tee (I), and the rotary sample injection valve (F) were obtained from Larry Bell and Associates, Hopkins, MN. The capillary metering type, Teflon-glass valves (D) and the flowmeters (E) were obtained from Roger Gilmont Instruments, Inc., Great Neck, NY. Teflon-glass connectors attached to the Teflon-glass valves and holders for the flowmeters

Figure III-2. Schematic diagram of liquid chromatograph

A	Helium tanks
B	Eluent reservoir
C	Buffer reservoir
D	Flow control valves
E	Flow meters
F	Sample injection valve
G	Cation-exchange column
H	Anion-exchange column
I	Mixing chamber
J	Disk detector
K	Potentiostat
L	Stripchart recorder

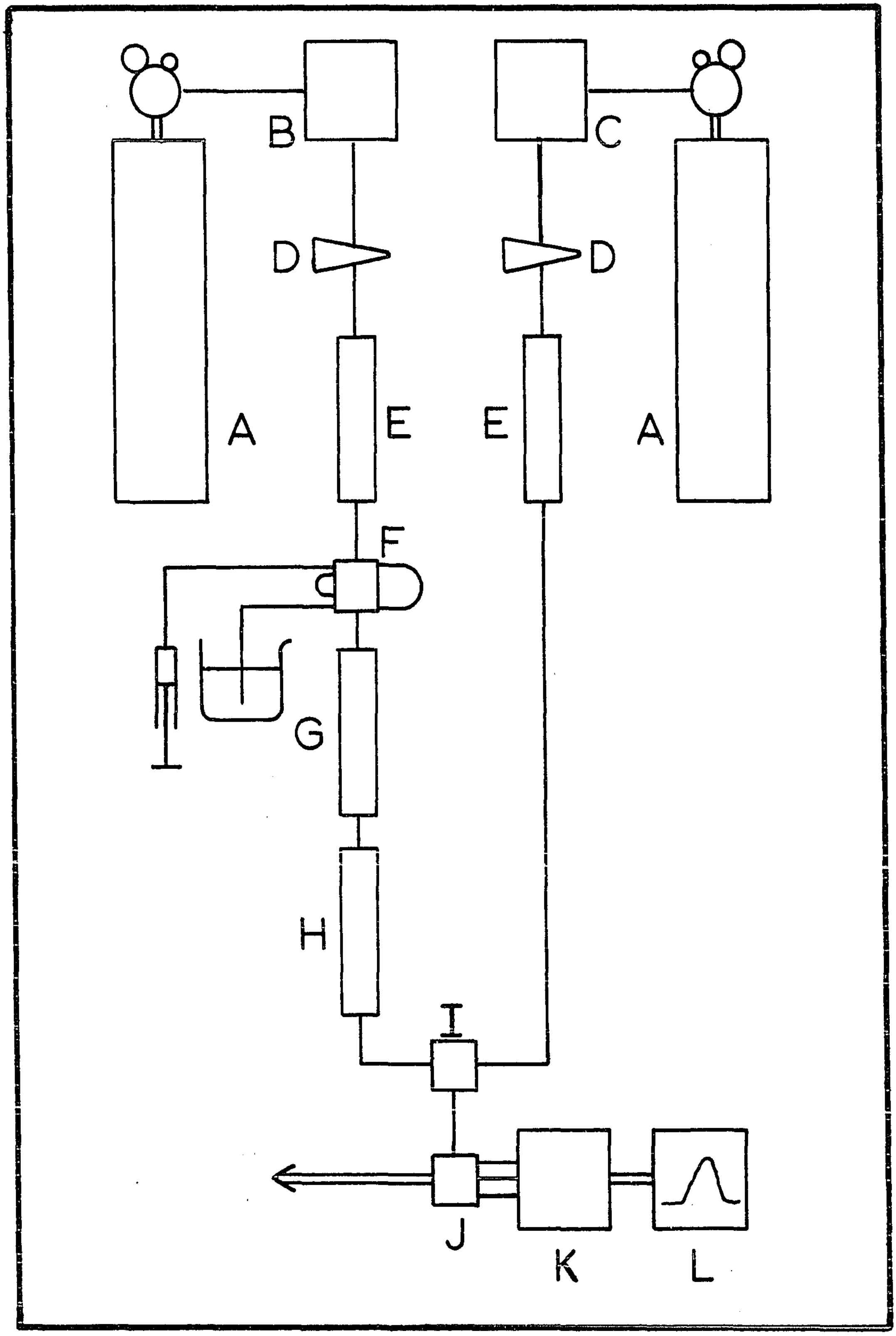
B
C
D
D
A
E
E
A
F
G
H
I
J
K
L

were constructed in the Chemistry Shop of Iowa State University.

Two helium tanks were used to supply pressure to two reagent reservoirs. The pressure, as measured by two stage regulators was not allowed to exceed 40 psi. The reservoirs are described elsewhere (85). One reservoir contained eluent, the composition of which varied from 2-5 mM perchloric acid. The other reservoir contained a pH 8 buffer composed of 0.5 M THAM and 0.22 M perchloric acid. Helium was bubbled through both the eluent and the buffer before pressurization to remove oxygen. This was necessary because oxygen is electrochemically active at the detector. To minimize accumulation of oxygen in the flow stream by permeation through the Teflon tubing, chromatographic components were arranged as close as possible such that very short pieces of Teflon tubing could be used for connection. The velocities of the fluid streams from the reservoirs were controlled independently by the manipulation of the pressure applied to the respective reservoirs and/or by the manipulation of the Teflon-glass valves in the flow streams. The velocity of the eluent was maintained at a value approximately 4 times that of the buffer.

The cation- and anion-exchange columns (G and H) were made in the Chemistry Glass Shop. The dimensions of the columns were 6 mm o.d. x 4 mm i.d. x 9 cm and 6 mm o.d. x 2 mm i.d. x 10 cm, respectively.

The only cation-exchange column was prepared with 100-200 mesh AG^{R} 50W-X8 Analytical Grade Cation Exchange Resin in the H^{+} form. The resin was used as received from Bio-Rad Laboratories. The column was repacked periodically with fresh resin.

Several anion-exchange resins were investigated. Discussion of the preparation of, and of the interaction of nitrate with, these resins are discussed in Sections III.B.2 and III.C.3, respectively. The resin that gave the best results was Dowex 1-X8, Bio-Rad Laboratories.

Effluent from these columns during chromatographic analysis was mixed with the buffer solution in the Kel-F tee (I). Complete mixing was effected by loosely packed glass wool in a short section of Teflon tubing between the mixing tee and the detector (J).

The potential of the electrochemical detector was controlled with the three-electrode potentiostat described in Section II.C.2. Current at the working electrode was recorded as a function of time, by monitoring the output of the current follower in the potentiostat with a Heath-Schlumberger Strip Chart Recorder (Model SR-255 A/B), Ann Arbor, MI. It was necessary, particularly at the more sensitive settings of the recorder and current follower, to offset a rather large background signal which resulted from the reduction of oxygen which had permeated the system lines.

The sample injection loop was calibrated against a 2-mL pipette by acid-base titrimetry. The loop was found to have a volume of 0.3086 ± 0.0011 mL.

5. Experimental procedures

At the beginning of each work period operation of the liquid chromatograph was initiated in the following fashion. The solution reservoirs were pressurized and the volume flow rates of the eluent and buffer were adjusted to approximately 1.0 and 0.25 mL min^{-1}, respectively. The cadmium-electrode tip was taken out of the flow-through disk detector and the surface was wiped with a paper towel to remove copper present from previous use. If the cadmium surface was observed to be pitted, it was polished with 6 µ and 1 µ diamond polishing compounds, according to standard metallurgical practice. The tip was swirled in a 0.08 M copper sulfate solution for approximately 10 sec and then was rinsed with a stream of deionized water. The copperized cadmium-electrode tip was then screwed into the working electrode chamber of the detector body until the flow meter in the buffer stream indicated a decrease in the flow rate of the buffer. Since there was no back pressure in the buffer stream, this was a very sensitive way of telling when the distance between the disk and the entrance channel orifice was just large enough to allow free flow of solution. This optimum distance, so determined, is discussed in Section III.C.1. The reference electrode was then removed so that gas bubbles trapped in the passage between the working electrode and reference electrode chambers could be washed out through the latter chamber. As the reference electrode was reinserted, the sudden increase in the flow rate of solution was usually sufficient to dislodge gas bubbles trapped in other detector channels and in the Teflon tubing connected to the exit ports of the detector body. To be sure that all bubbles were removed, first one of the exit channels, and then the other, was temporarily blocked until free flow from both channels was observed. The exit tubes were positioned against the wall of a flask so that a continuous stream of solution was formed on the flask wall. If the streams were not continuous, the falling of drops of solution that formed at the ends of the tubes was observed to coincide with periodic spikes in the background signal of the detector. The electronic components of the system were then turned on and the potential of the working electrode was adjusted to the desired value. Occasionally, the latter adjustment was impossible because of gas bubbles trapped in the passage between the working electrode and auxiliary electrode chambers. When this occurred, there was no electrical contact between those two electrodes and it was necessary to remove the auxil ary electrode, block the ends of both of the exit tubes and flush the offending gas bubbles from the system. When the desired working electrode potential was achieved, the flow rates of the solutions were again adjusted to the previously stated values. It was usually necessary to wait about 30 min for the background signal to decay to a steady value. Part of this background signal resulted from charging of the electrode; but most of it resulted from the decaying concentration of oxygen in the Teflon lines of the system. Problems related to the permeation of the system by oxygen are discussed in Section III.C.4.

The nitrate in several unknown samples was determined by the liquid chromatographic method described in this work. These included two natural water samples, a spinach extract, and a commercially available salt for curing meat. The nitrite in the meat curing salt was also determined with the liquid chromatograph by a different method following chemical oxidation of the nitrite to nitrate. In all cases, except for the spinach extract, an attempt was made to obtain a value for the concentrations of the desired constituents by a second analytical method.

Details of the preparation and treatment of each sample are given below. It may be said that all of the liquid chromatographic analyses were performed by the method of standard addition. I applied this technique by comparing the measured areas of the peaks obtained when aliquots of samples containing unknown amounts of nitrate and aliquots of the same samples to which a known amount of nitrate had been added were injected into the liquid chromatograph. Peaks areas were measured with a planimeter obtained from Keufel and Esser Co., Germany. For the chromatographic method, two aliquots of each sample prepared were injected alternately with two aliquots of the corresponding spiked sample. Also, most of the solutions which were analyzed by this method were purged of oxygen by bubbling nitrogen through the solutions for 5 to 10 min.

The 5-mL portions of a sample of well water which was thought to contain nitrate were provided by the Veterinary Diagnostic Laboratory, Iowa State University. The portions were identical accept that the laboratory personnel had added extra nitrate to one, the amount of which was unknown to me until after the analysis was complete. Two mL of each portion was combined with 0.5 mL of 1.0 M potassium chloride and diluted to the mark in a 5 mL volumetric flask with deionized water. To another 2 mL of each portion, treated in the same way, I added a known amount of potassium nitrate.

A larger sample of water from the Saylorville Reservoir in Central Iowa was obtained from the Engineering Research Institute, Iowa State University. The sample was acidified when taken from the reservoir with approximately 2 mL of concentrated sulfuric acid to prevent bacterial consumption of the nitrate (86). A piece of pHydrion Paper, Micro Essential Laboratory, Brooklyn, NY, was used to determine that 0.6 mL of 1.0 M potassium hydroxide was sufficient to neutralize the acid in a 10 mL portion of the sample. Therefore, 10 mL of sample, 2.5 mL of 1.0 M potassium chloride and 0.6 mL of 1.0 M potassium hydroxide were diluted to the mark in a 25 mL volumetric flask. A second 25 mL solution containing identical amounts of these chemicals plus a known amount of standard nitrate was also prepared. This sample was analyzed for nitrate by a colorimetric method in the Energy Research Institute, Iowa State University.

The spinach sample was obtained at a local food market. A 7.8 g sample, weighed as received, was ground in a Waring Blender with a small amount of deionized water. The mixture was filtered to remove the small amount of solids which remained and the sample was then diluted to 250 mL. A portion of this final solution of the sample was used to dilute a known quantity of potassium nitrate to 100 mL.

Four solutions, designated Solutions 1 through 4 were prepared from the meat curing salt as follows. Approximately 2.5 g of the salt was dissolved in 500 mL of deionized water to produce Solution 1. Solution 2 was prepared by combining 98 mL of Solution 1 with 2 mL of 10.0 mM potassium nitrate. Solution 3 was prepared by combining 90 mL of Solution 1 with 10 mL of 3% hydrogen peroxide. Solution 4 was prepared by combining 88 mL of Solution 1, 2 mL of 10 mM potassium nitrite, and 10 mL 3% hydrogen peroxide. A second 2.5 g sample of the meat curing salt, which had been dried in an oven at 90 °C for about 4 hr, was treated in the same way to produce Solutions 5 through 8, where Solution 1 corresponds to Solution 5, 2 to 7, etc. Two aliquots of each of the eight solutions were injected into the liquid chromatograph. The hydrogen peroxide was added to Solutions 3, 4, 7, and 8 to oxidize any nitrite present to nitrate so that the nitrite could be determined by difference.

The colorimetric procedure described by the Environmental Protection Agency of the United States for the determination of nitrite and nitrate in water and waste water samples was also used to analyze the meat curing salt (38). Approximately 0.9 g of the salt was dissolved in 500 mL of deionized water. The above procedure was followed without modification to determine the nitrite and nitrate content of this solution. A nitrite calibration curve was prepared with a series of potassium nitrite standard solutions. Aliquots of the unknown solution were passed through a copperized cadmium reductor column, as prescribed by the procedure, to reduce the nitrate to nitrite. Because the efficiency of the reductor column was unknown, the nitrate in a series of potassium nitrate standard solutions was also reduced by this method, and a nitrate calibration curve was prepared. The nitrite content of all solutions that had been passed through the reductor column was determined by comparison of that solution's absorbance to the nitrate calibration curve. Approximately 0.9 g of the meat curing salt, which had been dried as described above was also dissolved in 500 mL of deionized water. This solution was analyzed colorimetrically in the same manner.

The results of the analysis of each of these samples are discussed in Section III.C.8. Also, Section III.C.5, is devoted to the discussion of the chloride loading phenomenon which was discovered when the salt sample was analyzed chromatographically. Several other investigations were performed with the liquid chromatograph or modifications thereof to determine optimum analysis conditions. Procedural details of these experiments are given along with the discussion of results in Sections III.C.1 through III.C.7.

C. Results and Discussion

1. Evaluation of flow-through disk detector

The design of the cadmium tubular electrochemical detector described by Davenport (3) was found to be inadequate for this investigation. The internal working surface of the tube could not easily be polished, and it could not be visually inspected following electrochemical or chemical treatment. The cylindrical surface of the tubular geometry was concluded to be significantly different from the planar surface of the cadmium-disk electrode (Section III.B.3) because of difficulty experienced in obtaining a tube surface on which the reduction of nitrate occurred. Procedures that activated the disk surface did not activate the tube surface. It was, therefore, necessary to investigate other detector configurations which meet the following criteria:

1) the working electrode must be planar;
2) the working electrode must be physically accessible;
3) the working electrode should be adaptable to the rotator;
4) the detector should have a small cell volume.

Detectors based on two configurations reported in the literature were considered.

A thin-layer amperometric detector was constructed after the design of Kissinger (87). The working electrode was a disk of cadmium imbedded in one of two blocks of silica-loaded Teflon. A rectangular channel for flow of solution was formed by cutting a 2 mm x 1 cm slit in a 50-μ Teflon gasket and sandwiching the gasket between the two blocks of Teflon. The working electrode surface was one wall of the channel. This detector failed under experimental conditions because solution was found to leak between the gasket and blocks resulting in serious tailing of injected analyte and in corrosion of the unexposed cadmium. Also, as designed, this detector did not meet criteria 3, above.

A second detector was constructed which is similar to that of the wall-jet electrode described by Fleet and Little (88). This detector was described in Section III.B.3. Although the geometry of the working electrode in this detector is identical to that of Fleet and Little, I have chosen to use the name "flow-through disk detector rather than "wall-jet detector" for reasons discussed below.

Glauert used the term, "wall-jet" in 1956 to describe the flow pattern of a fluid issuing from a circular nozzle onto a planar surface (wall) positioned perpendicular to the direction of flow from the nozzle (89). Under these conditions the fluid disperses radially on the wall and back away from the wall into the space around the nozzle. A two-dimensional drawing of this flow pattern is shown in

Figure III-3-A. The vectors in the figure are meant to be a representation of the direction of flow.

Yamada and Matsuda evaluated a wall-jet electrode for which the term wall jet is very descriptive of the configuration (90). A circular disk, coincident with the plane of the wall and concentric with the nozzle, formed their working electrode surface. The diagonal lines in Figure III-3-A represent this disk. They derived Equation III-1 from fundamental principles which gives the limiting current, I, at the wall-jet electrode as a function of the steady state supply of an electroactive species in the fluid issuing from the nozzle.

$$I = (1.60\ k)nFD^{2/3}\nu^{-5/12}V_f^{3/4}a^{-1/2}R^{3/4}C^b \qquad \text{(III-1)}$$

In Equation III-1:

I = steady-state current at the working electrode;

n = number of electrons transferred in the electrode reaction;

k = proportionality constant;

V_f = volume flow rate;

a = radius of the nozzle;

R = radius of disk in the wall.

These workers experimentally verified the predicted dependence of I on each variable except D in Equation III-1.

It is noteworthy that electrode current was not predicted to depend on the distance between the nozzle and disk, d.

Figure III-3. Two dimensional drawing representing flow patterns near the working electrode within (A) a wall-jet detector and (B) a flow-through disk detector

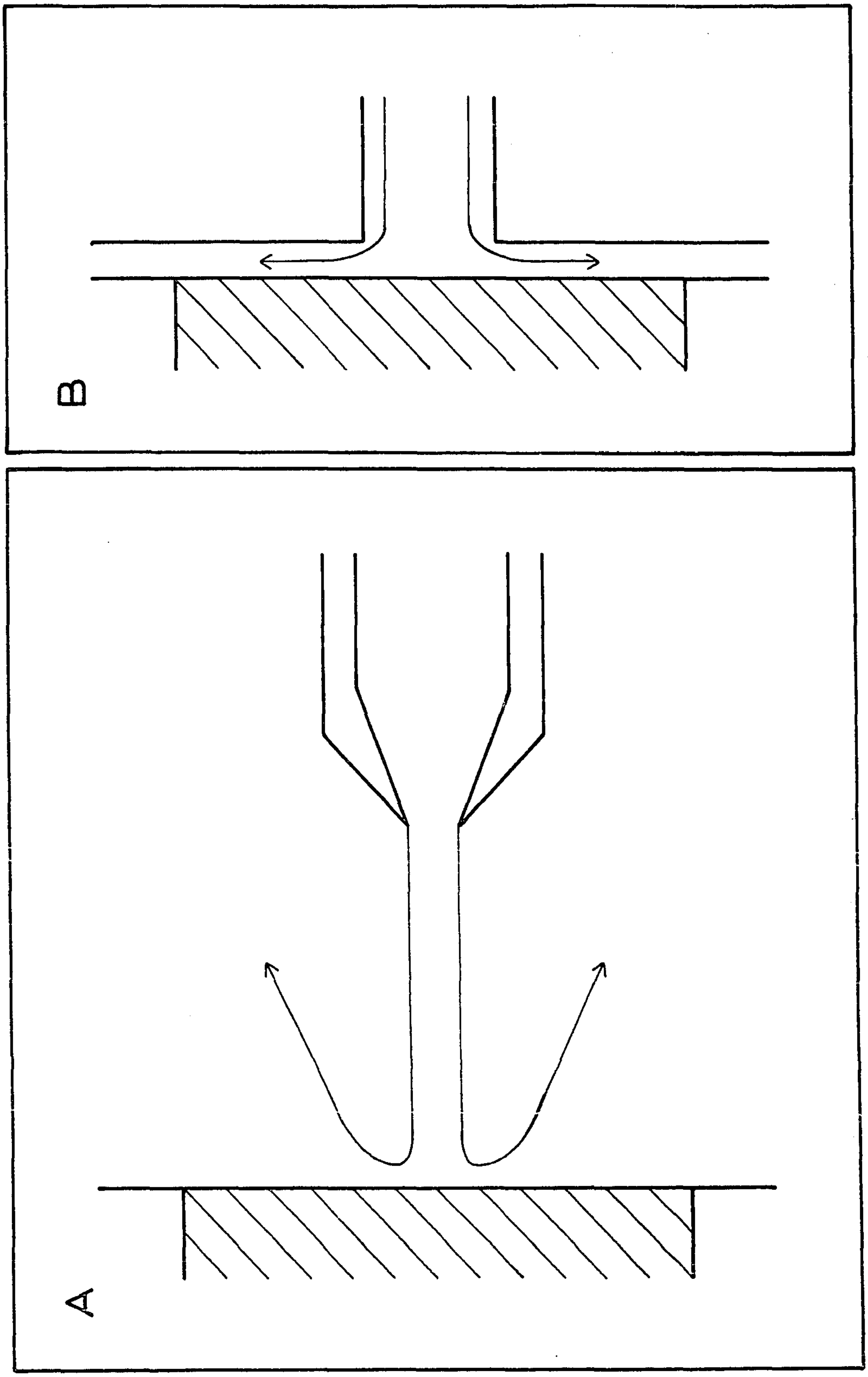
B
A

Yamada and Matsuda reported that for large values of V_f (20 m /min) and small values of the parameter a (0.3 mm) the current was indeed independent of d for values of d between 2 and 10 mm. These conditions for V_f and a, correspond nicely to the dictionary definition of the word jet (91) "a forceful rush of liquid, gas, or vapor through a narrow opening or nozzle".

Fleet and Little based their detector design on the wall-jet electrode just described; however, they made a significant modification (88). They mounted the working electrode disk in a wall as in the former, but replaced the nozzle with a channel orifice in second wall parallel to the first, and separated from it by a distance d. The orifice was again concentric with the disk so that solution issuing from the orifice still disperses radially on the disk, but the presence of the second wall hinders flow away from the working electrode surface. The vectors in Figure III-3-B represent this flow pattern. Kissinger has not had recently classified this detector as a "thin-layer detector" (87).

Fleet and Little report some data that support the contention that the two designs are different. They found that electrode current varied with d to a greater extent than Yamada and Matsuda reported. Specifically, they observed that current increased to a maximum value at d equal to about 0.5 mm and decreased rapidly as d increased to 3 mm. For values of d less than 0.2 mm, it was impossible to make useful measurements because of turbulence at the disk. Unfortunately, Fleet and Little do not report the diameter of the channel orifice or the magnitude of the volume flow rates for their detector. Also, they do not report the results of any experiments that would have verified the predicted dependence of electrode current on variables in Equation III-1. Results reported below from investigations I performed with the flow-through disk detector, indicate that electrode current does not depend on d or V_f as Equation III-1 predicts.

For the investigation of the response of the flow-through disk detector it was necessary to choose an electrode reaction for which the heterogeneous rate constant is large resulting in mass-transport limited electrode current. The oxidation of iodide to iodine occurs between 0.6 and 0.85 V vs. SCE on platinum in 0.1 M sulfuric acid. The linearity of the plot of limiting current for this process vs. the square root of rotation speed in Figure III-4 verifies that even at high rates of mass transport the necessary condition is satisfied. The data for Figure III-4 are listed in Table III-1.

The investigation of the dependence of electrode current at the flow-through disk detector on d and V_f was

Figure III-4. Dependence of iodide oxidation current on rotation speed of a platinum-disk electrode at 0.70 V vs. SCE in 0.10 M sulfuric acid

Iodide concentration = 0.12 mM
Electrode area = 0.033 cm^2

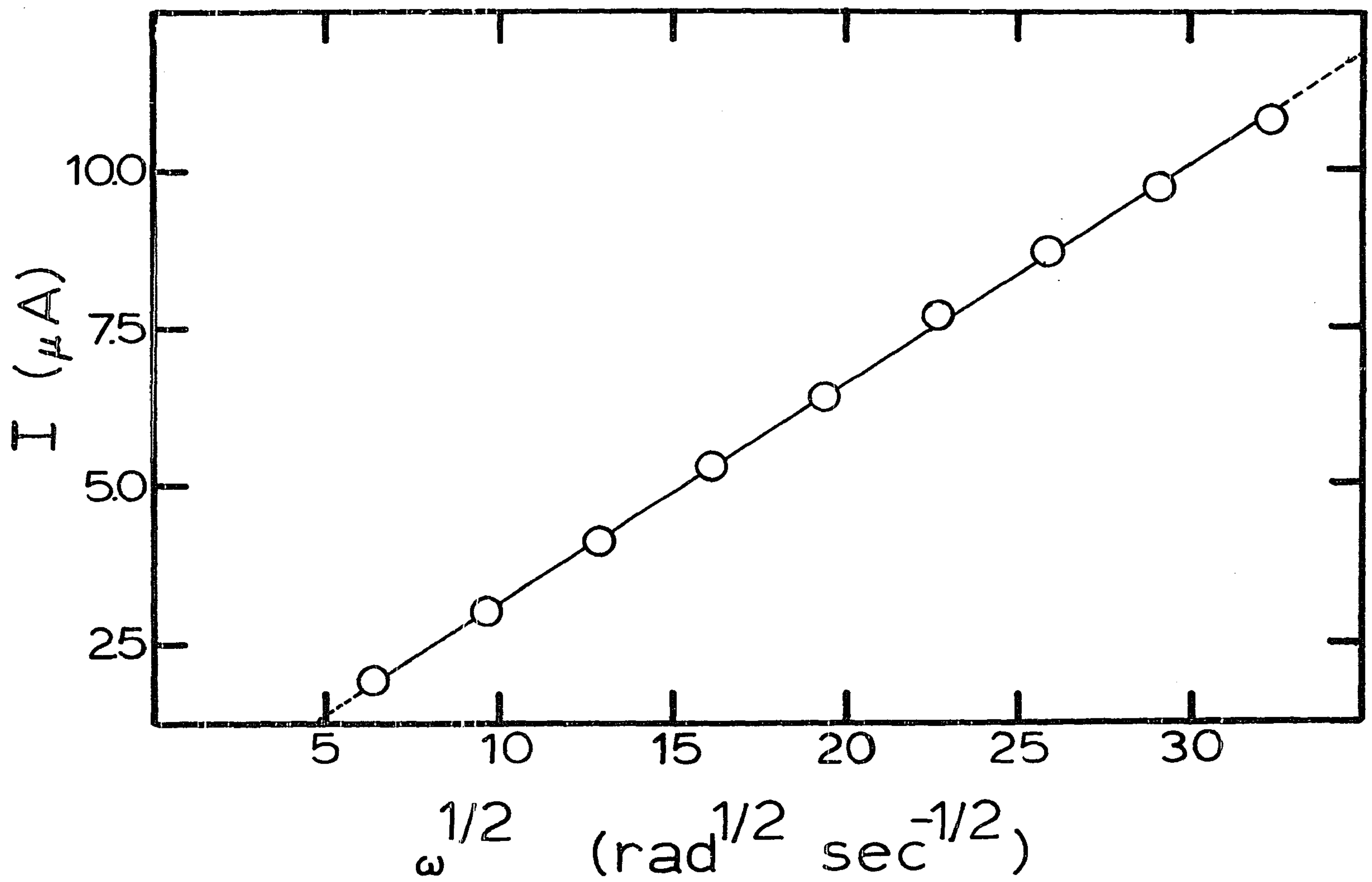
10.0
7.5
5.0
2.5
I (μA)
5
10
15
20
25
30
ω^1/2 (rad^1/2 sec^-1/2)

Table III-1. Dependence of iodide oxidation current on rotation speed of a platinum-disk electrode at 0.70 V vs. SCE in 0.10 M sulfuric acid[a]

$\omega^{1/2}$ ($rad^{1/2}$ $sec^{-1/2}$)	I (mA)
6.5	1.92
9.7	3.00
12.9	4.10
16.2	5.26
19.4	6.41
22.6	7.70
25.9	8.70
29.1	9.70
32.4	10.76

[a] Data shown graphically in Figure III-4.

performed as follows. The buffer in the liquid chromatograph described in Section III.B.4 was replaced by a 0.120 M potassium iodide solution in deoxygenated 0.1 M sulfuric acid. The volume flow rate was monitored by measuring the volume of effluent flowing from the detector into a burette during a known amount of time as measured with a stop watch. The platinum tip used in the rotation speed study of the oxidation of iodide to iodine was inserted into the flow-through disk detector body, and potentiostated at 0.70 V vs. SCE. The value of d was estimated by unscrewing the tip from a completely closed position in quarter turn increments. Each quarter turn corresponded to approximately 0.2 mm. At values of d less than 0.2 mm, constriction in the working electrode chamber resulted in a significant decrease in V_f, making measurements in this region meaningless.

The results of the experiment are shown graphically in Figure III-5. The data for Figure III-5 are listed in Table III-2. The slope of the plot of In I vs. In V_f is 0.329, which is not in agreement with the value of 0.750 as predicted for the wall-jet configuration by Equation III-1. The slope of the plot of ln I vs. ln d is approximately -0.75 which is not equal to 0 as predicted by Equation III-1. These results are taken as evidence that the wall-jet and flow-through disk configurations are not

Figure III-5. Dependence of mass-transport limited current at working electrode of flow-through disk detector on volume flow rate, V_f, of solution and on distance, d, between disk and channel orifice

Iodide concentration in 0.10 M sulfuric
acid = 2 mM
Electrode potential = 0.70 V vs. SCE
Electrode area = 0.033 cm^2

For Volume flow rate study
d = 0.20 mm

For study of dependence of current on d
V_f = 0.22 mL min^{-1}

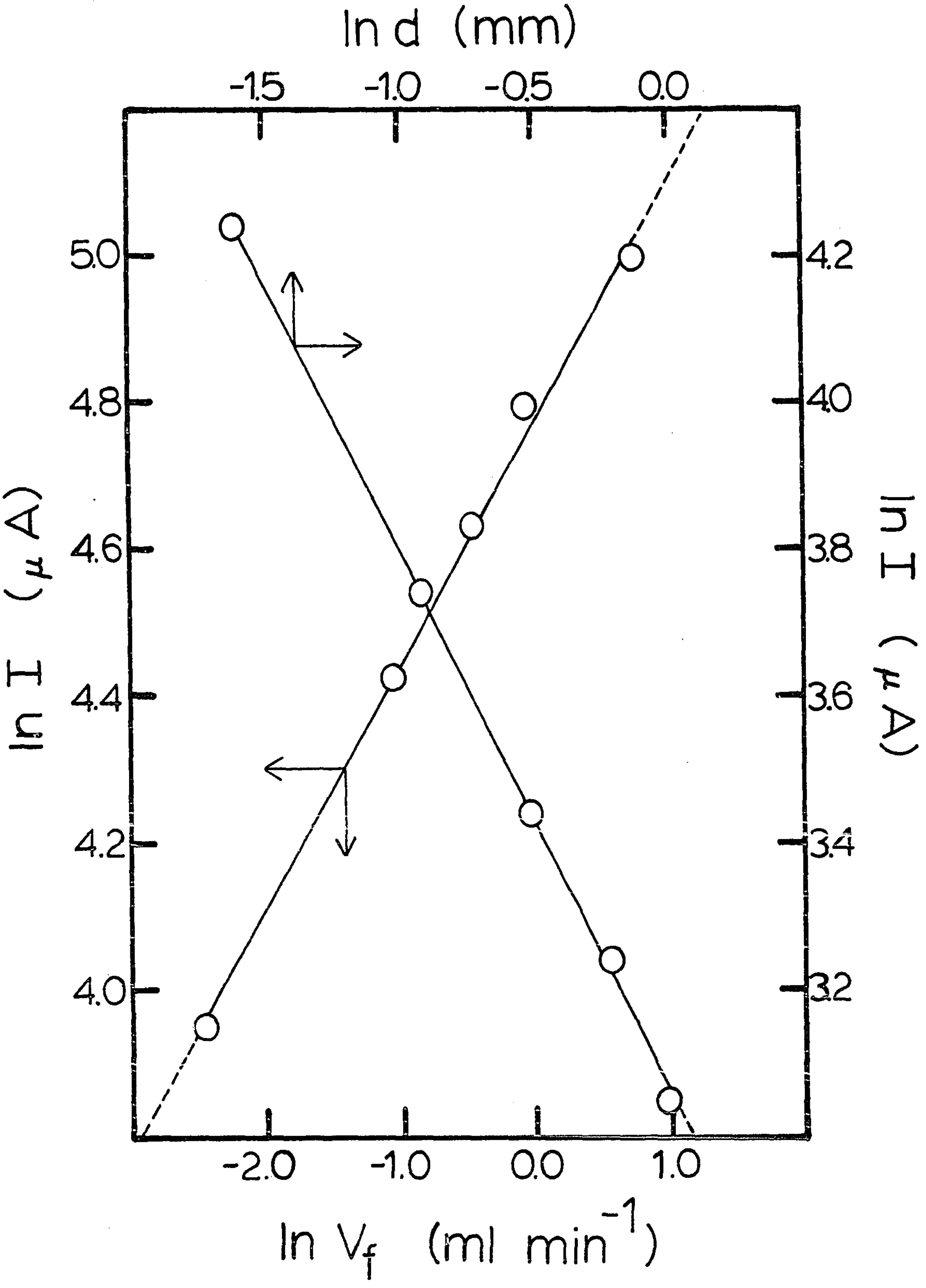
ln d (mm)
-1.5
-1.0
-0.5
0.0
5.0
4.8
4.6
4.4
4.2
4.0
ln I (μA)
4.2
4.0
3.8
3.6
3.4
3.2
ln I (μA)
-2.0
-1.0
0.0
1.0
ln V_f (ml min^{-1})

Table III-2. Dependence of mass-transport limited current at working electrode of flow-through disk detector on volume flow rate of solution stream, V_f, and on distance, d, between disk and channel orifice[a]

I (μA)	V_f (mL min^{-1})	I (μA)	d (mm)
52	0.09	69.6	0.20
84	0.35	42.0	0.40
103	0.63	31.3	0.60
121	1.05	25.6	0.80
148	2.12	21.1	1.00

[a] Data shown graphically in Figure III-5.

the same. Electrode current for this detector is shown in Section III.C.6 to vary linearly with C^b.

It should be noted, before proceeding further, that for the liquid chromatograph used in this work the dependence of current on $V_f^{1/3}$ applies to the total volume flow rate of the combined eluent stream, $V_{f,E}$ plus buffer stream, $V_{f,B}$. This total flow rate is designated $V_{f,T}$. One might be tempted to increase $V_{f,B}$ to improve the sensitivity of the detector by virtue of a larger $V_{f,T}$, but this is actually detrimental. The bulk concentration in the final stream is the product of C^b in the eluent stream and a dilution factor, $V_{f,E}/V_{f,T}$. When the flow rate dependence of the detector is multiplied by this dilution factor, current is seen to vary in proportion to $V_{f,E}/(V_{f,T})^{2/3}$.

The flow-through disk detector is most sensitive when d is adjusted to a value near 0.2 mm, when $V_{f/E}$ is large, and when $V_{f,B}$ is minimal. The practical limitation on the magnitude of $V_{f,E}$ is set by the pumping capacity of the system and the pressure drop experienced across the chromatographic columns. Furthermore, $V_{f,B}$ must be large enough so that the pH of the final solution is at the desired value. The limitations for this parameter are, therefore, set by the solubility of the buffering agent and the ability to completely mix the two streams.

2. Choice of detector potential

Voltammetric data may not always give adequate indication of the optimum detector potential to be used for amperometric analysis at constant potential. This has been shown to be the case, for instance, for glassy carbon where the proportion of hydroxyl, carbonyl, carboxy, and quinoid functional groups on the glassy carbon surface change as the surface potential is varied (92). Currents recorded during a potential scan can, therefore, be the result of phenomena related to the rapidly changing potential, as well as charging and the faradaic process of interest.

Therefore, the optimum detector potential for the chromatographic determination of nitrate was ascertained from pseudo-voltammograms which were constructed point by point from amperometric data obtained at fixed potential values. The data were obtained by allowing the background current in the detector to decay to a constant value after adjusting the detector potential. A sample of nitrate in deionized water was then injected into the flowing stream of the chromatograph. The electrical current for the background, the oxygen peak, and the nitrate peak were measured by monitoring the output of the current follower of the potentiostat with a digital voltmeter. The detector potential was then changed by a small increment and the procedure repeated until a complete set of data were obtained

This technique for obtaining pseudo-voltammograms is similar to that described by Blaedel and Jenkins (93) which they called "steady-state voltammetry". They measured steady-state currents resulting from a continuous supply of analyte. Here, peak currents have been assumed to be linearly proportional to the steady-state currents that would have been observed had Blaedel and Jenkins been rigorously followed. The experimental results are shown in Figures III-6 and III-7. The data for Figures III-6 and III-7 are listed in Table III-3. The general shape of the curves obtained for the reduction of nitrate and of oxygen are quite similar to those obtained from conventional voltammetry. Also shown are the net curves for the reduction processes corrected by subtracting the background current from the total current. From the net curve for nitrate reduction, it can be seen that beyond a certain value, more negative detector potentials actually diminish the reduction current and, therefore, the analytical sensitivity of the system. This decrease in current might be the result of an increased rate of hydrogen reduction at more negative potentials which would deplete the double layer concentration of hydrogen ion needed to support the reduction of nitrate. The evolution of hydrogen gas bubbles might also decrease the number of available sites on which the nitrate reduction process occurs, thereby causing a decrease of the current for

Figure III-6. Pseudo-voltammograms of nitrate reduction at working electrode of copperized cadmium-disk detector in pH 8 buffer

Nitrate concentration = 0.5 mM

○ Background current

□ Total nitrate reduction current

◇ Net nitrate reduction current

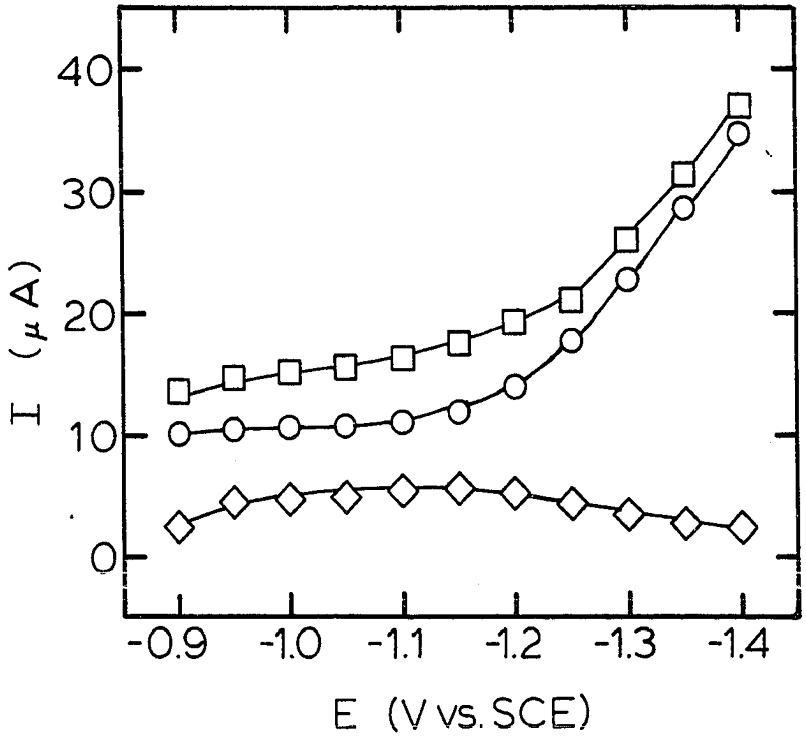
40
30
20
10
0
I (μA)
-0.9
-1.0
-1.1
-1.2
-1.3
-1.4
E (V vs. SCE)

Figure III-7. Pseudo-voltammogram of oxygen reduction at working electrode of copperized cadmium flow-through disk detector in pH 8 buffer

Air saturated solutions

○ Background current

□ Total oxygen reduction current

◇ Net oxygen reduction current

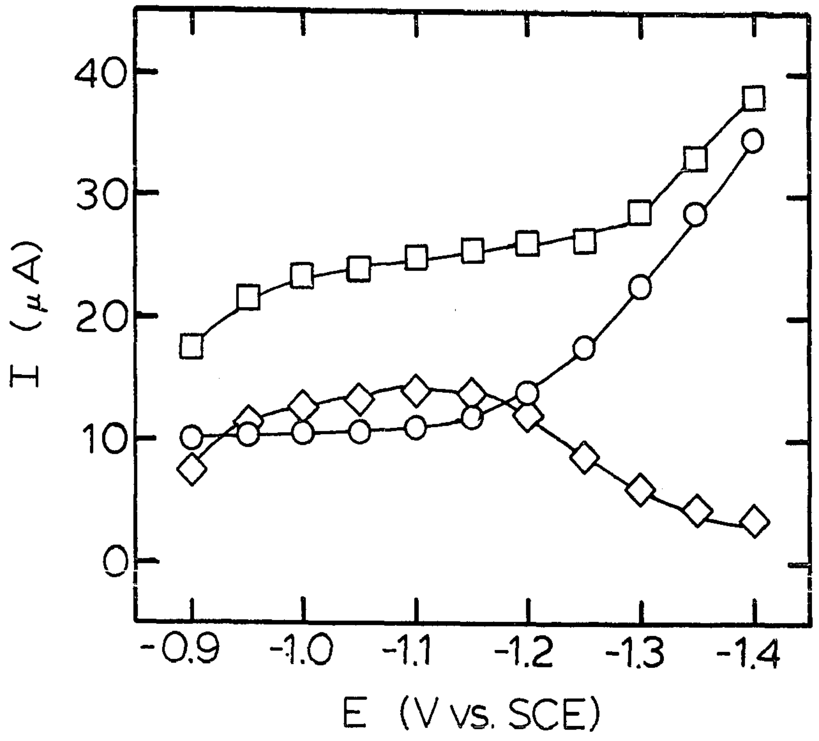
I (μA)
40
30
20
10
0
-0.9
-1.0
-1.1
-1.2
-1.3
-1.4
E (V vs. SCE)

Table III-3. Data for pseudo-voltammograms of nitrate and oxygen reduction current at working electrode of copperized cadmium-disk detector in pH 8 buffer[a]

Electrode potential (V vs. SCE)	Background current (μA)	Total nitrate reduction current (μA)	Net nitrate reduction current (μA)	Total oxygen reduction current (μA)	Net oxygen reduction current (μA)
-0.90	10.0	13.4	3.4	17.5	7.6
-0.95	10.3	14.7	4.4	21.7	11.4
-1.00	10.4	15.1	4.7	23.3	12.8
-1.05	10.7	15.6	4.9	24.0	13.3
-1.10	11.0	16.3	5.3	25.0	14.0
-1.15	11.9	17.4	5.5	25.7	13.8
-1.20	13.9	19.2	5.3	26.1	12.1
-1.25	17.6	22.0	4.4	26.4	8.8
-1.30	22.7	26.0	3.3	28.8	6.1
-1.35	28.6	31.3	2.7	33.1	4.5
-1.40	34.6	37.0	2.4	38.1	3.5

[a] Data shown graphically in Figures III-6 and III-7.

the reduction of nitrate. The detector potential chosen for analysis was -1.15 V vs. SCE which corresponds to the maximum in the curve for the reduction of nitrate in Figure III-6.

3. Evaluation of anion-exchange columns

Davenport has reviewed the various media that have been used to separate nitrate in water samples from other constituents. He concluded that none of those media were compatible with his cadmium tubular detector; however, he was able to develop a chromatographic separation of nitrate, nitrite, and oxygen using Amberlite IRA-900, a strongly basic, macroreticular anion-exchange resin, and an eluent of 0.01 M perchloric acid (3). Attempts to reproduce the conditions of Davenport's separation are described in Section III.B.2. Equivalent results were not obtained, partially because Davenport's description of his resin is brief and the column probably was not duplicated in my research. The technology used by Davenport for preparing the Amberlite IRA-900 was obtained from individuals who were contemporary graduate students at Iowa State University with both Davenport and myself and who had observed his work.

Two columns designated C-1 and C-2, were prepared from Amberlyst A-26 and Dowex 1-X8, respectively. The number of theoretical plates in each column, N_E was calculated from the shape of chromatographic peaks for nitrate. A value for N_E was also calculated for Davenport's column, designated C-D, from figures in his thesis. The parameter N_E is defined by Equation III-2 and is an indication of the efficiency of a chromatographic column.

$$N_E = 16(t_r/t_w)^2 \tag{III-2}$$

In Equation III-2:

t_r = retention time, the time necessary to elute a specie to maximum concentration;

t_w = base width of a peak, measured as the segment of baseline defined by drawing lines tangent to the inflection points on each side of the peak, also in time units.

A column is said to be "efficient" if N_E is large and, therefore t_r is large relative to t_w. N_E is not, however, a convenient basis for comparing various columns unless all the columns are equal in length. Such was not the case for columns compared here. The height equivalent of a theoretical plate, H, is better for intercomparison of columns of different length. H is the ratio of column length, L, to N_E; therefore, the more efficient column will have a smaller value for H. Values of H for the three columns compared are given in Table III-4.

Amberlyst A-26 and Amberlite IRA-900 are both strongly basic, macroreticular, anion-exchange resins. The

Table III-4. Comparison of efficiencies of anion-exchange columns

Column designation	Column packing[a]	H (cm)[b]	L (cm)[c]
C-1	Amberlyst A-26	0.20	11
C-2	Dowex 1-X8	0.12	9
C-D	Amberlite IRA-900	0.08[d]	11

[a] See Section III.B.2.

[b] H = height equivalent of a theoretical plate.

[c] L = length of column.

[d] Value measured from published figure (3).

difference in the values of H reported for the two columns packed with these resins probably reflects differences in resin preparation and/or packing technology. Whatever the specific cause for this difference, C-1 as I prepared it, was deemed inadequate for the separation of nitrate and oxygen.

The influence of particle size and shape, and of various packing techniques, on column efficiency has been extensively discussed by Hadden, et al. in Reference 94. They conclude that greater column efficiencies, i.e., smaller values for H, are obtained when the packing material consists of small particles of uniform size and shape. Dowex 1-X8 is commercially available in the form of small spherical beads in the size range of 200-400 mesh. While it was necessary to further size the resin by sieving, it was not necessary to grind this resin (see Section III.B.2). Therefore, a packing material with more uniform geometry was obtained. On the other hand, Dowex 1-X8 is a microreticular resin. Anions migrate in the relatively stagnant solution within the micropores of a microreticular bead by diffusion only. This slow form of mass transport contributes greatly to band broadening. Also, this type of resin tends to change volume with changes in ionic strength of the eluent (95) and with applied pressure. Nevertheless the value of H measured for C-2 packed with Dowex 1-X8 is somewhat smaller than that obtained for C-1. Even though C-2 was still not as efficient as C-D, all further investigative and analytical work reported in this thesis was performed with C-2.

From the data in Table III-4, one can calculate that there are only 75 theoretical plates in C-2. It would, therefore, be predicted from column theory that only those species with substantially different distribution coefficients could be separated on this column (94). Also, the time necessary to achieve a satisfactory separation is increased for a low value of N_E.

The efficiency of any column can be improved, theoretically, without changing the column packing material by increasing the length of the column. This is achieved at the expense of increased back pressure, however. Greater back pressure in turn requires greater pumping capability because the rate of flow of eluent must be increased to perform the separation in approximately the same amount of time. As described in Section III.B.4, gas pressure was applied to the glass reservoirs in this work to force the solutions along their respective flow streams. For C-2, 40 psi were required to achieve a rate of flow of approximately 1 mL min^{-1}. It was deemed unwise for reasons of safety to increase the reservoir pressure much above that value, therefore, C-2 was used without further improvement.

The Dowex 1-X8 resin packed in C-2 was found to be sufficient for the separation of nitrate from oxygen. Very little separation of nitrate from other anionic species is expected. One advantage of electrochemical detection is that the detector can be chosen to be quite selective, either through selection of the appropriate working electrode potential or, as is the case here, through selection of electrode material. An interference study is described and discussed in the next section which shows that the selectivity of the copperized cadmium flow-through disk detector for nitrate adequately compensates for the poor efficiency of the chromatographic separation.

4. Interference study

A study of possible interferences was performed to determine the selectivity of the copperized cadmium surface for reduction of nitrate. This study was also made to determine how the potentially interfering species might alter the interaction of nitrate with chromatographic column C-2 possibly causing detrimental changes in the chromatographic resolution of the nitrate peak from the peak attributed to dissolved oxygen and injection artifacts. Solutions were prepared containing 0.5 mM nitrate and 5 mM of a potentially interfering species. The species investigated as possible interferences are listed in Table III-5. A solution containing only 0.5 mM nitrate was injected onto C-2 before and after each injection of solution containing a chemical interference. There was no cation-exchange column present in the chromatograph for this study. The detector was the copperized cadmium flow-through disk electrode described in Section III.B.3. The eluent was 2 mM perchloric acid.

Peak areas were measured and the percent relative error in peak areas resulting from the presence of interfering species was calculated. The results are given in Table III-5. The relative uncertainty for a liquid chromatograph with amperometric detection is usually about 5%. Therefore, a substance was not considered an interference at the

Table III-5. Detection of 0.50 mM nitrate in the presence of potentially interfering ions

Interference (5.0 mM)	% Relative error in peak areas	Peak distortion
NaCl	+ 2.8	
NaBr	+ 1.4	fronting
NaI	- 3.3	
$Ca(OCl)_2$	+ 2.8	
$NaClO_3$	- 5.6	broadening
$NaClO_4$	+ 0.2	
$Na_2Cr_2O_7$	- 4.6	
Na_2HPO_4	+ 4.0	broadening
$NaHSO_4$	- 2.0	
$NaHSO_3$	+ 2.0	
$HClO_4$	+ 1.6	
$CuSO_4$	+85	
$Fe(NH_4)(SO_4)_2$	+ 5.3	

particular concentration tested unless it gave rise to a relative error in peak area greater than 5%.

Among the anions investigated, only chlorate was found to be an interference producing a negative error. An injection of 5 mM sodium chlorate gave a small reduction signal and it is probable that chlorate, which is not separated from nitrate, competes for the active sites on the electrode surface thereby diminishing the extent of nitrate reduction. Because the chlorate reduction rate is very small, the effect is a decrease in the net reduction current. Dichromate and hydrogen phosphate are marginal interferences; however, they did not give detection peaks when injected without the presence of nitrate.

Three anions did cause some change in the shape of the chromatographic peaks for nitrate. Bromide caused fronting, but the peak area was still accurate within the precision desired. The other two anions, hydrogen phosphate and chlorate, caused considerable broadening of the nitrate peak which may in part account for the error observed in peak area.

Many cations would be expected to be reduced on the electrode surface at the negative potentials used for detection of nitrate. While they would probably not be retained on the anion exchange column in dilute perchloric acid, they might be reduced all the way to their metallic form and be deposited on the surface, thus poisoning the surface. In the case of copper, further activation of the surface toward nitrate reduction would occur.

The presence of copper(II) and iron(II) were found to interfere with the detection of nitrate as shown in Table III-5. When the cation-exchange column described in Section III.B.4, was inserted before C-2 in the liquid chromatograph, these cations no longer interfered. There was a slight increase in the width of the nitrate peak, i.e., a decrease in the apparent efficiency of the separation, due to the increase in the dead volume of the system when the cation-exchange column was inserted in the chromatograph. No work was done to determine the lifetime of the cation-exchange column. The cation-exchange resin is inexpensive and the amount needed to pack the column is small. Therefore, it is suggested that the column be repacked at least once every 30-50 working hours, unless concrete data is obtained showing that the capacity of the cation-exchange column is large enough to be used for longer periods of time.

It is concluded that the detector is not appreciably sensitive to the anions investigated and that the poor efficiency of the anion-exchange column used is tolerable because of the selectivity of the detection system.

This high degree of selectivity, plus the fact that oxygen can be purged from an aqueous solution would seem to make it plausible to perform the analysis without an anion-exchange column. It was found that dissolved oxygen can be removed from the sample solutions in the manner suggested from neutral or alkaline solutions of nitrate without loss of nitrate as volatile nitric acid. The use of Teflon tubes in the flow stream of the chromatographic system, however, complicated the situation because Teflon is permeable to oxygen (96). Therefore, the oxygen concentration in the stream reaching the detector is greater than the weighted sum of the oxygen concentrations in the two solutions in the reservoirs, which have also been purged. This concentration is a function of the sum indicated and the amount of time that the solutions are in contact with the Teflon tubing. Samples, which have been purged of oxygen, are injected into the eluent stream after the eluent has already contacted several inches of Teflon tubing. The oxygen concentration in the sample plug is, therefore, less than that of the eluent before and after the plug, such that a negative peak is observed. This corresponds to a decrease in the background signal due to the reduction of oxygen in the stream. Therefore, without going to an oxygen impermeable system it was impossible to determine nitrate in aqueous samples by flow injection analysis without an anion-exchange column. However, removal of the oxygen from samples is desirable for reasons discussed in Section III.C.7 and III.C.8.

5. Effect of chloride loading of sample

The results of the analysis of several unknown samples will be discussed in Section III.C.8. One sample that was particularly interesting was Tender Quick Meat Cure, a meat curing product for home use, marketed by Morton Salt Company of Chicago. Tender Quick Meat Cure is designated as the "salt sample" or simply the "salt" in this report. According to the list of ingredients on the salt package, it contains about 0.5% sodium nitrate. A portion of the salt was prepared to give a solution of about 0.3 mM nitrate which was analyzed by the liquid chromatographic procedure. The eluent was 2 mM perchloric acid.

The chromatograms obtained for aliquots of the solution of salt with and without added spikes of potassium nitrate were markedly different from those obtained for standard potassium nitrate solutions of comparable concentrations. Examples of these chromatograms are given in Figure III-8. It is clear from the figure that nitrate in the salt sample is retained longer on the analytical column than is nitrate in deionized water. Much more surprising is the observation that the peak corresponding to nitrate elution is narrower for the salt sample even though the retention time is greater. Such behavior is opposite that predicted from theoretical considerations (94). It was desirable, therefore, to further investigate this phenomenon to obtain an explanation. Also, it was reasoned that there might be an improvement in the detection limit of the liquid chromatograph if the same effect could be produced for other nitrate samples. Therefore, it was desirable to determine which constituents of the salt sample were causing the observed effect and to determine what concentration of those constituents would optimize the observed changes in the nitrate peaks.

Figure III-8. Comparison of chromatogram of Tender Quick Meat Cure® sample to that of nitrate standard

A Standard nitrate

B Tender Quick Meat Cure® sample

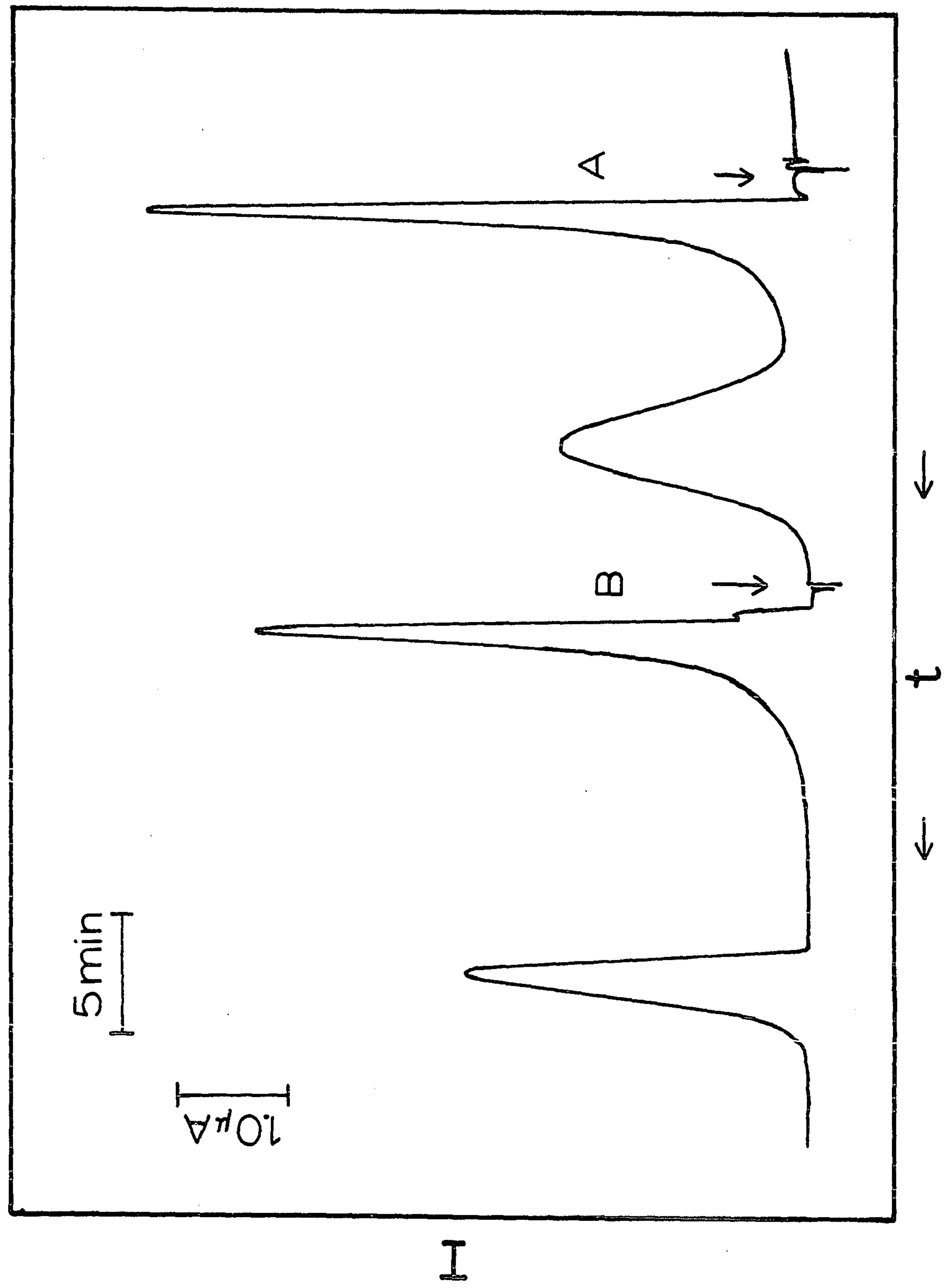
A
B
5min
1.0μA
t
I

A solution of each of the ingredients of the salt was prepared at a concentration approximately equal to the concentration of that ingredient in the salt sample. Each solution was spiked with 0.3 mM nitrate and was injected into the liquid chromatograph. The chromatogram for the solution containing sodium chloride, the major constituent of the salt, was found to be virtually identical to that for the salt sample (97). It was concluded, therefore, that the sodium chloride was responsible for the observed effect on the nitrate peak.

A series of solutions was prepared containing 0.4 mM potassium nitrate with varying concentrations of sodium chloride from zero to 0.7 M as listed in Table III-6. Aliquots of each solution were injected into the liquid chromatograph and the chromatograms recorded. The eluent used was 5 mM perchloric acid. Sample chromatograms are shown in Figure III-9.

The liquid chromatograph was then modified to permit the detection of chloride in the effluent. The pH 8 buffer was replaced with 0.5 M perchloric acid. A silver wire detector, briefly described in Section III.B.3 was used in place of the copperized-cadmium detector. The silver detector was potentiostated at +0.250 V vs. SCE. The detector current was produced by the oxidation of silver in the presence of chloride to form insoluble

Table III-6. Influence of chloride loading phenomenon on retention of nitrate by anion-exchange column packed with Dowex 1-X8[a]

Chloride concentration (M)	I_{pl}[b] (μA)	$W'_{1/2}$[c] (min)	T_{r,NO_3^-}[d] (min)
0.00	--	--	6.36
0.02	21.7	5.64	6.64
0.04	24.5	6.70	6.84
0.06	25.7	7.28	7.58
0.08	26.4	8.16	8.08
0.10	27.1	8.60	8.54
0.12	27.4	9.18	8.84
0.14	27.6	9.60	9.56
0.20	28.0	10.74	10.36
0.40	28.7	13.80	13.28
0.70	29.1	16.84	16.28

[a] Data shown graphically in Figure III-10.

[b] Highest current on the plateau of the chair shaped chloride chromatogram.

[c] Time necessary to wash chloride off column, measured from injection to tail of the response to chloride at 1/2 I_{pl}.

[d] Retention time of nitrate.

Figure III-9. Variations in nitrate and chloride chromatograms as a function of concentration of chloride in injected sample

Nitrate concentration = 0.40 mM
Perchloric acid eluent concentration = 5 mM

For nitrate detection (upper curves):
Potential of working electrode of copperized cadmium flow-through disk detector = -1.15 V vs. SCE
Eluent mixed with pH 8 buffer

For chloride detection (lower curves):
Potential of working electrode of silver-wire detector = 0.25 V vs. SCE
Eluent mixed with 0.5 M perchloric acid

Curve	Chloride Concentration (M)
A	0.00
B	0.06
C	0.14
D	0.40
E	0.70

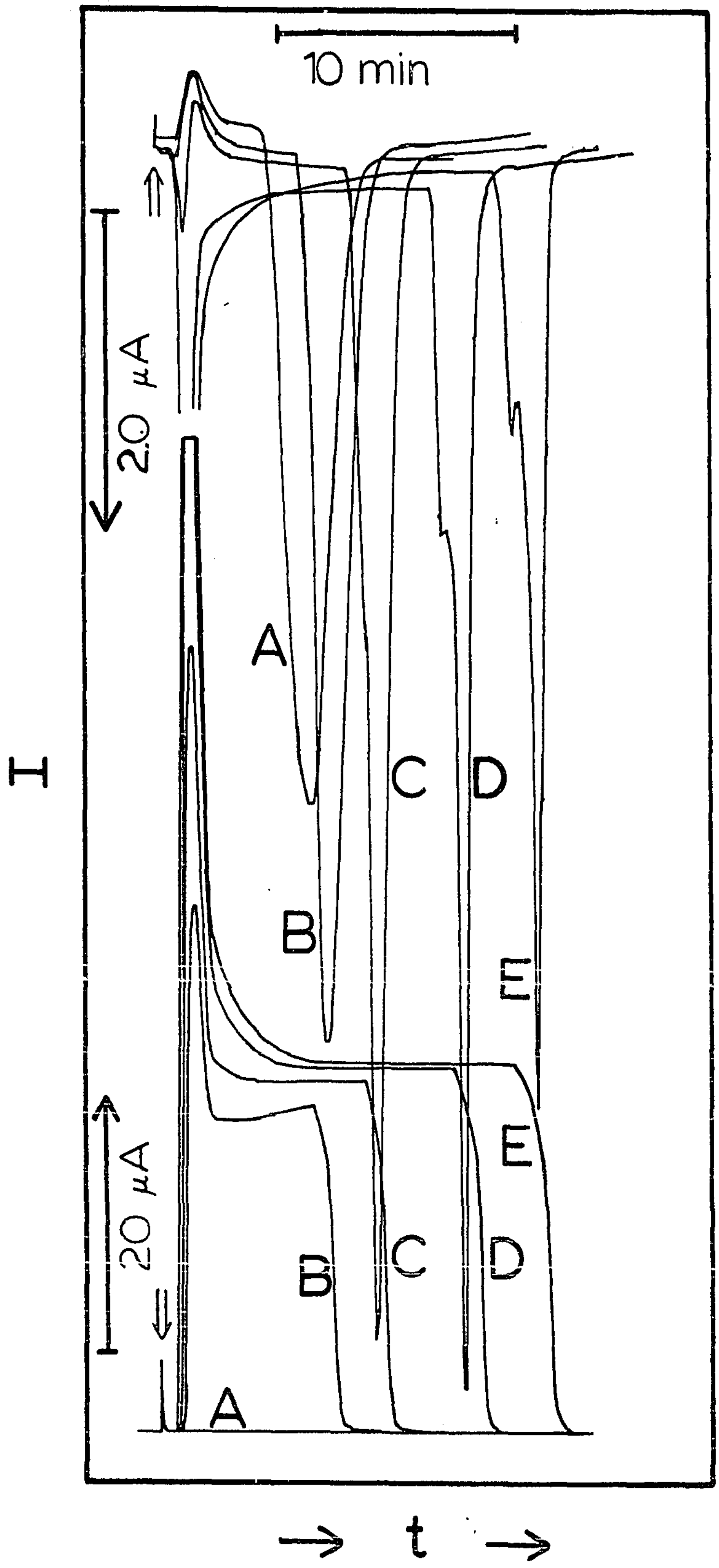
10 min
2.0 μA
20 μA
I
A
B
C
D
E
A
B
C
D
E
→ t →

Figure III-10. Influence of chloride loading phenomenon on retention of nitrate by anion-exchange column packed with Dowex 1-X8

○ Nitrate retention time, T_{r,NO_3^-}

□ Elution of chloride, $W'_{1/2}$

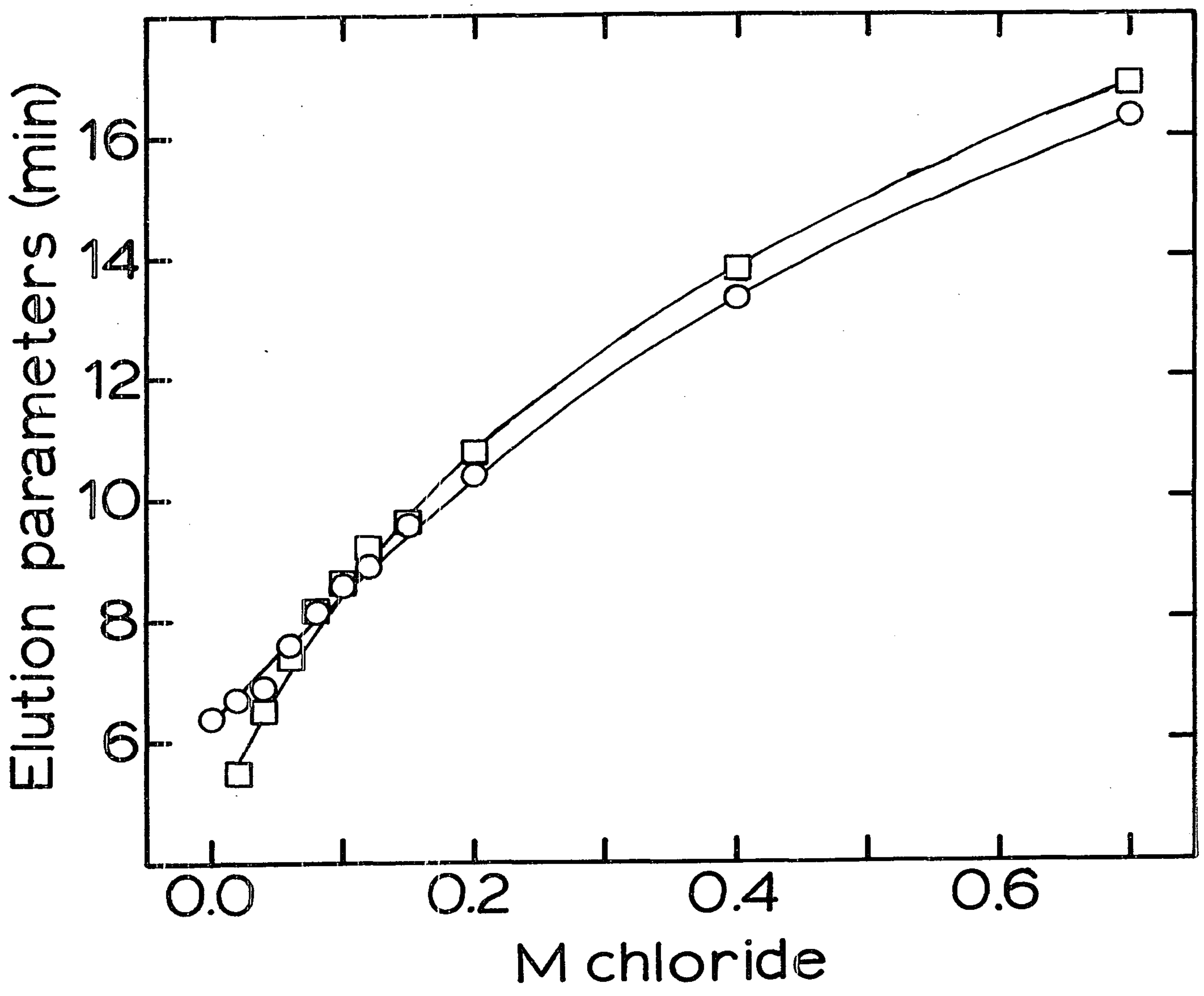
Elution parameters (min)
6
8
10
12
14
16
0.0
0.2
0.4
0.6
M chloride

silver chloride. Aliquots of the same solutions described in Table III-6 were again injected and the chromatograms recorded. A representative selection of both sets of chromatograms are included in Figure III-9.

It is obvious from the nitrate chromatograms in Figure III-9 that with each increase in the concentration of chloride in the sample injected the nitrate is retained for a longer time. The nitrate peaks get narrower and the peak currents increase for chloride concentrations up to about 0.2 M. It should also be noted that the larger chloride concentrations cause severe fronting of the nitrate peak. The chloride chromatograms, for the chloride concentrations above 0.06 M, are characterized by a large current spike followed by a current plateau. The current spike corresponds to the sample front indicating that some chloride is not retained by the column. The height of the chloride current spike and of the chloride current plateau increases with increasing chloride concentrations.

Several parameters are used to compare the chromatograms obtained. T_{r,NO_3^-} is the retention time of the nitrate on the analytical column and has its usual chromatographic significance, I_{pl} is the highest current on the plateau of the chair-shaped chloride chromatograms. $W'_{1/2}$ corresponds to the amount of time necessary to elute the chloride off the column, measured from the injection to the tail of the response to chloride at 1/2 I_{pl}. Values for these parameters are given in Table III-6. T_{r,NO_3^-} and $W'_{1/2}$ are plotted in Figure III-10 vs. the concentration of injected chloride. An examination of that figure shows that the nitrate is being eluted from the column about the same time as the last of the retained chloride. There is, however, an intersection of the two curves occurring at a chloride concentration of something less than 0.1 M. This probably represents an optimum chloride concentration, above which the increasing height of the nitrate peak is accompanied by detrimental peak distortion.

It is necessary to attempt to explain the influence chloride concentration has on the shape of the nitrate and chloride chromatograms. A very reasonable explanation for the shape of the chloride chromatogram can be developed starting with the observation that not all of the chloride in the injected samples is retained. Evidently the dynamic capacity of all of the resin in the column for chloride is exceeded by the amount of chloride injected. In the previous sentence, the word "dynamic" is used to modify the word "capacity" in recognition of the fact that the large amount of chloride in the injected samples can not completely equilibrate with the functional groups on the column resin during the short residence of the sample plug in the column bed. It is probable that only those functional groups on or near the exterior surface of the anion-exchange resin beads are converted to the chloride form. The number of functional groups converted to the chloride form evidently depends on the chloride concentration, because both the height of the current plateaus and the time needed to elute all of the chloride increase with increasing amount of injected chloride. The plateau shape can be explained by recognizing the following. The last portion of the sample plug is followed by a new eluent front which immediately begins to release the retained chloride. In later stages, those chloride ions being released at the top of that portion of the column still loaded with chloride are unretained by the rest of the column and, therefore, produce a steady state signal at the detector until the injected chloride is completely eluted from the column.

An explanation for the observed changes in the shape of the nitrate chromatograms as a function of the concentration of chloride co-injected is not so easy to develop. Factors discussed in the literature are helpful, however, in developing two separate explanations.

Gregor, et al. reported data showing that the affinity of perchlorate for a Dowex anion-exchange resin similar to that in C-2 decreases drastically as the mole fraction of the total exchange capacity of the resin in the chloride form, X_{Cl^-}, is increased (98). Conversely, the affinity of nitrate for the resin is virtually unaffected by the value of X_{Cl^-}. The relative affinity for the anions was observed to change from perchlorate > nitrate > chloride, to nitrate > perchlorate > chloride. If the effect of the parameter X_{Cl^-} is similar to the effect of converting a portion of the resin in the column to the chloride form, then it is hypothetically possible that the eluting strength of the perchlorate, which is proportional to its affinity for the resin, decreases with the increasing amounts of injected chloride. If this is the case, an increased retention time for the nitrate is predicted, because the perchlorate could not elute the nitrate as quickly. The hypothesis does not account for the observed changes in the nitrate peak shape. The hypothesis is also weak because the data reported by Gregor et al. were obtained in batch experiments, i.e., the interactions between anions of interest and the resin were allowed to arrive at equilibrium. Therefore, it may be unreasonable to expect that the eluting strength of the perchlorate decreases very much as the amount of chloride injected is increased.

Furthermore, the above hypothesis can be experimentally tested because Gregor et al. also report the observation that the affinity of iodide for their resin increases as

X_{Cl^-} is increased (opposite from the perchlorate case). Therefore, the perchlorate in the eluent could be replaced by iodide and aliquots of the same series of chloride-loaded nitrate samples injected. On the basis of the hypothesis it was predicted that the eluting strength of the iodide would increase and the nitrate would be retained for shorter periods of time as the amount of chloride co-injected with the nitrate was increased. The perchloric acid eluent in the liquid chromatograph was replaced by 5 mM sodium iodide, and several of the chloride containing nitrate solutions were injected. Only chromatograms for nitrate detection were obtained. T_{r,NO_3^-} was observed to increase with the concentration of chloride in the injected samples and the changes in the nitrate peak shape were identical to those for the perchloric acid eluent. Therefore, it is concluded that if the hypothetical changes in the affinity of perchlorate for the resin occur when large amounts of chloride is injected onto the resin, they are not sufficiently large to account for the increase in T_{r,NO_3^-} or the other changes observed.

The relative mobilities of nitrate and chloride in the resin matrix may be important to an understanding of the influence that co-injected chloride has on the shape of the nitrate peak. Helfferich illustrates the effect of relative mobilities with the following example:

> "First, let us examine particle-diffusion controlled exchange between a resin in A form and a solution containing two electrolytes BY and CY. If the mobilities of B and C in the resin are about equal, both these species are taken up at approximately equal relative rates. The situation is different, however, if B is much more mobile than C. Now, B will rapidly replace A in the resin, and the uptake of C will lag far behind. Later, C will follow, partly replacing the B ions that were taken up in the earlier stages. Thus, the concentration of B in the resin goes through a maximum." (99)

The second explanation for the observed changes in the nitrate peak shape can be developed by analogy. If chloride is much more mobile than nitrate in Dowex 1-X8, the concentration of nitrate in the resin would be expected to go through a maximum some time after the beginning of the residence of the nitrate band in the column.

Unfortunately, this explanation is not easily tested. The relative mobilities of nitrate and chloride in the resin matrix are not known. It is probably unwise to use the mobilities of the ions predicted from measurements of the ionic conductivities of chloride and nitrate in water, because the ions may or may not be hydrated in the resin matrix and because the environment experienced by the ions in the resin matrix is undoubtedly different from that in water. Future research into the mobilities of the ions in the resin will be helpful in explaining the phenomenon.

6. Calibration curves and detection limit

The nitrate in unknown samples was quantitatively determined by the technique of standard addition. This was necessary because the activity of the copperized cadmium flow-through disk detector varied from day to day, making the use of a calibration curve impractical. One set of calibration curves was prepared, however, to determine the extent of the concentration range over which the system's response to nitrate is linear; the standard addition technique is only applicable when the analytical response is linear.

Four calibration curves were prepared from two sets of standard calibration solutions. One set of solutions was prepared in deionized water and the other was prepared in 0.1 M potassium chloride. A pair of calibration curves was generated from each set of standard solutions by measuring both the area of the nitrate peaks and the peak heights. The peak areas were converted to microcoulombs of charge transferred and the peak heights were converted to peak currents. The log of the response measured is plotted vs. the log of the concentration of nitrate in Figure III-11. The data are also given in Table III-7.

Linear regressions were performed on the data for each curve, excluding those data points that were obviously beyond the linear range of concentrations. All four calibration curves were found to have linear regression

Figure III-11. Response of liquid chromatograph to nitrate concentration with and without 0.10 M chloride

For chloride concentration = 0.00 M
○ Peak area measured
⊖ Peak height measured

For chloride concentration = 0.10 M
⊕ Peak area measured
● Peak height measured

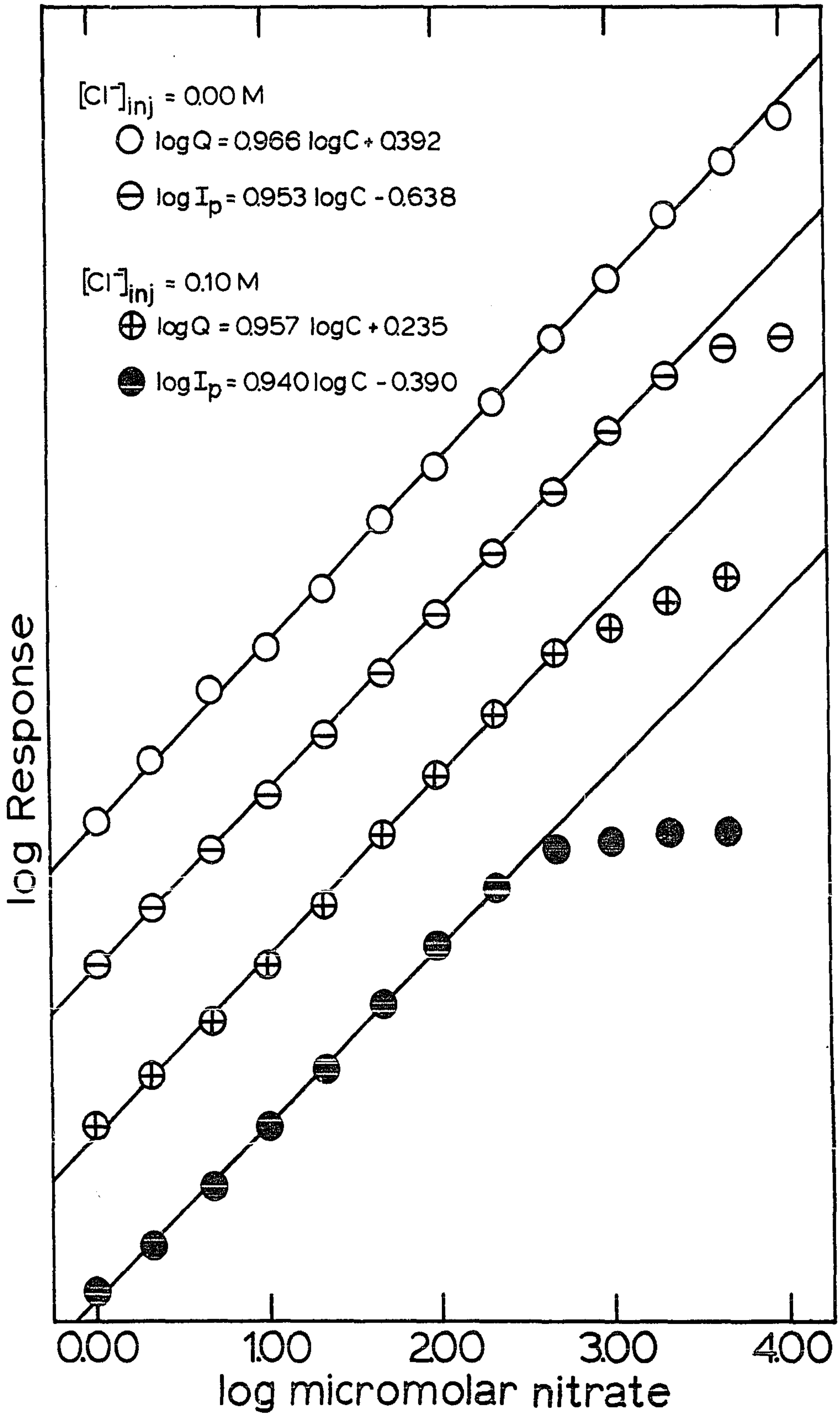
[Cl⁻]inj = 0.00 M
○ log Q = 0.966 log C + 0.392
⊖ log Ip = 0.953 log C - 0.638
[Cl⁻]inj = 0.10 M
⊕ log Q = 0.957 log C + 0.235
● log Ip = 0.940 log C - 0.390
log Response
0.00
1.00
2.00
3.00
4.00
log micromolar nitrate

Table III-7. Response of liquid chromatograph to nitrate concentration with and without 0.10 M chloride[a]

0.00 M Chloride			0.10 M Chloride		
Nitrate concentration (log μM)	Peak area (log μcoul)	Peak height (log μA)	Nitrate concentration (log μM)	Peak area (log μcoul)	Peak height (log μA)
0.02	0.41	-0.60	0.00	0.29	-0.34
0.34	0.73	-0.30	0.33	0.56	-0.10
0.68	1.11	-0.01	0.68	0.85	0.22
1.01	1.33	0.30	1.00	1.15	0.54
1.34	1.65	0.62	1.33	1.47	0.84
1.68	2.02	0.95	1.68	1.84	1.19
2.00	2.30	1.26	1.99	2.16	1.50
2.33	2.64	1.59	2.33	2.48	1.81
2.68	2.98	1.92	2.68	2.81	2.01
3.00	3.30	2.24	3.00	2.94	2.05
3.33	3.64	2.53	3.33	3.08	2.10
3.67	3.93	2.68	3.67	3.21	2.10
4.00	4.17	2.74	--	--	--

[a] Data shown graphically in Figure III-11.

coefficients that were greater than 0.999, when the criterion described above for the exclusion of data was used. The slopes and intercepts obtained from the linear regression treatment of the data are also given in Figure III-11.

The largest range of concentrations, almost four orders of magnitude, for which the system response is linear is obtained in the absence of chloride and when the nitrate peak areas are measured. The lower limit of this range, 1.0 μM (62 ppb), corresponds very nearly to the detection limit of the system for nitrate in the absence of large amounts of chloride. This limit corresponds to about 20.0 ng nitrate for a 0.3 mL sample loop. Above the upper limit of this linear range, the nitrate peaks were quite distorted, possibly indicating that the analytical column was being overloaded by the amount of nitrate in the sample. It can be seen by comparing the top two curves in Figure III- that the distortion of the nitrate peaks affects the peak height measurements at lower nitrate concentrations than it affects the peak area measurements. It is, therefore, concluded that peak area is a slightly better indication of nitrate concentration.

It can be seen, by comparing the bottom pair of curves in Figure III-11 with the top pair, that the range of concentrations for which the system response is linear is smaller when chloride is present in the nitrate calibration solutions. The increased separation of the nitrate peak from the oxygen-related injection phenomenon, explained in Section III.C.4, and the improved peak height make it easier to determine where the baseline should be drawn. The detection limit is improved by about an order of magnitude. The nitrate present in the potassium chloride reagent used to make up these solutions was actually the limiting factor. A chromatogram for an injected aliquot of a 0.1 M potassium chloride to which no nitrate was added is compared with one containing standard nitrate in Figure III-12. The fact that the detection limit is lower in the presence of the chloride illustrates that the limiting factor of the overall system which determines the detection limit is the efficiency of the separation, not the sensitivity of the detector.

7. Precision study

The reproducibility of the analytical method for the determination of nitrate was investigated, with and without added chloride, at nitrate concentrations of 0.10 and 0.01 mM. Two solutions at each concentration were prepared by appropriate dilution of the stock potassium nitrate solution. One of each of these pairs of solutions was spiked with sufficient potassium chloride to produce a final concentration of 0.1 M chloride. All solutions were purged of oxygen.

Figure III-12. Chromatograms of 0.1 M potassium chloride (A) without added nitrate and (B) with 0.1 μM nitrate

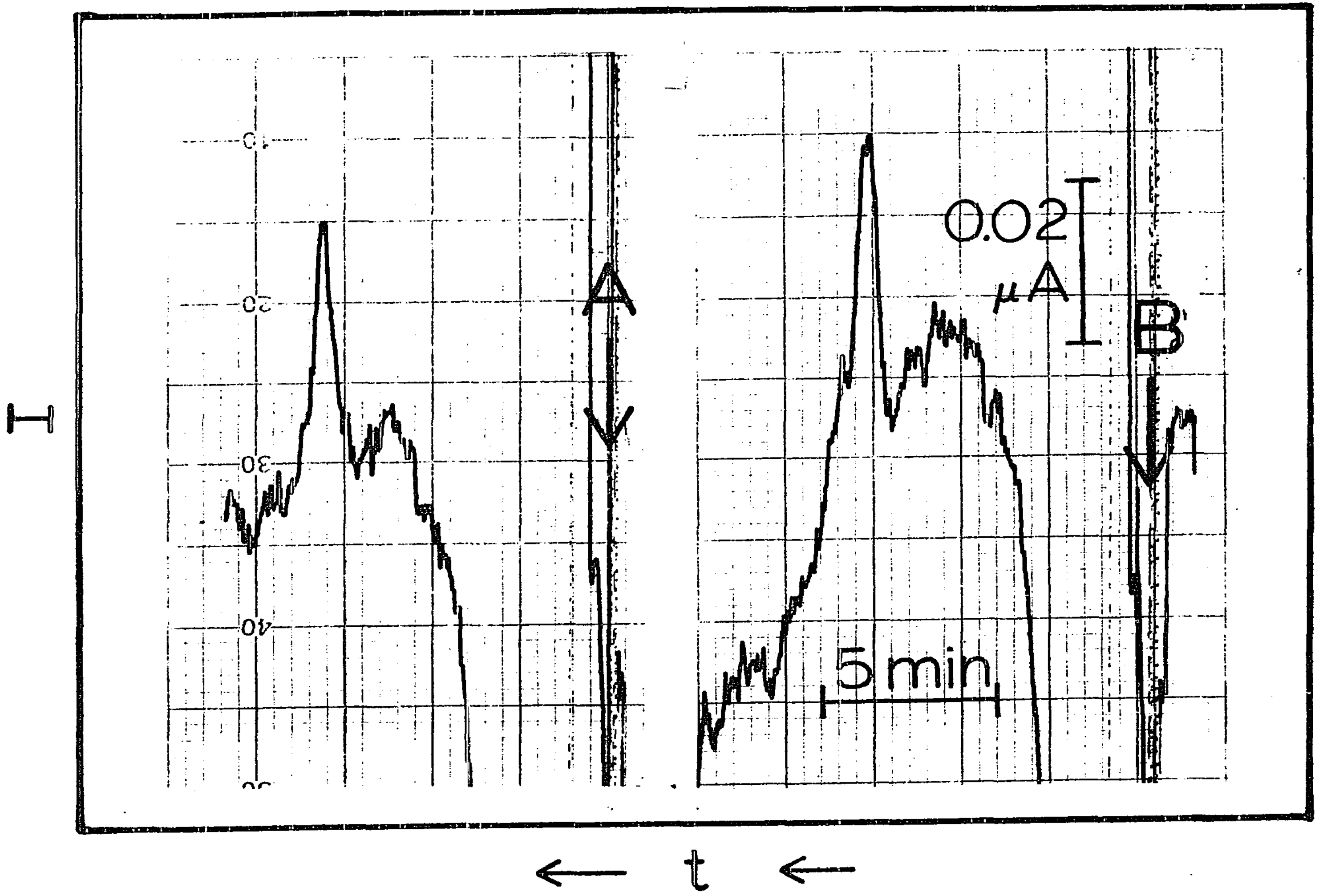
I
10
20
30
40
A
0.02
μA
B
5 min
t

Six aliquots of each solution were injected into the liquid chromatograph for analysis. The area of each nitrate peak, A_p, was measured four times with a planimeter and the results were averaged. The relative standard deviation of the four measurements of each peak area, RDS_p, was calculated. The average of the areas of the six nitrate peaks, A_t, was obtained for each solution and the relative standard deviation, RDS_t, was calculated as an indication of precision of the analytical method for nitrate.

The summary of analytical results is given in Table III-8. For three cases, the RDS_t values are less than 5% and are considered to be satisfactory. The result for the solution of 0.01 mM nitrate containing no chloride is not satisfactory. One of the chromatograms of that solution is shown in Figure III-13. The nitrate peak is not well-separated from the negative oxygen-related injection phenomenon, which was explained in Section III.C.4. The baseline is not re-established following the negative peak before the nitrate begins to elute from the column. It was, therefore, necessary to estimate where the base of the nitrate peak should be drawn as is illustrated in Figure III-13. A line was drawn tangent to the front side of the nitrate peak at the inflection point. A second line was drawn tangent to that part of the curve between the negative injection peak and the nitrate peak at the inflection

Table III-8. Precision study - summary of data

	A_p	RDS_p	A_t	RDS_t
0.100 mM KNO_3/H_2O	125.0	0.7	126.0	3.7%
	134.0	1.6		
	125.0	0.0		
	127.0	1.4		
	119.0	1.5		
	125.8	0.7		
0.098 mM KNO_3/0.1 MKCl	133.3	0.9	135.6	2.5%
	141.0	0.6		
	137.0	0.6		
	136.0	0.6		
	130.8	0.4		
	135.5	0.7		
0.0103 mM KNO_3/H_2O	53.3	1.8	57.2	9.1%
	58.0	1.4		
	63.8	0.8		
	62.0	1.3		
	48.8	1.0		
	57.5	2.3		
0.0100 mM KNO_3/0.1 M KCl	65.5	1.5	63.5	2.7%
	64.3	1.5		
	61.5	0.9		
	64.8	1.5		
	63.0	0.0		
	61.8	1.5		

Figure III-13. Illustration of construction of baseline for nitrate peak not resolved from oxygen-related injection phenomenon

Nitrate concentration = 0.01 mM

Chloride concentration = 0.10 M

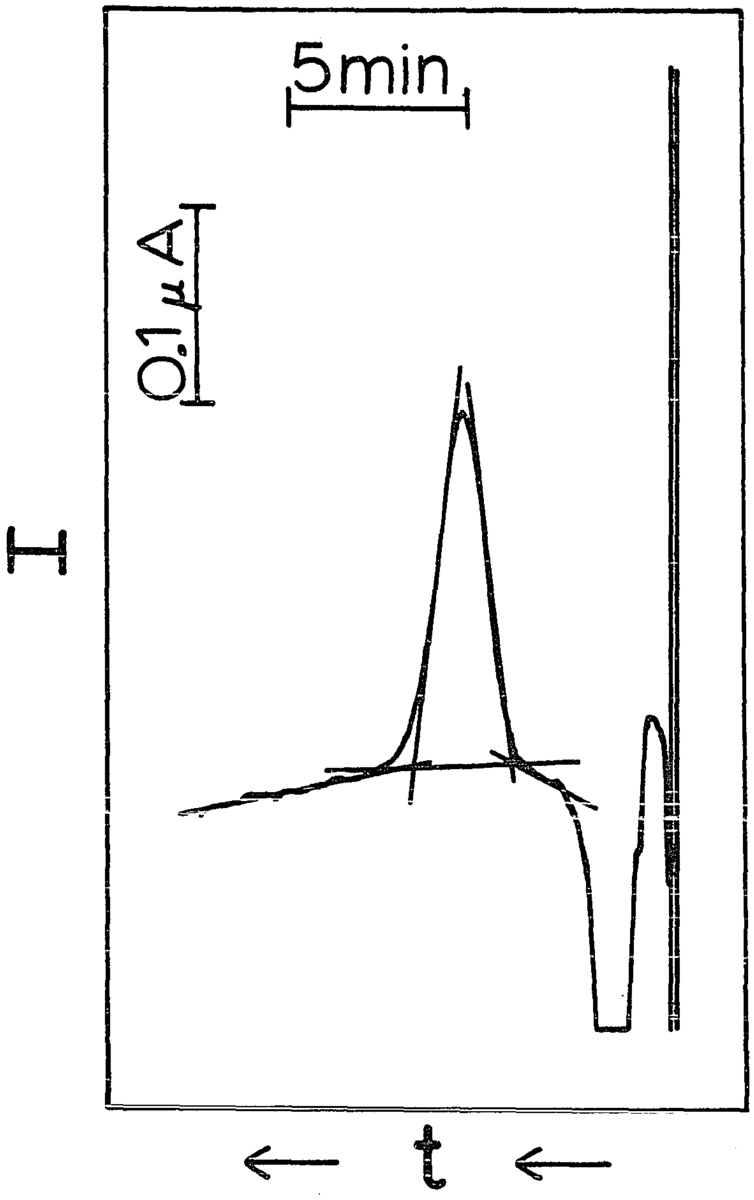
5min
0.1μA
I
← t ←

point. The intersection of these two lines was considered to be one of two points needed to construct the base of the peak. The other point was the intersection of a line drawn tangent to the back side of the nitrate peak at the inflection point and a backwards extrapolation of the base line which followed the nitrate peak. Even with this careful construction of the base of the peak, the reproducibility of the peak area at lower nitrate concentrations is poor as reflected by the high value of RDS_t, 9.1%, for this case.

It is apparent from a comparison of this value with the one obtained for the 0.01 mM nitrate in 0.1 M chloride that one way to improve the precision at lower concentrations is to load the nitrate samples with chloride. For this solution it was easy to determine where the base of the peak should be drawn because a better separation was achieved and the peak height was improved. While it is true that a better separation can also be achieved by lowering the concentration of perchloric acid in the eluent, the poorer shape of the nitrate peaks obtained would be detrimental to the detection limit.

8. Analysis of unknown samples

It was shown in Sections III.C.6 and III.C.7 that the response of the copperized cadmium flow-through disk detector during any given work period is reasonably constant and linear with nitrate concentration. Therefore, the method of standard addition can be used to determine the concentration of nitrate in a solution of an unknown sample, C_u. In this technique, a known amount of nitrate was added to a portion of the sample solution to produce a new concentration C_{u+s}. An expression for C_{u+s} as a function of the volumes of the unknown and the standard solutions, V_u and V_s, respectively, is given in Equation III-4.

$$C_{u+s} = \frac{V_u C_u + V_s C_s}{V_u + V_s} \qquad \text{(III-4)}$$

When aliquots of the spiked and the unspiked solutions were injected into the liquid chromatograph, nitrate peaks of areas of A_{u+s} and A_u, were obtained. The relationship between these parameters is given in Equation III-5.

$$C_u = \frac{A_u}{A_{u+s}} C_{u+s} \qquad \text{(III-5)}$$

The details for preparation of samples for chromatographic analysis were given in Section III.B.5. The results of the analysis of these samples are summarized in Table III-9. Note that comparison results obtained by a second analytical method, or taken from manufacturer's specifications, are also given in Table III-9.

The spinach extract provides an example of an aqueous sample which is difficult to analyze for nitrate. While

Table III-9. Analytical results

Sample	Chromatographic results	Comparison results	Comparison results determined by
Spinach extract	0.034% NO_3^-	None	
Iowa well water	0.7 ppm NO_3^-	1.6 ppm NO_3^-	Comparison to spiked portion of sample[a]
Saylorville Reservoir water	23.6 ppm NO_3^-	22.8 ppm NO_3^-	SCM[b]
Morton Tender Quick®	0.54% $NaNO_3$	0.50% $NaNO_3$	Company value[c]
		0.56% $NaNO_3$	SCM[b]
	0.34% $NaNO_2$	0.50% $NaNO_2$	Company value[c]
		0.49% $NaNO_2$	SCM[b]
Dried Morton Tender Quick®	0.73% $NaNO_3$	0.50% $NaNO_3$	Company value[c]
		0.33% $NaNO_3$	SCM[b]
	0.76% $NaNO_2$	0.50% $NaNO_2$	Company value[c]
		0.49% $NaNO_2$	SCM[b]

[a] See discussion of this sample.

[b] Standard colorimetric method (38).

[c] Value reported on the package.

nitrate ion-selective electrodes have been successfully used to determine nitrate in spinach (77, 78), it is impossible to do so colorimetrically unless the chlorophyll present in the sample extract is removed. A nitrate ion-selective electrode was not available for this research and only the chromatographic results are reported for spinach.

Chromatograms obtained for the spinach extract and for the spiked spinach extract are shown in Figure III-14. Oxygen was not purged from these solutions. The first peak in the chromatogram corresponds to the reduction of oxygen present in the sample. Note that there is still current at the detector due to the reduction of oxygen when the nitrate begins to elute from the column. At higher current sensitivities this tailing of the oxygen peak would interfere greatly with the determination of low levels of nitrate. Therefore, oxygen should be removed from all samples. The matter of deoxygenation during the preparation of the samples does not contribute very much to the overall analysis time because one sample can be analyzed as the next is being deoxygenated.

The second unknown listed in Table III-9, a sample of water from a well in Iowa, was provided by the Veterinary Diagnostic Laboratory of Iowa State University. The well water was thought to be contaminated with bacteria, sulfate

Figure III-14. Chromatograms (A) of spiked spinach extract and (B) of spinach extract

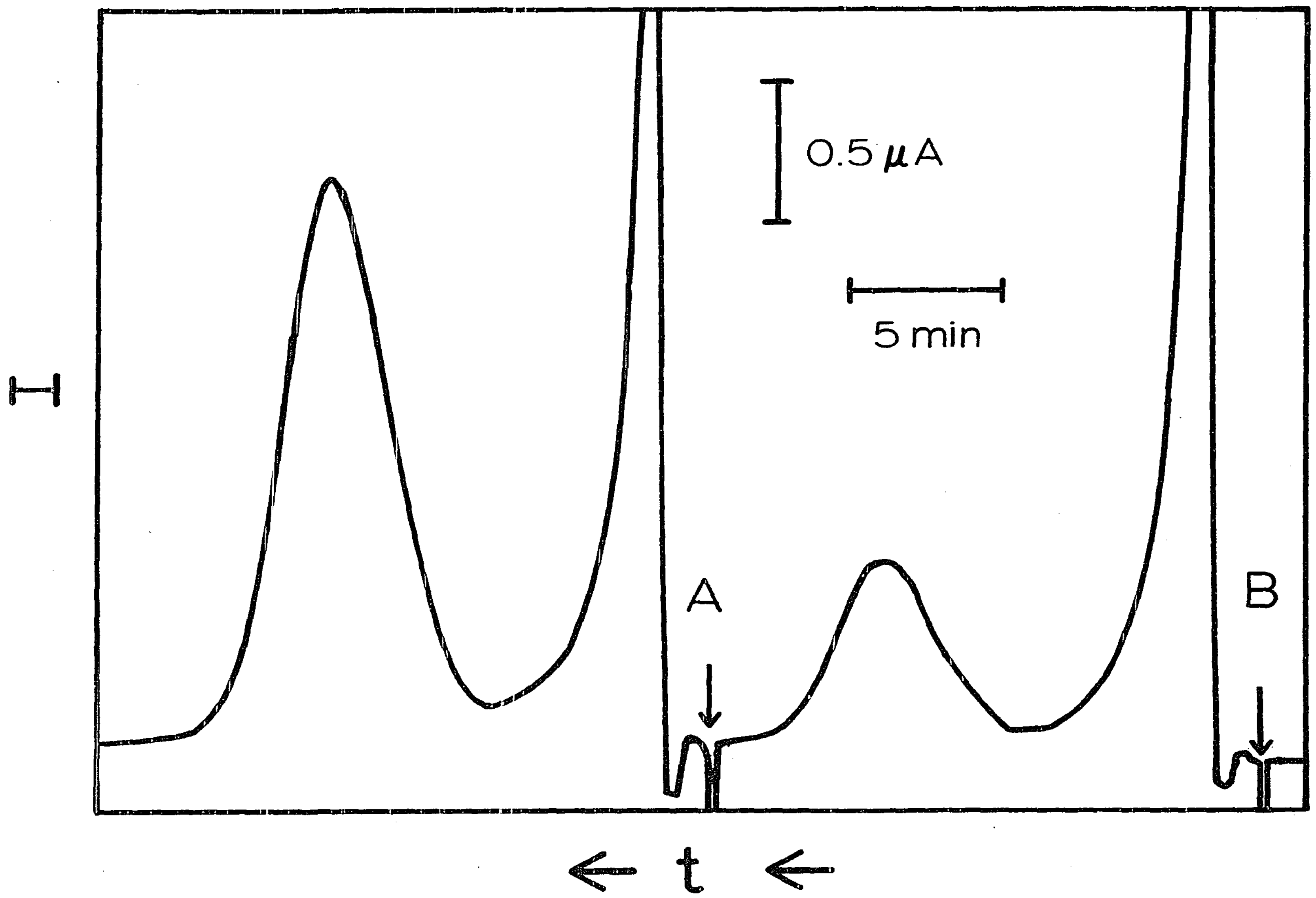
0.5 μA
5 min
I
A
B
← t ←

and nitrate. Personnel from the Veterinary Diagnostic Laboratory had encountered difficulty in applying the standard colorimetric procedure for nitrate to this particular sample. Only 9 mL of sample was made available to me for analysis. This sample had been divided into two portions of 5 mL and 4 mL each. To the second portion 1 mL of 60 ppm standard nitrate solution was added.

The procedure applied for analysis of these two well water samples is described in Section III.B.5. Let it suffice here to note that this analysis was difficult because of the volumes of the samples provided were small. I found 0.7 ppm nitrate in the unspiked portion of the sample and 13.3 ppm in the spiked portion. Assuming that the latter result was accurate, it was possible to calculate from Equation III-5 that the concentration of nitrate in the original 4 mL of sample was 1.6 ppm prior to spiking. Based on the foregoing assumption and calculation, the chromatographic result obtained for the unspiked portion is low. The relative error in the analysis, obtained by comparing 0.7 ppm and 1.6 ppm, was about 44%. The relative error involved in the measurement of the small volumes was large; therefore, the result of the analysis of the well water sample is considered to be satisfactory.

The sample of water from the Saylorville Reservoir was provided by the Energy Research Institute of Iowa

State University. This sample was also analyzed for nitrate by Energy Research Institute personnel by the colorimetric procedure approved by the Environmental Protection Agency (38). Assuming that the result they obtained was correct, the relative error in the chromatographic analysis was less than 4%.

The sample of Morton Tender Quick Salt turned out to be a very interesting sample. It was discovered while analyzing this sample with the liquid chromatograph that large amounts of chloride co-injected with the nitrate cause the nitrate to be retained on the anion-exchange column for a longer time period. Although retained longer, the nitrate is eluted in a narrower band than observed for the absence of chloride. Section III.C.5 is devoted to the description and discussion of this phenomenon. Further details concerning the sample and the preparation of aqueous samples thereof are given in Section III.B.5.

A portion of the salt was dried. Both the dried salt and the wet salt were analyzed by the liquid chromatographic method and a colorimetric method. In the liquid chromatographic method, nitrite was determined by difference following chemical oxidation with hydrogen peroxide to nitrate. In the colorimetric method, nitrate was determined by difference following chemical reduction in a copperized cadmium column to nitrite. Only the results for direct liquid chromatographic determination of nitrate in the wet salt and the colorimetric determination of nitrate and nitrite in the wet salt are satisfactory.

The poor results obtained for the chromatographic determination of nitrite in the wet salt can be explained as follows. It had been observed that a large amount of hydrogen peroxide would oxidize the nitrite in standard solutions to nitrate. The optimum conditions for this reaction were not determined, but an attempt was made to determine the nitrite in this sample with the liquid chromatograph. The result obtained for the liquid chromatographic determination of nitrite in the wet salt is low. Even so, the possibility of being able to determine nitrite with the liquid chromatograph is illustrated by this attempt.

Another reagent that was successfully used to oxidize nitrite in standard solutions was permanganate in acid solution. This reagent is probably better than hydrogen peroxide because the excess hydrogen peroxide could not be removed and it reacted chromatographically and electrochemically in the same way that oxygen reacts. It is proposed that the nitrite in an acidified sample can be oxidized by the dropwise addition of permanganate solution. It is not necessary to add a large excess of permanganate because the reaction proceeds with sufficient speed and the first persistent pink color from excess permanganate can be taken as an indication that all the nitrite is oxidized. The small amount of excess permanganate can be reduced by the dropwise addition of very dilute hydrogen peroxide, which need not be added in excess. The manganous ion, which is the product of the permanganate reduction, is retained on the cation-exchange column and, therefore, does not interfere. It should be noted that any acid added to the sample must be neutralized if the sample is to be purged of oxygen; otherwise nitric acid will volatilize. The details of this proposed procedure for the liquid chromatographic determination of nitrite are left for a future investigator to determine.

The poor analytical results obtained for the determination of nitrite and nitrate in the dried salt by both methods are thought to be due to reactions that occurred during the drying of the salt. Nitrate is an oxidizing agent, whereas nitrite is both an oxidizing and a reducing agent. The salt formulation also included sucrose and propylene glycol. Following the drying operation there were brown crystals present in the salt sample, indicating that the sample had partially decomposed and was no longer homogeneous.

It is concluded that the anion-exchange separation and copperized cadmium flow-through detector described in this report can be used to determine nitrate in a variety of aqueous samples. As with all analytical methods of analysis, the procedure used to prepare the sample and to perform the analysis may vary as a function of the nature of the sample, the accuracy required, and imposed time limitations. Also, it seems promising that the same system can be used to determine nitrite by difference.

IV. SUMMARY

A method for the determination of nitrate in aqueous samples was described in this thesis. The method is an improvement of the method described by Davneport and Johnson which involved the separation of nitrate, nitrite, and oxygen by anion-exchange chromatography with amperometric detection of nitrate and nitrite in the effluent by electroreduction at a tubular cadmium detector. The improved method described here also uses anion-exchange chromatography, but copperized cadmium was chosen for the working electrode material because the reduction of nitrate was observed to be electrocatalyzed by the copper deposited on the cadmium electrode surface. The electrocatalyzed rate of the reduction of nitrate on copperized cadmium was observed to be mass-transport limited at pH 8. The replacement of the cadmium by the copperized cadmium in the chromatographic detector constituted a major advance in the method for the determination of nitrate because the electrode surface was observed to be much more reproducible in activity for nitrate reduction than the detector of Davenport.

The electrocatalytic effect of the copper was investigated and it was proposed that an unpaired d electron in the copper-cadmium alloy might be involved in the formation of an adsorption bond between the electrode surface and the adsorbed reactant such that the overall electrochemical energy of activation is smaller at a copperized-cadmium electrode than at a cadmium electrode. Experimental results were described which support the proposed explanation of the electrocatalytic effect of the deposited copper.

The copperized-cadmium electrode was used in a flow-through disk detector which was interfaced with an anion-exchange column to form an analytical system for the determination of nitrate. The source and preparation of the anion-exchange packing material for chromatographic separation of nitrate from oxygen was fully described. It was discovered that the shape of the nitrate peak obtained with this analytical system was improved if the injected sample was loaded with a large amount of chloride. The chloride loading phenomenon resulted in an order of magnitude improvement in the detection limit of the system for nitrate (from 0.1 μM to 1 μM for a 0.3 mL sample injection loop). The precision of the method was found to be ±5% at nitrate levels above 10 μM and the response of the analytical system to nitrate was found to be linear over three to four orders of magnitude. No significant interferences were found for common anions. Electroactive metal cations were removed in the chromatographic process by adsorption in a cation-exchange column.

The nitrate in several unknown samples was determined and the results were found to be in good agreement with those obtained by other analytical methods. Nitrite was determined in one unknown sample. The method involved the determination of nitrate with the anion-exchange chromatograph before and after the chemical oxidation of nitrite to nitrate with hydrogen peroxide. The increase in the peak area for nitrate was taken as a measure of nitrite present in the sample.

V. SUGGESTIONS FOR FUTURE RESEARCH

The mechanism of the electrocatalytic reduction of nitrate on copperized cadmium needs further investigation. A mathematical expression for the currents observed during the activation studies described in Section II.D.3 should be very helpful in determining how many surface atoms of cadmium and/or copper are involved in the activated complex of the reaction.

It is possible that a pH between 1 and 8 might be chosen such that the copperized cadmium flow-through disk detector would respond to nitrite without excessive hydrogen evolution. Nitrate and nitrite could be separated with the packing material used in the method described here; however, the column would have to be lengthened and the pumping capacity increased by selection of appropriate equipment.

It is suggested that nitrate might be analyzed in a flow-injection analysis system without a separation column at pH 8, if oxygen is removed in a reproducible fashion. Such a system would have to be oxygen impermeable: stainless steel would probably work for the interconnection of chromatographic components because of the high pH of the flowing stream.

VI. APPENDIX: ELECTROLYSIS AT CONTROLLED POTENTIAL

The rate at which an electroactive analyte is depleted by electrolysis is described by Faraday's law as described in Equation A-1.

$$\frac{dN^b}{dt} = \frac{dC^b}{Vdt} = \frac{-I}{nF} \qquad \text{(A-1)}$$

In Equation A-1:

N^b = quantity of electroactive species in solution (moles);

t = time (sec);

C^b = bulk concentration of electroactive species (μ moles cm^{-3});

V = volume of solution (cm^3);

I = electrode current (coul sec^{-1});

n = electrons (equiv $mole^{-1}$)

F = Faraday constant (9.65×10^4 coul $equiv^{-1}$).

The maximum current at an electrode is controlled by the maximum rate of convective-diffusional mass transport as described empirically by Equation A-2.

$$I_\ell = \frac{nFADC^b}{\delta} \qquad \text{(A-2)}$$

In Equation A-2:

I_ℓ = mass-transport limited electrode current (mA);

A = electrode area (cm^2)

D = diffusion coefficient (cm^2 sec^{-1});

δ = thickness of diffusion layer (cm).

The thickness of the diffusion layer at a rotating disk electrode is accurately given by Equation A-3.

$$\delta = 1.61D^{1/3}\omega^{-1/2}\nu^{1/6} \tag{A-3}$$

In Equation A-3:

ω = angular velocity of electrode rotation (rad sec^{-1});

ν = kinematic viscosity of the solution (cm^2 sec^{-1}).

Equation A-1 and A-2 can be combined and integrated for a constant rate of electrode rotation to yield the value of N^b at time t in the electrolysis, $N^b{}_t$, as compared to N at t=0, $N^b{}_{t=0}$

$$N^b{}_t = N^b{}_{t=0} \exp\{-\lambda t\} \tag{A-1}$$

$$\lambda = \frac{AD}{V\delta}$$

For electrodeposition of a metal, the quantity of accumulated metal at time t, $N^a{}_t$, is

$$\begin{aligned} N^a{}_t &= N^b{}_{t=0} - N^b{}_t \\ &= N^b{}_{t=0}(1 - \exp\{-\lambda t\}) \end{aligned} \tag{A-5}$$

Equation A-5 is also given in this thesis as Equation II-23. The number of atoms deposited is related to $N^a{}_t$ by Avogadro's number, $(N^a{}_t)(6.023 \times 10^{23}$ atoms mole$^{-1})$. The number of atomic layers in the metal deposit is predicted for a hexagonal close-packed deposit by Equation A-6.

$$\text{Number of layers} = 6.023 \times 10^{23}\ N^{a}_{t}\ A_{atom}/A \qquad \text{(A-6)}$$

$$= 6.023 \times 10^{23}\ N^{b}_{t=0}(1 - \exp -kt\ )A_{atom}/A$$

In Equation A-6, A_{atom} is the area occupied by the close-packed atom which is calculated from the geometry of the hexagon and the covalent radius, r, by Equation A-7.

$$A_{atom} = 2r^{2}(\sec 30° + \tan 30°) \qquad \text{(A-7)}$$

Values for r of copper and cadmium atoms are 1.28×10^{-8} cm and 1.48×10^{-8} cm, respectively (100). The values for D of copper(II) and cadmium(II) are the same, 7.2×10^{-6} $cm^{2}\ sec^{-1}$ (101). The disk electrode areas are 0.60 cm^{2} for copper, 0.95 cm^{2} for polycrystalline cadmium, and 0.35 cm^{2} for monocrystalline cadmium.

VII. BIBLIOGRAPHY

1. Nicholas, D. J. D. Biol. Rev. 1963, 38, 530.

2. Skinner, K. J. Chem. Eng. News 1976, 54(41), 24.

3. Davenport, R. J., Ph.D. Dissertation, Iowa State University, Ames, IA, 1974.

4. Lee, D. H. K. Environ. Res. 1970, 3, 484.

5. Nichols, M. S. J. Am. Water Works Assoc. 1965, 57, 1319.

6. Davidsohn, I.; Henry, J. B. "Clinical Diagnosis by Laboratory Methods", 14th ed.; W. B. Saunders Co.: Philadelphia, 1969; p 135, 592.

7. Barnes, J. M.; Magee, P. N. Br. J. Med. 1954, 11, 167.

8. Inoue, Y. Hisoshima Daigaku Igaku Zasshi 1972, 20, 347.

9. Hawksworth, G.; Hill, M. J. J. Biochem. (Tokyo) 1971, 122, 28P.

10. "Water Quality Criteria"; McKee, J. E., Wolf, H. W., Eds.; Resources Agency of California, State Water Quality Control Board Publication No. 3-A: Sacramento, CA, 1963; p 224.

11. Davenport, R. J.; Johnson, D. C. Anal. Chem. 1973, 45, 1979.

12. Griess, P. Ber. Dtsch. Chem. Ges. 1879, 12, 426.

13. Morrison, R. T.; Boyd, R. N. "Organic Chemistry", 2nd ed.; Allyn and Bacon: Boston, 1966; Chapter 24.

14. Adriaanse, A.; Robbers, J. E. J. Sci. Food Agric. 1969, 20, 321.

15. Hosvay, M. L. Bull. Soc. Chim. Fr. 1889, 2, 388.

16. Follett, M. J.; Ratcliff, P. W. J. Sci. Food Agric. 1963, 14, 138.

17. Bratton, A. C.; Marshall, E. D. J. Biol. Chem. 1939, 128, 537.

18. Wada, E.; Hattori, A. Anal. Chim. Acta 1971, 56, 233.

19. Raganowicz, E.; Niewiadomy, A. Bromatol. Chem. Toksykol. 1976, 9, 213; Chem. Abstr. 1977, 86, 25532p.

20. Foris, A.; Sweet, T. R. Anal. Chem. 1965, 37, 701.

21. Kamm, L.; McKeown, G. G.; Morrison Smith, D. J. J. Assoc. Off. Agric. Chem. 1965, 48, 892.

22. Lambert, J. L.; Zitomer, F. Anal. Chem. 1960, 32, 1684.

23. Toei, K.; Kiyose, T. Anal. Chim. Acta 1977, 88, 125.

24. Fawcett, R.; Tame, D. A.; Johnson, T. E. J. Assoc. Public Anal. 1976, 23, 14.

25. Bray, R. H. Soil Sci. 1945, 60, 219.

26. Foyn, E. Rep. Norw. Fish. Mar. Invest. 1951, 9, 7.

27. Chow, T. J.; Johnstone, M. S. Anal. Chim. Acta 1962, 27, 441.

28. Litchfield, M. H. Analyst (London) 1962, 92, 132.

29. Mullen, J. B.; Riley, J. P. Anal. Chim. Acta 1955, 12, 464.

30. Terrey, D. R. Anal. Chim. Acta 1966, 34, 41.

31. Austin, K. H.; Strickland, J. D. H. J. Cons., Cons. Perm. Int. Explor. Mer. 1959, 24, 446.

32. Potzl, L.; Reiter, R. Z. Aerosol Forsch. Ther. 1960, 8, 252.

33. Brewer, P. G.; Riley, J. P. Deep Sea Res. 1965, 12, 765.

34. Fudge, R.; Truman, R. W. J. Am. Pharm. Assoc. 1973, 11, 19.

35. Morris, A. W.; Riley, J. P. Anal. Chim. Acta 1963, 29, 272.

36. Grasshoff, K. Kiel. Meeresforsch 1964, 20, 5.

37. Strickland, J. D. H.; Parsons, T. R. "A Manual of Seawater Analysis"; Bull., Fish. Res. Board Can., 1969, No. 125.

38. "Methods for Chemical Analysis of Water and Wastes"; Crowe, R. E., Ed.; *Environ. Prot. Technol. Ser.*: Washington, DC, 1974; p 201.

39. Wood, E. D.; Armstrong, F. A. J.; Richards, F. A. *J. Mar. Biol. Assoc. U. K.* 1967, *47*, 23.

40. Lambert, R. S.; Dubois, R. J. *Anal. Chem.* 1971, *43*, 955.

41. Nydahl, F. *Talanta* 1976, *23*, 349.

42. Otsuki, A. *Anal. Chim. Acta* 1978, *99*, 375.

43. Stainton, M. P. *Anal. Chem.* 1974, *46*, 1616.

44. Lowe, R. H.; Hamilton, J. L. *J. Agric. Fd. Chem.* 1967, *15*, 359.

45. Srinivasan, S.; Wroblowa, H.; Bockris, J. O'M. *Adv. in Catal.* 1967, *17*, 351.

46. Bockris, J. O'M.; Wroblowa, H. *J. Electroanal. Chem.* 1964, *7*, 428.

47. Trasatti, S. *La Chemica e L'Industria* 1969, *51*, 1063.

48. Galus, Z. "Fundamentals of Electrochemical Analysis", Engl. Transl.; Reynolds, G. F., Ed.; Halsted: New York, 1976; Chapter 3.

49. Tur'yan, Ya. I.; Ruvinskii, O. E. *J. Electroanal. Chem. Interfac. Electrochem.* 1969, *23*, 61.

50. Rao, M. L. B.; Damjanovic, A.; Bockris, J. O'M. *J. Phys. Chem.* 1963, *67*, 2508.

51. Agladze, R. I.; Karchava, D. E.; Kvaratskheliya, R. K. *Soobschch. Akad. Nauk Gruz. SSR* 1968, *50*, 75; *Chem. Abstr.* 1969, *70*, 63421d.

52. Kvaratskheliya, R. K.; Agledze, R. J. *Electrokhimiya* 1969, *5*, 911.

53. Kabanov, B. N.; Tomashova, N. N.; Kiseleva, J. G. *Electrokhimiya* 1970, *6*, 612.

54. Kortum, G. "Treatise on Electrochemistry", 2nd Engl. ed.; Elsevier: New York, 1965; Chapter 12.

55. Bockris, J. O'M.; Davanathan, M. A. V.; Muller, K. Proc. Roy. Soc. 1963, 55, A274.

56. Guidelli, R.; Foresti, M. L. Electrochim. Acta 1973 18, 301.

57. Foresti, M. L.; Guidelli, R. J. Electroanal. Chem. 1974, 53, 219.

58. Foresti, M. L.; Cozzi, D.; Guidelli, R. J. Electroanal. Chem. Interfac. Electrochem. 1974, 53, 235.

59. Guidelli, R.; Foresti, M. L. J. Electroanal. Chem. 1976, 67, 239.

60. Landsberg, R.; Thiele, R. Electrochim. Acta 1966, 11 1243.

61. Scheller, F.; Muller, S.; Landsberg, R.; Spitzer, H. -J. J. Electroanal. Chem. 1968, 19, 187.

62. Lindeman, J.; Landsberg, R. J. Electroanal. Chem. 1971, 29, 261.

63. Sharma, B.; Ahlert, R. C.; Saldick, J. J. Environ. Sci. Health 1976, A11(3), 255.

64. Vdovenko, V. M.; Gurikov, Yu. V.; Legin, E. K. Radiokhimiya 1966, 8, 323.

65. "Handbook of Chemistry and Physics", 52nd ed.; Weast, R. C., Ed.; Chemical Rubber Co.: Cleveland, OH, 1972; p D-223.

66. Amenson, J., Energy Research Institute, Iowa State University, personal communication, 1978.

67. Bockris, J. O'M.; Reddy, A. D. N. "Modern Electrochemistry"; Plenum/Rosetta: New York, 1970; Vol. II, p 708.

68. Trepak, N. M.; Il'ina, L. K.; L'vov, A. L.; Rodnikova, V. N. Electrokhimiya 1972, 8, 939.

69. Cullity, B. D. "Elements of X-ray Diffraction"; Addison-Wesley: Reading, MA, 1967; p 38.

70. Shahine, S.; Ismael, N. Mikrochim. Acta 1976, 2, 75.

71. Cresser, M. S. Analyst (London) 1977, 102, 99.

72. Senn, D. R.; Carr, W.; Klatt, L. N. Anal. Chem. 1976, 48, 954.

73. Kiang, C-H.; Kuan, S. S.; Guilbault, G. C. Anal. Chem. 1978, 50(9), 1319.

74. Mertens, J.; Vander Winkel, P.; Massart, D. L. Anal. Chem. 1975, 47, 522.

75. Hopirtean, E.; Stefaniga, E.; Liteanu, C. Chem. Anal. (Warsaw) 1976, 21, 867.

76. Nomura, T.; Nakagawa, G. Anal. Lett. 1975, 8, 873.

77. Pfeiffer, S. L.; Smith, J. J. Assoc. Off. Anal. Chem. 1975, 58, 915.

78. Liedtke, M. A.; Meloan, C. E. J. Agric. Food Chem. 1975, 24, 410.

79. Bodini, M. E.; Sawyer, D. T. Anal. Chem. 1977, 49, 485.

80. Cox, J. A.; Litwinski, G. R. Anal. Chem. 1979, 51, 554.

81. Tesch, J. W.; Rehg, W. R.; Sievers, R. E. J. Chromatogr. 1976, 125, 743.

82. Wheeler, G. L.; Lott, P. F. Microchem. J. 1974, 19, 390.

83. Small, H.; Stevens, T. S.; Baumans, W. C. Anal. Chem. 1975, 47, 1801.

84. Snider, B. G. Ph.D. Dissertation, Iowa State University, Ames, IA, 1978.

85. Larochelle, J. Ph.D. Dissertation, Iowa State University, Ames, IA, 1977.

86. Gaunt, J., Energy Research Institute, Iowa State University, personal communication, 1978.

87. Kissinger, P. T. Anal. Chem. 1977, 49, 447A.

88. Fleet, B.; Little, C. F. J. Chromatogr. Sci. 1974, 12, 747.

89. Glauert, M. B. *J. Fluid Mech.* 1956, *1*, 625.

90. Yamada, J.; Matsuda, H. *J. Electroanal. Chem. Interfacial Electrochem.* 1973, *44*, 189.

91. "Webster's Seventh New Collegiate Dictionary"; G. & C. Merriam Co.: Springfield, MA, 1965; p 456.

92. Lewis, E. C. Ph.D. Dissertation, Iowa State University, Ames, IA, 1977.

93. Blaedel, W. J.; Jenkins, R. A. *Anal. Chem.* 1974, *46*, 1952.

94. Hadden, N.; Baumann, F.; MacDonald, F.; Munk, M.; Stevenson, R.; Gere, D.; Zamaroni, F.; Majors, R. "Basic Liquid Chromatography"; Varian Aerograph: Palo Alto, CA, 1971; Chapters 2 and 3.

95. "Materials, Equipment, and Systems for Chromatography, Electrophoresis, Immunochemistry, and Membrane Filtration"; product literature of Bio-Rad Laboratories: Richmond, CA, 1977; p 7.

96. Karel, M. *Food Tech.* (*Chicago*) 1974, *28*(8), 50.

97. Langler, J., Research Laboratories, Morton Salt Co., Woodstock, IL, personal communication, 1978.

98. Gregor, H. P.; Frederick, M. *Ann. N. Y. Acad. Sci.* 1953, *57*, 87.

99. Helfferich, F. "Ion Exchange"; McGraw-Hill: New York, 1962; p 175.

100. "Table of Periodic Properties of the Elements"; distributed by Sargent-Welch Scientific Co.: Skokie, IL, 1968; Catalog No. S-18806.

101. Kolthoff, I. M.; Lingane, J. J. "Polarography", 2nd ed.; Interscience Publishers: New York, 1952; Vol. I, p 52.

VIII. ACKNOWLEDGEMENTS

I would like to thank Dr. Dennis C. Johnson for skillfully guiding me through the graduate program which has culminated in this Ph.D. thesis. His concern for the total development of his graduate students is gratefully acknowledged.

I wish to thank the members of Dr. Johnson's research group for their contribution to my graduate education. Also, I owe a special note of thanks to Mr. Douglas Gjerde, who helped considerably in the development of the anion-exchange separation described in this thesis.

A special thanks is offered to two personal friends, Dr. Benjamin Strohbehn and Mr. Craig Hastings, for their encouragement during the writing of this thesis. Finally, I thank my wife, Becky, and my children, Matthew and Hannah, for the sacrifices they have made in order to get me educated.